FURTHER STUDIES OF THE ANALOGY BETWEEN FLUID FRICTION AND HEAT TRANSFER IN A STEADY-STATE, TWO-DIMENSIONAL TURBULENTLY FLOWING AIR STREAM.

Thesis by

Franklin Page, Jr.

In Partial Fulfillment of the Requirements

For the Degree of

Doctor of Philosophy

California Institute of Technology

Pasadena, California

1950

Acknowledgments

This thesis is dedicated to my wife. Without her unceasing, though not always untiring, assistance it might have been impossible to process the tremendous body of data reported herein.

Dr. B. H. Sage has provided the inspirational leadership and the frequently needed advice which has made possible the success of the entire Chemical Engineering Transfer Research Program.

Numerous fellow students have made important contributions to the work reported herein. They have assisted in the construction, maintenance and operation of the heat transfer apparatus. The most valuable assistance has been rendered by Dr. David M. Mason, Stuart D. Cavers, John L. Mason and Virgil J. Berry.

Many employees of the California Institute have rendered valuable assistance in the construction and operation of the heat transfer apparatus. The most important contributions were those of Hollis H. Reamer and Darlton K. Breaux.

Abstract

Velocity and temperature distributions have been measured in a steady-state, two-dimensional, turbulently flowing air stream. These measurements have been made both in an essentially isothermal stream and in one upon which a temperature gradient had been imposed. The heat flux and shear and the thermodynamic state of the fluid were determined at the same positions in the air stream.

From these data, the eddy conductivity and eddy viscosity distributions were calculated for fifteen different flow conditions.

The results of the eddy property calculations have been compared with eddy property distributions predicted by other investigators. The data have been correlated in a manner which appears to simplify prediction of eddy properties in other similiar situations.

TABLE OF CONTENTS

TABLE OF CONTENTS, cont'd.

Section I

Introduction:

A complete understanding of the analogy between the transfer of thermal energy and the transfer of momentum in turbulent fluids appears to be desirable. Such an understanding might assist in improving the analysis of turbulent processes and certainly would provide useful assistance in the prediction of heat flux in engineering situations. This analogy has attracted the attention of many investigators but a complete understanding is still lacking.

An investigation of the relationship between eddy viscosity and eddy conductivity appears to offer a means of obtaining additional understanding of the mechanism of this analogy. The principal purpose of the investigations reported herein is the determination of the relationship between eddy conductivity and eddy viscosity in a two-dimensional, turbulently flowing air stream.

Almost every writing on the analogy between heat transfer and fluid friction pays tribute to Osborne Reynolds (1) who originally reported this phenomenon. The Prandtl (2) and Taylor (3) theories of turbulent action appear to yield, as a corollary, the proposal that the eddy conductivity and the eddy viscosity are

identical quantities. By the use of this assumption and of either experimental or assumed eddy viscosity distributions, heat transfer relations may be calculated.

Karman (4) tacitly assumed the identity of the eddy viscosity and of the eddy conductivity by considering the existence of only one quantity, the "turbulent diffusivity", which possessed the properties of both of the eddy quantities. Using this identity assumption he derived expressions which approximately indicate the heat transfer coefficients for circular tubes for a wide range of fluids and a wide range of flow conditions.

Boelter, et.al., (5), and Martinelli (6) recognized that possibly the eddy conductivity and the eddy viscosity were not identical, but presumed that their relationship might be represented as a ratio. This ratio was assumed to be single-valued for any one stream. Using this ratio they derived complicated expressions for heat transfer coefficients for circular tubes and parallel plates. In their actual numerical computations they used the value of unity for this ratio.

In any fluid situation for which the eddy conductivity and velocity distributions may be accurately estimated, the heat transfer problem is capable of a complete solution. This approach to the heat transfer problem has obtained engineering importance only since the development of such computational aids as the analog

computer and high speed digital computers. The application of eddy conductivity data to the solution of heat transfer problems is not within the realm of the present writer's investigations. Several other graduate students in the Chemical Engineering Department of the California Institute have been demonstrating the use of eddy conductivity data with the analog computer for the prediction of thermal flux and of temperature fields in turbulent streams. One paper (7) reports the use of an arbitrarily assumed eddy conductivity distribution. A later study utilized, at least in part, eddy conductivity distributions determined by the present writer and reported in this thesis.

The use of high speed computational aids makes unnecessary the simplifying assumptions which have characterized all previous work in this field. Previous investigators have been forced to distort their data to yield expressions which are capable of analytical integration. This capability of analytical integration is perhaps still desirable for those engineers who do not yet have access to high speed computational aids. However, such equipment is becoming widely available and it seems desirable to abandon the use of simplifying assumptions which do not adequately describe the heat transfer situation.

An apparatus has been constructed in the Chemical

Engineering Department at the California Institute for the direct and simultaneous determination of the eddy conductivity and of the eddy viscosity in a turbulently flowing air stream. This apparatus was largely constructed by students who preceded the present writer. Their preliminary measurements did not yield reliable values of the eddy quantities and the present writer has had the assignment of accurately determining these quantities in a turbulently flowing two-dimensional air stream. It has been the hope of the present investigators that the ratio of eddy conductivity to eddy viscosity determined in this investigation might be used to indicate the eddy conductivity under other flow conditions where the eddy viscosity might be independently determined.

A large body of data has been collected which shows the distributions of the eddy properties in a two-dimensional turbulent air stream under a variety of experimental conditions. However, the problem of predicting the eddy conductivity distributions is not completely solved. In fact, the eddy viscosity distributions predicted in the literature (4), (5), (6), do not agree with the data obtained on our apparatus. The ratio of the eddy properties seems to depend upon the position in the stream and upon the Reynolds number.

Section II

Equipment Used in this Investigation:

The equipment used in this investigation has been previously described. As it is believed that the previous descriptions are quite adequate, a complete and detailed description of this equipment has not been included in this thesis. The Chemical Engineering Department heat transfer apparatus has been described in the Ph. D. theses of W. H. Corcoran (8), Glenn W. Billman (9), and David M. Mason (10), and in Chemical Engineering Department Manuscript No. 292 (11) which has been submitted for publication in Industrial and Engineering Chemistry.

The present writer has assisted in the redesign of the calorimetric equipment. The isolated-wall-section calorimeters designed by the writer have been further modified and are being described in the Ph. D. thesis of fellow student, Stuart D. Cavers (12). The present writer has assisted in the modification of the anemometry equipment and in the development of operating procedures for this equipment. The presently used anemometry equipment and methods are described in section VI of this thesis.

The heat transfer apparatus consists of a wind tunnel approximately 0.7 inches in thickness, 13 inches wide and 14 feet long. Air is circulated through this

channel by means of a suitable blower and control system. The air flow rate may be set at any desired value by adjusting the speed of the blower with a continuously variable speed controller. The temperature of the entering air may be held within approximately 0.03°F of any desired control setting. The air flow rate is monitored by a suitable venturi meter and the entrance air temperature is monitored by means of a platinum resistance thermometer.

The two 13 inch by 14 foot walls of the channel are heavy copper plates backed by suitable oil baths. The oil baths are provided with electric heaters, refrigeration coils, circulation pumps and appropriate control equipment. The oil baths may be controlled within approximately 0.01°F of a desired setting. The oil bath temperatures are monitored with platinum resistance thermometers and the plate temperatures are monitored by means of copper-constantan thermocouples and a precision potentiometer.

The two plates may be maintained at two different temperatures, thus imposing a temperature gradient across the air stream; or they may be maintained at the same temperature for the study of the transfer of momentum under essentially isothermal conditions. A uniform, steady-state, flow with transfer of thermal energy and of momentum or with the transfer of momentum alone may

thus be established in the apparatus.

The apparatus contains a fine platinum wire which may be used for the measurement of temperature and velocity at almost any point within the flow channel. This thermanemometer is described in some detail in Section VI of this thesis. Other instrumentation is provided which enables the determination of the pressure at any point in the apparatus and of the pressure gradient in the direction of flow.

The previous papers, (8), (9), (10), and (11) have described this apparatus in considerable detail. However, a few illustrations are offered to help the reader visualize its general characteristics. Figure 1 is an overall schematic view of the apparatus, showing the air circulation circuit and the oil circulation systems. Figure 2 shows a cross section through the air channel and the oil baths. Figure 3 is a view of the downstream end of the apparatus. The working section and oil baths and the air return line may be seen. On the right is the power control panel. Figure 4 is a close-up view of the working section and traversing mechanism. Figure 5 shows the centralized location for all electrical measurements and for control of the various apparatus temperatures.

Figure 6 shows the bank of manometers used in this work and the special cathetometer built for this apparatus.

Figure 7 shows the micromanometer used with the pitot tube measurements. Figure 8 shows one of the two calorimeters before mounting in the apparatus and Figure 9 shows the same calorimeter in position and connected to the vacuum pump. Figure 10 shows a sectional view of one of the calorimeters.

Section III

Measurements of Temperature and Velocity Distributions in a Two-Dimensional Turbulently Flowing Air Stream.

This thesis records the primary data for twenty-four different traverses representing fifteen sets of nominal operating conditions. These traverses were taken at four different distances downstream of the entrance to the channel. The most important data are those at the extreme downstream position. The various nominal conditions are indicated diagrammatically on Figure 11, which indicates the relationship between the various traverses and serves as a sort of index to the data. (It should be noted that the nominal values of some of the descriptive parameters are sometimes quite different from the actual values measured during a traverse and reported in the tables.)

The present author does not wish to represent these data as the result of his exclusive efforts. The heat transfer project has been a cooperative effort with as many as five students and employees assisting in the operation of the apparatus during a single traverse. Considerable additional effort was required to free the various dial readings of the equipment calibrations and obtain the primary data recorded in these tables. However, the present author has had the primary responsibility for the calibration calculations and is

responsible for all the primary data recorded in the accompanying tables.

The test numbers assigned to the data have no particular significance except that they were assigned consectutively. In general, a new test number is taken whenever any of the nominal parameters is changed. Whenever a single test number has been applied to more than one traverse, decimal suffixes have been applied to the basic test numbers to designate the second traverses.

Several of these tests have been identified by other "test numbers" in Chemical Engineering Department Manuscripts Nos. 292 (11) and 5006 (13) which have been submitted for publication. Several of the figures prepared for these manuscripts and also used in this thesis have the curves labeled with these extraneous "test numbers". In these cases appropriate foot notes have been attached to the figures to indicate the corresponding test numbers as used in this thesis.

The various data which apply to each entire traverse are tabulated in Table I. The data in Table I are actual measurements rather than nominal values and are, in general, believed to have the accuracy and precision indicated by the number of significant figures reported. In this table are reported the distance between the plates, the traverse position (in terms of distance

downstream of the channel entrance), the incoming air temperature, the plate temperatures, the bulk velocity, the piezometric pressure at the traversing point, the pressure gradient in the direction of flow, the heat flux density and the weight fraction of water in the air.

For purposes of convenience, the second portion of Table I lists several derived quantities which apply to each entire traverse. These are expected to be especially useful in comparing one traverse with another and in comparing this work with that of other investigators. These are the Reynolds number, the Fanning friction factor, and the "friction velocity".

In Table I, the data given for y_o, the distance between the plates, represents a direct measurement at the time of the traverse. This measurement is performed with a traversing gear optical system and cathetometer, using the reflection method described in Reference 9. The y_o data seem to divide themselves into two distinct sets. This is the result of a major adjustment of the plate separation distance between test 34 and test 37.

The entrance air temperatures reported are those measured with a precision platinum resistance thermometer mounted in the center of the channel at the entrance of the converging section. In the case of every traverse reported in this thesis, this temperature has been con-

trolled within approximately 0.05°F of the nominal setting. The plate temperatures reported in Table I are those indicated by thermocouples buried in the plates opposite the traverse locations. An attempt was made to choose oil bath control temperature settings which would result in the nominal plate temperatures at the traverse location. As may be seen from the data, this effort was usually successful.

The pressure gradient, dP/dx was determined by analysis of data obtained from piezometer bars located upstream of the traversing location and from piezo taps located on the traversing gear. Upstream of the measuring equipment, the pressure gradient appeared to be independent of the position in the channel. That is, the pressure decreased linearly in the downstream direction.

The heat flux density was measured with the isolated-wall-section type of heat flux calorimeters being described in the Ph. D. thesis of fellow student, S. D. Cavers (12).

The weight fraction of water was determined by wet bulb and dry bulb thermometer measurements.

The "bulk velocities" reported here are the result of direct integration of the velocity across the traverse. Other definitions of "bulk velocities" have been suggested for use in streams whose intensive thermo-

dynamic properties are not constant across the stream. No universal custom has been adopted and a mass rate integration is rejected as not yielding the units of velocity. Any other flow rate designation which is desired may be obtained from the primary data presented in this thesis.

The Reynolds number, the friction velocity, and the Fanning friction factor have been defined in terms of the bulk velocity (as described above), the average fluid shear at the wall, and the properties of the fluid midway between the upper and lower plates. These definitions are:

$$U = \frac{1}{y_o} \int_0^{y_o} u \, dy \qquad \text{(Eq. 1)}$$

$$Re = \frac{2 y_o U}{(\nu)_{\frac{y}{y_o}=0.5}} \qquad \text{(Eq. 2)}$$

$$u^* = \sqrt{\frac{\tau_o}{(\rho)_{\frac{y}{y_o}=0.5}}} = \sqrt{\frac{y_o}{2(\rho)_{\frac{y}{y_o}=0.5}} \left(-\frac{dP}{dx}\right)} \qquad \text{(Eq. 3)}$$

$$f = \frac{y_o}{(\rho)_{\frac{y}{y_o}=0.5} U^2} \left(-\frac{dP}{dx}\right) = 2\left(\frac{u^*}{U}\right)^2 \qquad \text{(Eq. 4)}$$

In the case of several of the non-isothermal traverses, the Reynolds number was also calculated, using

the alternative definition $2\int_0^{y_0}(u/U)\,dy$. The results were in substantial agreement with those calculated using the definition in Equation 2.

It should be noted that the data obtained in the experiments reported in this thesis do not directly yield any quantity comparable to a conventional heat transfer coefficient. This is the reason that no heat transfer coefficients are reported in this thesis.

Point values of the temperature and velocity for each of the traverses are tabulated in Table II. These temperatures and velocities are believed to be the time averages at the points indicated. The point locations are expressed in terms of y/y_o, the fractional distance from the lower wall. It should be emphasized that the data in Table II are the directly measured data which have been freed of apparatus calibrations but which have not been smoothed in any manner. On some of the traverses, these data are not as smooth as might be desired, but they are reported here candidly in the belief that they are more useful than any smoothed set which would invariably reflect the opinions of the person doing the smoothing. However, most of these data need no apology as the direct measurements are adequately smooth just as they are recorded. This is the result of very careful experimental work using adequate equipment. Each of the various traverses is discussed in detail and with

candor in the paragraphs that follow and these remarks should be consulted when using any of these data.

Tests 30, 31, 32, 33 and 34:

Tests 30, 31, 32, 33 and 34 all represent a 60°F difference between the two plate temperatures. The nominal velocities on these tests range from 7.5 ft./sec. to 90 ft./sec. These data were obtained before the installation of the piezo taps on the traversing gear. This difficulty made frequent anemometer calibrations impractical and prevented calibration checks during a traverse. The galvanometer damping elements had not yet been installed in the thermanemometer circuit and precise balancing was sometimes impossible. The point velocity data reported for these tests are thus not of the same high quality as the later measurements. The temperature data on these tests are of the usual high precision. As the temperature gradients on these tests were greater than those on any of the later tests, it is believed that the point values of the temperature gradients were established with high relative precision. The pressure gradient data for tests 30, 31, 32, 33 and 34 were mostly established from a friction factor plot for the apparatus. Direct measurements of the pressure gradient agreed approximately with the data reported. However, it is believed that leaks, which were stopped before any later measurements, make the direct measure-

ments less reliable than the friction factor values.

The temperature distributions for tests 30, 31, 32, 33 and 34 are shown in Figure 12. It should be noted that, in spite of a nine fold variation in the bulk velocity and in the Reynolds number, the temperature profiles are quite similiar. (Two of the curves have been displaced from the other three curves for clarity.)

Tests 37 and 39:

Tests 37 and 39 represent a nominal velocity of 30 ft./sec. with the air stream essentially isothermal at 100°F. The test 39 traverse was performed at the downstream end of the measuring section, 12.7 feet from the entrance of the apparatus. (This is the location of most of the later traverses for which eddy properties have been calculated.) The traverse labeled test 37.1 was taken at the furthest upstream position which could be reached by the traversing gear. The traverse labeled test 37 was taken at an intermediate point.

The point velocity distribution determined in test 39 is plotted in Figure 13. (The slight asymmetry apparent in this plot is due to an approximately constant error in position measurement which was eliminated from all tests after test 40.) As a comparison with work of other investigators, the ratio of the velocity deficiency to the friction velocity has been plotted as

a function of the position in the stream in Figure 14. For comparison, Karman's (14) universal velocity deficiency distribution has been shown on the same plot. In plotting the universal velocity distribution, the Karman universal constant "kappa" was taken to be 0.40. In the notation of this thesis, the Karman velocity deficiency distribution is given by:

$$\frac{u_{MAX}-u}{u*} = -2.50\left[\ln\left(1-\left|\frac{2y}{y_o}-1.0\right|^{\frac{1}{2}}\right)+\left|\frac{2y}{y_o}-1.0\right|^{\frac{1}{2}}\right]$$

(Eq. 5)

The experimental data are in approximate agreement with the Karman prediction except for the slight asymmetry noted above. However, our data do not appear to yield a pointed nose at the center of the channel as is predicted by the universal distribution.

In the eddy property calculations, a residual technique was used to magnify the velocity behavior in the central portion of the stream. (Further discussion of this residual technique, per se, will be found in Section IV of this thesis.) The same residual techniques are useful for the comparison of two or more traverses taken under similiar conditions. For the extreme downstream position, the reference equation,

$$u_{ref.} = 33.70 - 38.13\left(\frac{y}{y_o}-0.5\right)^2 \qquad \text{(Eq. 6)}$$

was used; leading to the residual equation,

$$\tilde{u} = u_{ref} - u$$

$$= 33.70 - 38.13\left(\frac{y}{y_o} - 0.5\right)^2 - u \qquad \text{(Eq. 7)}$$

The same residual expression was applied to the data from test 37 and test 37.1 after correcting these data to yield the same bulk velocity. Each point velocity was multiplied by the ratio of the test 39 bulk velocity to the test 37 (or 37.1) bulk velocity before calculation of the residual velocity. This correction to the same bulk velocity is necessary when comparing velocity distributionsas the operating conditions can not be reproduced exactly between traverses.

The three residual velocity profiles are plotted in Figure 15. These data indicate that the turbulent velocity profile is well developed upstream of the furthest upstream location at which the traversing gear may be used.

Tests 39, 43, 48, 49 and 50:

Tests 39, 43, 48, 49 and 50 were all performed with the air stream essentially isothermal at 100°F. The nominal velocities range from 10 ft./sec. to 90 ft./sec. In the case of tests 43, 48, 49 and 50, two traverses were taken at each nominal velocity, one at the extreme downstream position and one 5.7 feet upstream

of this position. The upstream traverses have been given the designation 43.1, 48.1, 49.1 and 50.1 and are reported in detail in this thesis, though very few derived data have been calculated from these traverses. Test 37 and 37.1 are upstream traverses with the nominal conditions the same as those for test 39. With the exception of test 50.1, all of the data reported for these isothermal tests are completely satisfactory. Almost all of them are smooth within the experimental uncertainty of the various determinations. The traverse reported as test 50.1 has an apparent discontinuity in the velocity distribution data, apparently due to some sudden change in one of the operating variables.

Tests 40, 41, 44 and 45:

Tests 40, 41, 44 and 45 represent nominal plate temperatures of 105 and 95°F. They represent nominal velocities varying from 15 ft./sec. to 90 ft./sec. One traverse at the extreme downstream position is reported for test 40 (nominal velocity 30 ft./sec.). Two traverses, one at the extreme downstream position and one 5.7 feet upstream of this position, were taken for each of the sets of nominal conditions represented by tests 41, 44 and 45 (nominal velocities 60, 90 and 15 ft./sec., respectively). The upstream traverses are identified in this thesis as tests 41.1, 44.1 and 45.1.

The data for tests 40, 41 and 45 (and tests 41.1 and 45.1) are completely satisfactory in every respect. Almost all of these data are smooth within the experimental uncertainties of the various determinations. As examples of these data, the point temperature distributions for tests 40 and 45 are shown in Figures 16 and 17 respectively. The point velocity distributions for tests 40 and 45 are shown in Figures 18 and 19 respectively.

The data for test 44 (and 44.1) are not as satisfactory and should be used with caution. These data have a great deal of scatter and are not of the same quality as the balance of the data taken subsequent to the installation of the piezo taps. Both the temperature and velocity data for both of these traverses have excessive and apparently random deviations from smooth curves. The cause of these deficiencies is not known.

Test 46:

Test 46 represents nominal plate temperatures of 115 and 85°F and a nominal velocity of 15 ft./sec. One traverse was taken at the extreme downstream position. The data seemed completely satisfactory in every respect.

Section IV

Calculation of the Eddy Properties:

In this investigation, the eddy properties have been defined by the equations used by Karman (4), though he did not, in the cited reference, distinguish between these two properties. It should be emphasized that these are point properties which vary with position in the flowing stream, and that the various quantities in the defining equations are those quantities at the particular point in the stream.

$$\epsilon_c = \frac{Q^\circ / \sigma c_p}{dt/dy} - K \qquad \text{(Eq. 8)}$$

$$\epsilon_m = \frac{\tau/\rho}{du/dy} - \nu \qquad \text{(Eq. 9)}$$

In these relationships, Q° is considered to be the heat flux parallel to the y axis and τ to be the shear perpendicular to the y axis. With these restrictions on the meaning of Q° and τ, the use of vector notations may be dispensed with for a uniform two-dimensional stream.

These relationships are considered by the present author to be the proper definitions of these properties, and are entirely analogous to the Fourier law of

molecular heat conduction and to the conventional definition of viscosity. The molecular definitions may be rearranged to a form similiar to the form in which we have expressed the definitions for the eddy properties:

$$K = \frac{k}{\sigma c_p} = \frac{Q^\circ / \sigma c_p}{dt/dy} \qquad \text{(Eq. 10)}$$

$$\nu = \frac{\eta}{\rho} = \frac{\tau/\rho}{du/dy} \qquad \text{(Eq. 11)}$$

The above definitions of the molecular quantities (Eqs. 10 and 11) are, of course, only applicable in the absence of turbulence.

To calculate the eddy conductivity and the eddy viscosity at a point in the stream, it is necessary to determine at the same point in the stream all the other quantities in the above defining equations (Eqs. 8 and 9). It is tacitly assumed that Q° is constant across any traverse. It has been shown that the temperature and velocity profiles are fully developed upstream of the traversing positions used in eddy property determinations, and that, therefore, the temperature gradient in the downstream direction is negligible. In addition, the friction in the fluid is negligible compared with Q° in the case of the tests used for the determination of eddy conductivity. By application of the principles of an energy balance, it is evident that Q° must be substantially constant across a section of the channel

and that the data obtained from the wall calorimeters are applicable at each point in the channel.

The point values of the shear, τ , are determined by integration of the expression,(15):

$$d\tau/dy = -dP/dx \qquad \text{(Eq. 12)}$$

As τ must have a zero value at the point of maximum velocity (where du/dy is zero) and as the pressure gradient in the downstream direction is independent of the distance from the center of the stream, the shear may be expressed in terms of the following integral expression:

$$\tau = \left(-\frac{dP}{dx}\right) \int_{\text{¢}}^{\text{point of interest}} dy \qquad \text{(Eq. 13)}$$

σ , ρ , c_p , η , and k are available from widely published data. Samples of the actual values chosen for use in these calculations have been included in Chemical Engineering Department Manuscript No. 5006 (13). σ and ρ were corrected for temperature and pressure in accordance with the conventional practices of chemical engineering thermodynamics. They were also corrected for water vapor by means of the ideal solution assumption (16). No correction of the viscosity for water vapor was made as the various authorities consulted did not yield satisfactory agreement and as the

effect appears to be negligibly small for the moisture concentrations reported in this thesis. The data on the thermal conductivity of air are quite unsatisfactory. However, the values of thermal conductivity chosen appear to be within one percent of the correct values.

ν and K are, of course, obtained from the defining relationships:

$$\nu = \eta/\rho \qquad \text{(Eq. 14)}$$

$$K = k/\sigma c_p \qquad \text{(Eq. 15)}$$

The derivatives du/dy and dt/dy are obtained by graphical differentiation of the experimental data. The temperature and velocity points for each traverse were plotted as ordinates versus the measured location in the stream as abscissas. The most probable line was placed through these data points. Figures 12, 13, 16, 17, 18 and 19 are typical examples of these plots. The slope of this most probable line at a point of interest was taken as the value of the derivatives at this point.

The graphical treatment was checked by a residual plotting technique. Reference velocity and temperature distributionswere obtained by the assumption of extremely simple analytical relationships which fit the data

reasonably well in the bulk of the turbulent core. For example, for test 40, the following reference equations were used:

$$u_{ref.} = 32.30 - 40.625\left(\frac{y}{y_o} - 0.5\right)^2 \qquad \text{(Eq. 16)}$$

$$t_{ref} = 97.60 + 4.80\left(\frac{y}{y_o}\right) \qquad \text{(Eq. 17)}$$

As will be recognized, these equations are consistent with the approximation of a constant value of the eddy properties across a major portion of the turbulent core. No claim is made for these reference equations near the wall.

The difference between the reference value at each data point and the measured value at this point was plotted as the residual velocity or residual temperature. As examples, the residual property plots for test 40 are shown in Figures 20 and 21. This procedure greatly magnifies minor variations in the data taken in the contral portion of the turbulent core but was useless elsewhere. Critically chosen lines were drawn through the residual plots without reference to the previously made direct data plots. Velocity and temperature gradients were determined by graphical differentiation of the residual plots plus analytical differentiation of the reference

expression. The gradients were thus determined by two more or less independent treatments of the data, and satisfactory agreement was obtained in most cases. The gradients thus obtained were plotted as functions of the position in the flow channel, however, little smoothing was done at this point and the plots were mostly used for purposes of inspection and checking.

These gradient plots all had characteristic shapes. As examples, the velocity gradient distributions for tests 39 and 40 are shown in Figures 22 and 23. The temperature gradient distributions for tests 30, 31, 32, 33 and 34 are shown in Figure 24. The temperature gradient distribution for test 40 is shown in Figure 25.

All the quantities in the equations defining the eddy properties are thus directly available from the experimental data and from the known properties of the fluid. The defining equations (Eqs. 8 and 9) may thus be used directly for the calculation of the eddy properties.

An apparent difficulty is encountered near the center line of the stream where both the shear and the velocity gradient become zero. However, inspection of the expression used for the determination of shear (Eq. 13) and of a plot of the velocity gradient as a function of position (e.g., Figures 22 and 23) reveals that both of

these quantities vanish in a regular analytic manner. In addition, of course, the shear and the velocity gradient vanish at the same point. Therefore, at the central axis of the stream, i. e. the point where the shear and the velocity gradient become zero, the eddy viscosity may be determined by the use of the derivatives of these quantities with respect to the position in the traverse:

$$\epsilon_m = \frac{(\partial \tau / \partial y)/\rho}{(\partial^2 u / \partial y^2)} - \nu \qquad \text{(Eq. 18)}$$

The values of the eddy conductivity and the eddy viscosity were calculated at twenty-five points in each traverse. These data were plotted as a function of position in the stream and smoothed with respect to position but not (at this point) cross-plotted and smoothed with respect to any other variable. No attempt was made at this point to eliminate any apparent asymmetry while smoothing. The resulting smoothed values of the eddy properties are reported in Table III.

The eddy property distributions are illustrated by several plots. The eddy conductivity distributions for tests 30, 31, 32, 33 and 34 are shown in Figure 26. The eddy viscosity and eddy conductivity distributions for test 40 are shown in Figure 27 and corresponding eddy property distributions for test 45 are shown in Figure 28. These plots correspond to the data reported in Table III.

It will be noted that the eddy conductivity is, at every point, greater than the eddy viscosity. The two eddy properties appear to vary in a more or less regular manner with position in the stream. The behavior of the eddy properties near the center of the channel is particularly interesting. Both eddy properties decrease somewhat from their maximum values as they approach the center line and they both decrease by approximately the same percentage.

There is some asymmetry in the eddy properties reported in Table III and shown in Figures 27 and 28. In general, this asymmetry appears to affect both eddy properties alike. This asymmetry appears to be actually present in the experimental data and is not the result of erroneous measurement or of erroneous interpretation of the data. The direction and magnitude of this asymmetry appears to be completely random as is illustrated by Figure 29 which presents the eddy viscosity distributions for tests 39 and 40.

The reason for this apparent asymmetry is not clearly understood. However, the actual experimental work during a traverse takes about six hours and some of the flow parameters may drift slightly during this period. Perhaps the most important drift is in the mass flow rate which depends, somewhat, upon the line voltage supply to the blower motor. The mass flow rate is the only im-

portant parameter not controlled by some sort of an automatic control device.

It does not seem likely that any actual asymmetry in the eddy properties exists at any one time. If it were possible to measure the entire temperature and velocity distributions at one instant, it is believed that no asymmetry would be found.

It has seemed desirable to eliminate this asymmetry from the eddy property distributions to obtain more valuable comparison between traverses and to improve any extension of these results to the prediction of eddy property distributions in other streams.

The eddy property distributions have been adjusted to a symmetrical basis about the horizontal axis of the flow channel. In most instances, this has been accomplished by simply averaging the data reported in Table III for points equidistant from the horizontal axis. However, in a few cases, greater weight has been given to the data on one side of the axis, as the result of a review of the record of minor changes in the operating conditions with time. These critically chosen symmetrical values of the eddy properties are reported in Table IV. For the purpose of further analysis of the data, the symmetrical pattern reported in Table IV will be employed.

The distributions of these smoothed and symmetrical

eddy properties are presented in Figures 30, 31, 32 and 33.

Figure 30 presents the eddy viscosities for isothermal flow conditions. The increase in the eddy viscosity with increasing Reynolds number is apparent. The highest magnitude shown in Figure 30 is approximately eighty-three times the magnitude of the corresponding molecular viscosity.

The eddy viscosity and eddy conductivity distributions obtained with nominal plate temperatures of 105°F and 95°F are shown in Figure 31. The data for test 44 have been omitted from this plot as the lack of smoothness of the primary data makes the eddy values quite uncertain.

The eddy conductivity and eddy viscosity distributions obtained with nominal plate temperatures of 115°F and 85°F are shown in Figure 32.

The eddy conductivity distributions obtained with nominal plate temperatures of 130°F and 70°F are shown in Figure 33. As these data were obtained before the perfection of the velocity measuring techniques, point values of the eddy viscosity are not available for these tests.

The Ratio of the Eddy Conductivity to the Eddy Viscosity:

The point values of the ratio of the eddy con-

ductivity to the eddy viscosity have been calculated from the smoothed symmetrical distributions of the eddy properties. These ratios are reported in Table IV along with the corresponding distributions of the eddy properties themselves. The distribution of the ratios for test 40, 41, 45 and 46 are plotted in Figure 34. It will be noted that these curves all exhibit a marked minimum and that the location of this minimum moves towards the wall with increasing Reynolds number.

Figure 35 presents a plot of the ratio of the eddy properties as a function of the dimensionless parameter y^+. The four dotted lines are the experimentally determined distributions. The solid line is a weighted mean of the experimental data. It is suggested that the solid line be used in extending these data to other situations.

Section V

Prediction of the Eddy Conductivity For Other Flow Conditions:

The ultimate purpose of the investigations described in this thesis is to enable the prediction of eddy conductivity distributions for other flow situations. It is of primary interest to investigate the extent to which other authors may have predicted the eddy properties in our stream.

Evaluation of Predictions by Other Authors:

Eddy viscosity distributions may be obtained by the differentiation of any of the analytical velocity distribution expressions. Thus we may assume the applicability of Karman's velocity expressions;

$$u^+ = -3.05 + 5.00 \ln y^+ \qquad \text{(Eq. 19)}$$

for the "buffer layer" between $5 < y^+ < 30$, and

$$u^+ = 5.50 + 2.5 \ln y^+ \qquad \text{(Eq. 20)}$$

for the "turbulent core", $30 < y^+$. These quantities may be differentiated and solved for the velocity gradients. The shear may be calculated from pressure drop measurements or may be assumed from a "friction factor"

generalization. The eddy viscosity distribution may now be obtained from Equation 9.

For the "buffer layer", this procedure leads to the eddy viscosity distribution suggested by Karman (4) and Martinelli (6);

$$\epsilon_m = \frac{u_* y_o}{5.00}\left(\frac{y}{y_o}\right)\left(1 - \frac{2y}{y_o}\right) - \nu \qquad \text{(Eq. 21)}$$

In the case of the "turbulent core" the subtracted term ν is usually ignored, (4), (6). This simplification appears to be justified as it simplifies analytical integration and the eddy viscosity distributions given by these expressions are, at best, approximations. The eddy viscosity distribution expression used by Karman and by Martinelli for the turbulent core is;

$$\epsilon_m = \frac{u_* y_o}{2.50}\left(\frac{y}{y_o}\right)\left(1 - \frac{2y}{y_o}\right) \qquad \text{(Eq. 22)}$$

The eddy viscosity distributions predicted by Equations 21 and 22 have been compared with those obtained by actual measurement. In applying these predictions, the actually measured pressure gradient data were used as the source of the friction velocity terms in the expressions. The comparison between the predicted and measured eddy viscosity distributions in an isothermal stream is shown in Figure 36, representing test 43.

The comparison between the predicted eddy viscosity distribution and the measured eddy viscosity and eddy conductivity distributions for a non-isothermal stream is shown in Figure 37 which presents data for test 40. These plots are quite typical of the relationship found between the experimental and predicted quantities. As shown in these figures, the Karman distribution prediction does fit our data fairly well for approximately two-thirds of the cross section of the channel.

The deviations found between the predicted and measured eddy property distributions are not surprising. Karman's velocity distribution is the result of an attempt to describe with two extremely simple equations a very complex natural phenomenon. These equations seem to have been obtained by plotting, on "semi-logarithmic" paper, the velocity distribution data of a large number of investigators and choosing two straight lines which describe these data rather well. The eddy properties, are, of course, dependent upon the derivatives of the velocity distribution, and a possible severe misfit in the derivative distribution might not be at all obvious in the inspection of the velocity data, per se. This is in keeping with the general principle of applied mathematics that the arbitrary selection of the distribution of a function does not critically determine the distribution of the derivative of the function.

The discontinuity in the predicted eddy property distribution at the outer edge of the buffer layer is a serious deficiency in Equations 21 and 22 as this region is of "controlling" importance in many engineering situations. The extreme misfit near the center of the channel is the most serious deficiency of the eddy property distributions predicted by Karman and by Martinelli. This misfit is of lesser importance when both walls are at the same temperature, and there is no net heat flux across the central axis of flow. However, the Karman distribution does not give any basis for the prediction of the net heat flux when the wall temperatures are not symmetrical with respect to the central axis of the stream.

It has been the purpose of the present writer to obtain values of the ratio of the eddy properties which could perhaps be applied to other engineering situations to predict heat transfer relationships. It has been naively assumed that the eddy viscosity distributions which must necessarily be multiplied by this ratio to obtain eddy conductivity distributions would be available when they were needed. It had been hoped that this ratio might be some sort of a single valued number, which, at least for one fluid, could be applied to a very wide range of conduit configurations and to almost any Reynolds number. The hope that this ratio might be a unique function of the fluid identity has been shared by others and is implied by the term "Turbulent Prandtl Number" which has

been applied to its reciprocal, (17).

Efforts to describe extremely complex phenomena by simple single valued numbers are rarely successful. As was shown in Figure 34, the eddy property ratio for air was found to vary with the Reynolds number and with position in the channel. However, for our channel the ratio of the eddy properties seems to have a single valued distribution when expressed as a function of the dimensionless parameter y^+. The effect of changes in the channel configuration or of changes in the fluid could not be readily investigated with our apparatus.

It was also determined that the popular predictions of the eddy viscosity distribution do not accurately describe the eddy viscosity distributions found in our apparatus.

The eddy viscosity distribution prediction of Karman and of Martinelli is a generalized prediction applicable to all turbulent Reynolds numbers, to a range of conduit shapes and, apparently, to all fluids. The distribution prediction of Karman and of Martinelli is amazingly versatile. In view of the versatility of their prediction, it is believed that their error in the prediction of the eddy viscosity distribution for the outer two-thirds of our stream is perhaps tolerable. It would be interesting to see this prediction checked by the

actual measurement of eddy viscosity distributions in other fluids.

Reduced Eddy Properties:

An examination of the eddy viscosity prediction equation (Equation 22) for the turbulent core reveals that the division of this equation by the product $u^* y_o$ yields:

$$\frac{\epsilon_m}{u^* y_o} = \left(\frac{1}{2.50}\right)\left(\frac{y}{y_o}\right)\left(1 - \frac{2y}{y_o}\right) \qquad \text{(Eq. 23)}$$

The right hand side of this equation is now a universal distribution, applicable to any turbulent Reynolds number and to any fluid. The same distribution law is also applicable to a circular conduit. Expressed in the notation of the circular conduit, we have:

$$\frac{\epsilon_m}{u^* D} = \left(\frac{1}{2.50}\right)\left(\frac{y}{D}\right)\left(1 - \frac{2y}{D}\right) \qquad \text{(Eq. 24)}$$

The dimensionless ratio $\epsilon_m / u^* y_o$ has been called the "reduced eddy viscosity" by the present author and has a companion property, the "reduced eddy conductivity", $\epsilon_c / u^* y_o$. It would be very useful to have some form of the eddy properties which would have the same distribution for all turbulent flow conditions, with all fluids and with a wide range of conduit shapes. The Karman-Martinelli distribution in the turbulent core, if expressed as the reduced eddy viscosity, has this universal

applicability to all fluids and all flow conditions.

The present eddy property data has been further examined by plotting the distributions of the "reduced eddy properties", ϵ_c/u^*y_o and ϵ_m/u^*y_o. It is observed that there is reasonably good agreement between the reduced eddy property distributions determined at any one nominal velocity. This agreement is shown by plotting the reduced eddy properties for each nominal bulk velocity on a separate plot. Figures 38, 39, 40, 41 and 42 present the reduced eddy property distributions determined for nominal velocities of 90, 60, 30, 15 and 10 ft./sec. respectively.

The direct plots of the eddy property distributions (Figures 30, 31, 32 and 33) showed that the eddy properties were greatly increased by an increase in the Reynolds number. (Actually the eddy properties are approximately proportional to the 0.9 power of the Reynolds number in our channel.) This spread is greatly reduced by plotting the reduced eddy properties instead of the direct eddy properties. In addition, at each nominal velocity, the reduced eddy property distributions seem rather closely bunched. At each nominal velocity, a mean value of the distribution of each of the reduced eddy properties may be selected which approximately represents all of the data obtained at or near the Reynolds number represented by this nominal velocity. The distribution of these

averages of the reduced eddy properties for each nominal bulk velocity have been plotted together in Figures 43 and 44.

Examination of Figures 43 and 44 reveals that the portion of the reduced eddy property distribution lying nearest the wall is shifted toward the center of the stream by a decrease in the Reynolds number or a decrease in the nominal bulk velocity. This shift of the residual eddy properties toward the center line of the stream extends much further than the inner edge of the Karman "buffer layer". In plot 45, the mean distributions of the reduced eddy properties for a nominal velocityof 15 ft./sec. are compared with the reference distribution;

$$\frac{\epsilon_m}{u_* y_o} = \left(\frac{1}{2.50}\right)\left(\frac{y}{y_o}\right)\left(1 - \frac{2y}{y_o}\right) \qquad \text{(Eq. 23)}$$

Also included on this plot is the reduced eddy property distribution obtained by rigorous differentiation of the Karman velocity distributions, not neglecting the molecular viscosity term. This distribution is;

$$\frac{\epsilon_m}{u_* y_o} = \left(\frac{1}{5.00}\right)\left(\frac{y}{y_o}\right)\left(1 - \frac{2y}{y_o}\right) - \frac{\nu}{u_* y_o} \qquad \text{(Eq. 25)}$$

for the "buffer layer", $5 < y^+ < 30$; and

$$\frac{\epsilon_m}{u_* y_o} = \left(\frac{1}{2.50}\right)\left(\frac{y}{y_o}\right)\left(1 - \frac{2y}{y_o}\right) - \frac{\nu}{u_* y_o} \qquad \text{(Eq. 26)}$$

for the "turbulent core", $30 < y^+$. It will be noted that the distribution obtained by rigorous differentiation treatment of the Karman velocity distribution improves somewhat upon the simplified reference expression (Equation 23). However, Equations 25 and 26 do not accurately predict the eddy viscosity distribution.

Residual Reduced Eddy Properties:

Examination of Figures 38 through 45 reveals that the eddy properties are approximated, for about two-thirds of the channel, by the very simple expression represented in Equation 23. The deviations from the distribution predicted by this expression are orderly and appear to increase with decreasing Reynolds number. It appears possible that the eddy property distribution behavior may be represented quite simply by a residual plotting technique. The "residual reduced eddy properties" have been defined as the difference between the reduced eddy properties predicted by Equation 23 and those calculated from the data. Thus the "residual reduced eddy viscosity" is defined as:

$$\left(\frac{\epsilon_m}{u_* y_o}\right)_{\sim} = \left(\frac{1}{2.50}\right)\left(\frac{y}{y_o}\right)\left(1 - \frac{2y}{y_o}\right) - \left(\frac{\epsilon_m}{u_* y_o}\right) \quad \text{(Eq. 27)}$$

The "residual reduced eddy conductivity" is defined as:

$$\left(\frac{\epsilon_c}{u_* y_o}\right)_{\sim} = \left(\frac{1}{2.50}\right)\left(\frac{y}{y_o}\right)\left(1 - \frac{2y}{y_o}\right) - \left(\frac{\epsilon_c}{u_* y_o}\right) \quad \text{(Eq. 28)}$$

The residual reduced eddy viscosity distributions determined from our data are shown in Figure 46 and appear to be well enough established to be used for the prediction of eddy viscosities in other situations or engineering interest. The residual reduced eddy conductivity distributions shown in Figure 47 are based on only four tests and are not as well established.

Prediction of the Eddy Properties for Other Situations:

These investigations have been limited to the two-dimensional flow of turbulent air in a channel approximately three-quarters of an inch thick. Any attempt to use these results as the basis for the prediction of eddy properties for the flow of other fluids in channels of other geometry is certainly presumptive. However, there are many engineering situations for which the results of this study may be more useful than any previously published procedure for the prediction of the heat transfer relationships.

Examination of Figures 34 and 35 indicates that a single number might be selected as an approximately mean value of the ratio of the eddy conductivity to the eddy viscosity. However, it seems preferable to use the distribution of the point values of this ratio which is predicted by Figure 35. If the eddy viscosity distribution were separately known, the eddy conductivity distribution could be obtained by simple multiplication. This procedure would permit the prediction of heat flux and of temperature fields in situations similiar to our channel with a greater accuracy than has been previously possible.

It is believed that the distribution of the ratio of the eddy properties predicted by Figure 35 may probably be applied without great error to the flow of air in a circular conduit as well as the flow in a two-dimensional channel. It seems probable that this distribution is also applicable to other fluids with Prandtl numbers similiar to that of air; e. g. any of the common gases.

The prediction of eddy viscosity in engineering situations is likely to introduce a greater error than that introduced by the multiplication of this prediction by an assumed ratio of the eddy properties. The rigorous application of Equations 25 and 26 will give better results than are obtained by ignoring the molecular

viscosity in the turbulent core. However, any analytical expression based upon the differentiation of a logarithmic velocity distribution law will predict a zero value for the eddy viscosity at the center of the flow stream. In addition to the error of the zero value prediction, the Karman-Martinelli distributions (Equations 21 and 22) predict too high a value in the region where y/y_o is approximately 0.25.

In the absence of more conclusive data, the eddy viscosity distributions for other engineering situations may be predicted using the residual reduced eddy viscosity plots shown in Figure 46. The effect of a change in the channel thickness or in the channel shape or in the identity of the fluid upon the residual reduced eddy viscosity distribution has, of course, not been investigated. The distribution shown in Figure 46 may be greatly changed by any change in these variables. However, it is believed that the use of this imperfect plot is preferable to ignoring the residual correction altogether. For other fluids, for other channel widths, and for other channel shapes, the choice of residual curve may be quite difficult. Tentatively it is suggested that the value of the parameter, u^*y_o/ν, be estimated and that this parameter be used as the basis for the selection of the proper curve in Figure 46.

The procedure tentatively suggested for the

estimation of the eddy conductivity for situations of engineering interest is:

1. Determine the shear either by a direct measurement of the pressure gradient or by estimation using a friction factor plot. Calculate u^*, u^*y_o and u^*y_o/ν. (For a circular conduit, u^*, u^*D and u^*D/ν should replace these quantities.)

2. Determine the distribution of the reduced residual eddy viscosity from Figure 46. Use a line labeled with approximately the same value of u^*y_o/ν or interpolate between two such lines. Determine this distribution in the region $0 < y/y_o < 0.4$.

3. Determine the distribution of the reduced eddy viscosity in the region $0 < y/y_o < 0.4$ by pointwise application of the appropriate one of the following formulas:

$$\left(\frac{\epsilon_m}{u^* y_o}\right) = \frac{1}{2.50}\left(\frac{y}{y_o}\right)\left(1-\frac{2y}{y_o}\right) - \left(\frac{\epsilon_m}{u^* y_o}\right)_{\sim} \quad \text{(Eq. 29a)}$$

$$\left(\frac{\epsilon_m}{u^* D}\right) = \frac{1}{2.50}\left(\frac{y}{D}\right)\left(1-\frac{2y}{D}\right) - \left(\frac{\epsilon_m}{u^* D}\right)_{\sim} \quad \text{(Eq. 29b)}$$

4. Calculate the distribution of the eddy viscosity by the solution of the distribution deter-

mined in Step 3. Assume that the value of the eddy viscosity obtained at $y/y_o = 0.4$ is also applicable between $0.4 < y/y_o < 0.5$.

5. Determine distribution of the ratio of the eddy properties from Figure 35.

6. Determine the eddy conductivity distribution by multiplying the results obtained in Steps 4 and 5 above.

Section VI

Velocity Measurement Techniques:

Description of the Thermanemometer:

The point temperatures and the point velocities reported in this thesis were measured with a fine platinum wire which, because of its dual usage, has been called a "thermanemometer". The physical appearance of this instrument is shown in Figure 48. A 0.0005" diameter pure platinum wire three-eighths of an inch long is mounted under slight tension between platinum extensions at the ends of the two steel needles. The platinum needle extensions are approximately 0.010" in diameter. The wire is mounted between the tops of the needle extensions, allowing the center line of the wire to approach within approximately 0.002" of the upper wall.

The needle mountings are adjustable in every direction so as to enable the alignment of the wire exactly parallel to the copper plates and exactly perpendicular to the flow of the air. These adjustments also place a slight tension in the wire to prevent its deflection due to the drag of the air stream.

The temperature measurements were performed using the thermanemometer wire as the sensing element of a four lead resistance thermometer. The use of the Mueller (18)

technique with a "Leeds and Northrup Precision Mueller Bridge" presumably cancelled out all of the lead resistance effects. Platinum leads were carried from the sensing element to an insulated junction box outside the channel, minimizing possible errors due to thermoelectric effects.

For velocity measurements, the "constant resistance" (19) technique was used. The constant resistance technique is particularly suited to the measurement of time-average velocities rather than of instantaneous velocities. In addition, the wide range of velocities measured appears to make the use of the "constant current" technique impractical.

In the constant resistance anemometric technique the sensing element is made, in effect, one leg of a Wheatstone bridge. The other legs of the bridge are set so as to balance the bridge at some previously chosen anemometer resistance. In the work described in this thesis the anemometer resistance was usually chosen so as to yield a wire temperature of 250°F.

The other bridge elements are all made of Manganin wire and their resistances remain approximately constant once they are set. The actual resistance of the anemometric sensing element was checked as part of each measurement.

The circuit used in the anemometric measurements is shown in Figure 49. The variable resistors R1 and R2 are actually complex resistor networks allowing precise setting of their effective values. They are adequately represented on a schematic diagram by a single variable resistor of the same effective value. Resistor R1 is adjusted to obtain the desired balance-point-resistance in the thermanemometer sensing element. R3 and R4 are carefully made fixed-value Manganin resistors.

When a velocity measurement is being made switch S1 is closed in the "down" position. The bridge is then balanced by adjusting the total current with resistor R2. This causes the wire to obtain the previously selected operating resistance and temperature. The current in the wire is determined by measuring the potential across the "shunt" resistor, R5. The potential across the thermanemometer itself is also measured at the E_{hw} terminals allowing calculation of the thermanemometer resistance.

When temperatures are being measured, switch S1 is "up", connecting the thermanemometer to the Mueller bridge. An "exercise" resistor, R6, replaces the thermanemometer in the bridge circuit, maintaining an approximately constant battery load and eliminating difficulties otherwise introduced by drifting battery polarization.

Resistors R7 and R8 allow selection of the galvanometer sensitivity. Resistor R9 provides approximately critical damping at all sensitivity selections. Resistors R8 and R9 are made of copper to eliminate possible thermoelectric effects in the galvanometer circuit. The galvanometer has a time constant many times the turbulent fluctuation period and is critically damped. Thus the anemometer indicates time-average velocities rather than instantaneous velocities.

Choice of Velocity Measuring Instrument:

The use of a platinum wire as the velocity-sensing element allows the measurement of temperature with the same element. This has the advantage that the velocity and temperature are measured at the same location. As a result derived eddy viscosity and eddy conductivity data are calculated at the same point and valid point values of their ratio may be obtained. If velocity and temperature were sensed with two different elements, any displacement error would significantly affect the calculated eddy-property-ratios in the region where the change of these properties with position is very rapid. As this region is of "controlling" importance in many heat transfer situations, such a displacement error is not tolerable.

Perhaps the outstanding advantage of the hot wire anemometry method in studies such as those reported in

this thesis is the retention of precision at low velocities. This is in marked contrast with the pitot tube which loses its precision at these same low velocities. This contrast is indicated clearly in Figures 50 and 51, which show the absolute precision and the percentage precision of the hot wire anemometer and of the pitot tube at low velocities.

In the construction of Figures 50 and 51, it was assumed that the pitot tube precision was limited by a possible error of one thousandth of an inch (of kerosene) in the micromanometer measurement. The hot-wire anemometry precision was presumed to be limited by a possible error of one microvolt in the measurement of the potential across the "shunt" resistor, R5, (Figure 49).

The hot wire anemometer is sensitive to the velocity of the air flowing around it. When used in the region of a high velocity gradient, it certainly must indicate some sort of an "average" of the velocities within the region which it senses. If it is near a wall of the channel, the wire itself must distort the gas flow and thereby change the velocity pattern. The hot wire data are assumed to represent the velocity of the undisturbed stream at the same point as that occupied by the wire at the time of the measurement. The uncertainty due to this assumption is believed to be much less than the corresponding uncertainty introduced by similiar use of a

pitot tube of any practical diameter.

The hot wire procedure is dependent upon the temperature of the air stream at the point where the measurement is made. In the case of many of the measurements reported in this thesis, temperature gradients were present. To minimize the effect of these gradients, the operating temperature of the hot wire was made as high as seemed practical.

In the case of several of the traverses, it was possible to determine the velocity gradient in the laminar layer from the hot wire data. This gradient was compared with the laminar layer velocity gradient calculated from the shear measurements. In each case the velocity gradients determined from the hot wire data was in approximate agreement with that calculated from the shear data. This agreement which is reported in more detail in the thesis of fellow student, Stuart D. Cavers, (12), is considered to indicate that the hot wire techniques employed in this work are valid in regions of high temperature gradients and high velocity gradients.

Calibration Procedure:

When the hot wire is being calibrated as an anemometer, the tilt mechanism is adjusted until the pitot tube is level and the anemometer and pitot tube are both

at the center of the stream. As all velocity derivatives are zero at the center of the stream, any possible error due to misalignment is minimized. The pitot tube is connected to one side of the micromanometer and a static-pressure-reading "piezo tube" is connected to the other side of the micromanometer.

The "piezo tube" is not shown in Figure 48 but is very similiar in appearance to the pitot tube which is shown there. When the "piezo tube" was constructed, it was carefully checked by comparison with one of the piezometer bars. It was "traversed" to all locations in line with this piezometer bar while air was flowing through the apparatus at a nominal velocity of 30 ft./sec. The pressure indicated by the "piezo tube" agreed with the pressure indicated by the piezometer bar within one thousandth of an inch of kerosene at all points in the channel. This not only proved the "piezo tube" design to be satisfactory, but also demonstrated the absence of pressure gradients in any other direction than the downstream direction.

Before and after each traverse, the thermanemometer is calibrated by adjusting the air flow to obtain several different velocities. The velocity is determined with the pitot tube using the kerosene-filled micromanometer shown in Figure 7. The hot wire current and potential are measured at the same time. For analysis of the hot

wire data, we have defined a quantity, Φ, as;

$$\Phi = \frac{i^2}{R_{h.w.} - R_a} \qquad \text{(Eq. 30)}$$

The numerator of Φ is proportional to the power expended in the hot wire when it operates at a constant resistance. The denominator of Φ is proportional to the difference in temperature between the hot wire and the ambient air. King (20) predicted a linear relationship between Φ and $\sqrt{u}$.

The calibration data on a freshly cleaned hot wire is presented in Figure 52. The radius of the circles approximately indicates the uncertainty due to a possible error of one thousandth of an inch in the micromanometer reading. It will be noted that the calibration line in Figure 52 shows a slight curvature. This curvature is typical of all the calibration data from the heat transfer apparatus and its existence has been quite well established.

Because of the pitot tube uncertainties at low velocities, it is impossible to obtain a calibration point at a laminar-flow velocity. However, a calibration point at zero velocity is available. As shown in Figure 52 the zero velocity point is in satisfactory agreement with an extrapolation of the higher velocity calibration data.

In the normal operation of the hot wire anemometer, calibrations are made at or near several standard velocities. At least three calibration points are obtained before and after each traverse. As a given hot wire may be used for several traverses between cleanings, the resulting statistical treatment of the pitot tube data improves considerably upon a one-point calibration. The values of the function Φ for each of these calibration points is adjusted (if necessary) to a standard velocity and then plotted as a function of time. This is done for at least three standard velocities. Such a plot is shown in Figure 53.

As indicated in Figure 53 the Φ associated with any given velocity changes slowly with time. This "drift" was found to be due to the collection of dirt on the wire. Removal of the dirt approximately restores the original calibration. Mechanical removal of the dirt was not practical because of the fragility of the fine platinum wire. The wire was cleaned periodically by heating electrically to a temperature between 600 and 1000°F. When this cleaning procedure was observed through a microscope, the dirt could be seen to char and to spall-off from the wire. This heating sometimes resulted in a slight change in the thermometric calibration and thus could not be applied during a traverse but only when it was practical to repeat the thermometric calibration.

A cross-plot of the several plots of $\oint$ versus the apparatus operating time may be constructed to represent any desired instant. Figure 54 is an example of such a cross-plot of $\oint$ versus $\sqrt{u}$. It indicates the instantaneous calibration of the hot-wire anemometer and could be used for the conversion of thermanemometer data to the corresponding velocities. However, the use of an instantaneous cross-plot such as Figure 54 for the treatment of hot-wire data would require the construction of such an individual cross-plot for the time represented by such hot-wire reading.

A procedure has been developed which simplifies the treatment of the data. This procedure represents merely the application of conventional "graphic-arts" methods for the treatment of data and is not described in detail in this thesis. Briefly the calibration data are approximated by a straight line through the calibration points at two of the standard calibration velocities. The slope and intercept for this line are plotted as functions of time and these plots are used in the treatment of the traverse data. A small residual correction is made for the curvature of the calibration line.

References

1. Reynolds, Osborne, Proc. Lit. & Phil. Soc. of Manchester, 14, 7-12 (1874). (Reprinted in Reynolds, Osborne, "Papers on Mechanical Subjects", Cambridge, 1900.

2. Prandtl, L., Physikalische Zeitshrift, 29, 487-489 (1928).

3. Taylor, G. I., Proc. Royal Soc. London, A135, 685-701, (1932).

4. von Karman, Th., Trans. Am. Soc. Mech. Engrs., 61, 705-710, (1939).

5. Boelter, L. M. K., Martinelli, R. C., and Jonassen, F., Trans. Am. Soc. Mech. Engrs., 63, 447-455, (1941).

6. Martinelli, R. C., Trans. Am. Soc. Mech. Engrs., 69, 947-959, (1947).

7. Jenkins, R., Brough, H. W., Sage, B. H., "Calculation of Temperature Distribution in Turbulent Flow", California Institute Chem. Eng. Dept. Manuscript No. 293.*

8. Corcoran, W. H., Ph. D. Thesis, California Institute, (1948).

9. Billman, Glenn W., Ph. D. Thesis, California Institute, (1948).

10. Mason, David M., Ph. D. Thesis, California Institute, (1949).

11. Corcoran, W. H., Page, F. Jr., and Sage, B. H., "Temperature Gradients in Turbulent Gas Streams, Methods and Apparatus", California Institute, Chem. Eng. Dept. Manuscript No. 292.*

12. Cavers, S. D., Ph. D. Thesis, California Institute, (1950).

13. Page, F. Jr., Corcoran, W. H., and Sage, B. H., "Temperature Gradients in Turbulent Gas Streams, Temperature and Velocity Distributions in Uniform Flow", California Institute, Chem. Eng. Dept., Manuscript No. 5006. *

---

* California Institute Chemical Engineering Department Manuscripts Nos. 292, 293 and 5006 have been submitted to Industrial and Engineering Chemistry for publication.

14. von Karman, Th., Journal of the Aeronautical Sciences, 1, No. 1, 1-20, (1934).

15. Rouse, H., "Elementary Mechanics of Fluids", John Wiley & Sons, p. 154, (1946).

16. Lewis, G. N., & Randall, M., "Thermodynamics & The Free Energy of Chemical Substances", p. 226, Mc Graw-Hill, (1923).

17. Corrsin, S., & Uberoi, S., N.A.C.A., Tech. Note No. 1865.

18. American Institute of Physics, "Temperature, Its Measurement and Control", Reinhold, pp. 162-179, (1941).

19. Willis, J. B., "Review of Hot Wire Anemometry", Australian Council for Aeronautics Report No. ACA - 19 (Oct.1945).

20. King, L. V., Phil. Trans. Royal Soc. London, A214, 373-432 (1914).

Nomenclature

English Letter Symbols:

c_p	Specific heat at constant pressure, BTU/lb.°F.
d	Differential operator.
E_{hw}	Time-average potential across the thermanemometer element, volts.
f	Fanning friction factor, defined by Equation 4, p 13, dimensionless.
i	Time-average current, thermanemometer element, amps.
k	Thermal conductivity (of fluid in channel), BTU/ft.sec. °F.
P	Piezometric pressure at the traversing point, lbs./ft.^{2}
Q^o	Heat flux density, BTU/ft.^{2} sec.
R_a	Thermanemometer resistance at the point temperature of the air stream, ohms.
R_{hw}	Thermanemometer resistance as determined when measuring velocity, ohms.
Re	Reynolds number, defined by Equation 2, p 13, dimensionless.
t	Temperature, °F.
$t_{ref.}$	Reference temperature, °F.
$t_\sim$	Residual temperature, °F.
u	Point velocity, ft./sec.
$u_{max.}$	Maximum point velocity for a given traverse, ft./sec.
$u_{ref.}$	Reference velocity, ft./sec.
$u_\sim$	Residual velocity, ft./sec.
u*	"Friction velocity", defined by Equation 3, p 13, ft./sec.

Nomenclature, cont'd.

u^+	u/u*, dimensionless.
U	Bulk velocity, defined by Equation 1, p 13, ft./sec.
x	Distance in downstream direction, ft.
y	Distance from the lower plate, ft.
y_o	Distance between upper and lower plates, ft.
y^+	yu^*/ν, dimensionless.

Greek Letter Symbols:

ϵ_c	Eddy conductivity, defined by Equation 8, p 21, $ft.^2/sec.$
ϵ_m	Eddy viscosity, defined by Equation 9, p 21, $ft.^2/sec.$
η	Absolute viscosity, $lb.sec./ft.^2$
K	Thermometric conductivity, $ft.^2/sec.$
ν	Kinematic viscosity, $ft.^2/sec.$
ρ	Specific mass, $lb.sec.^2/ft.^4$
σ	Specific weight, $lb./ft.^3$
τ	Shear stress at any point, $lb./ft.^2$
Φ	Thermanemometer calibration function, defined by Equation 30, p 53, $amps^2/ohm.$

Important Combinations:

y/y_o	Fractional distance from the lower wall, dimensionless.
dP/dx	Pressure gradient in the downstream direction, $lb./ft.^3$

Nomenclature, cont'd.

$\left(\frac{\epsilon_e}{u_* y_o}\right)$ Reduced eddy conductivity, dimensionless.

$\left(\frac{\epsilon_m}{u_* y_o}\right)$ Reduced eddy viscosity, dimensionless.

$\left(\frac{\epsilon_m}{u_* D}\right)$ Reduced eddy viscosity in a circular conduit, dimensionless.

$\left(\frac{\epsilon_m}{u_* y_o}\right)_{\sim}$ Residual reduced eddy viscosity, defined by Equation 27, p 41, dimensionless.

$\left(\frac{\epsilon_m}{u_* D}\right)_{\sim}$ Residual reduced eddy viscosity in a circular conduit, dimensionless.

$\left(\frac{\epsilon_c}{u_* y_o}\right)_{\sim}$ Residual reduced eddy conductivity, defined by Equation 28, p 41, dimensionless.

List of Figures

List of Figures, cont'd.

List of Figures, cont'd.

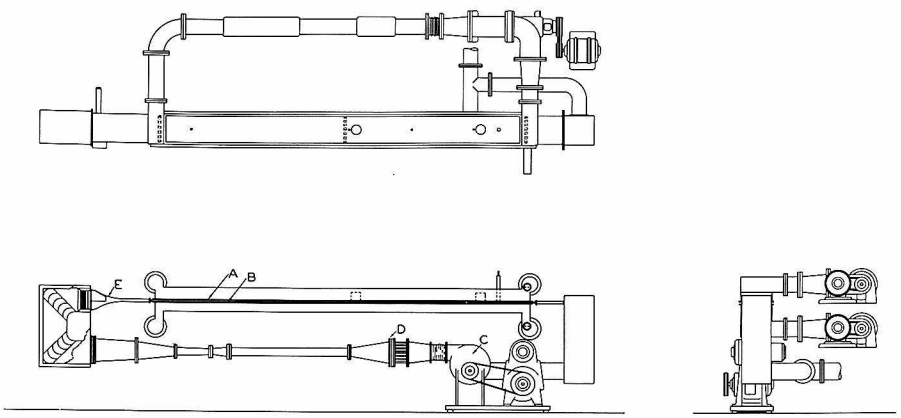

Figure 1

General Arrangement of Equipment

Legend: A. Upper Copper Plate

B. Lower Copper Plate

C. Blower

D. Air Heater

E. Converging Section

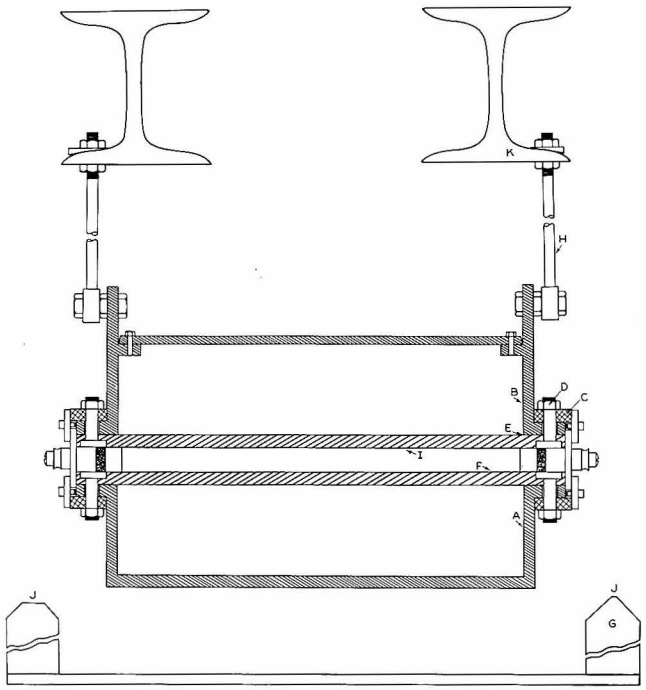

Figure 2

Sectional View of Flow Channel

Legend:

A & B.	Oil Baths.
C, D & E.	Oil Bath Seal and Channel Closure (See Reference 11 for detailed description.)
H & K.	Supports for upper oil bath and upper plate.
J & G.	Ways for traversing gear.

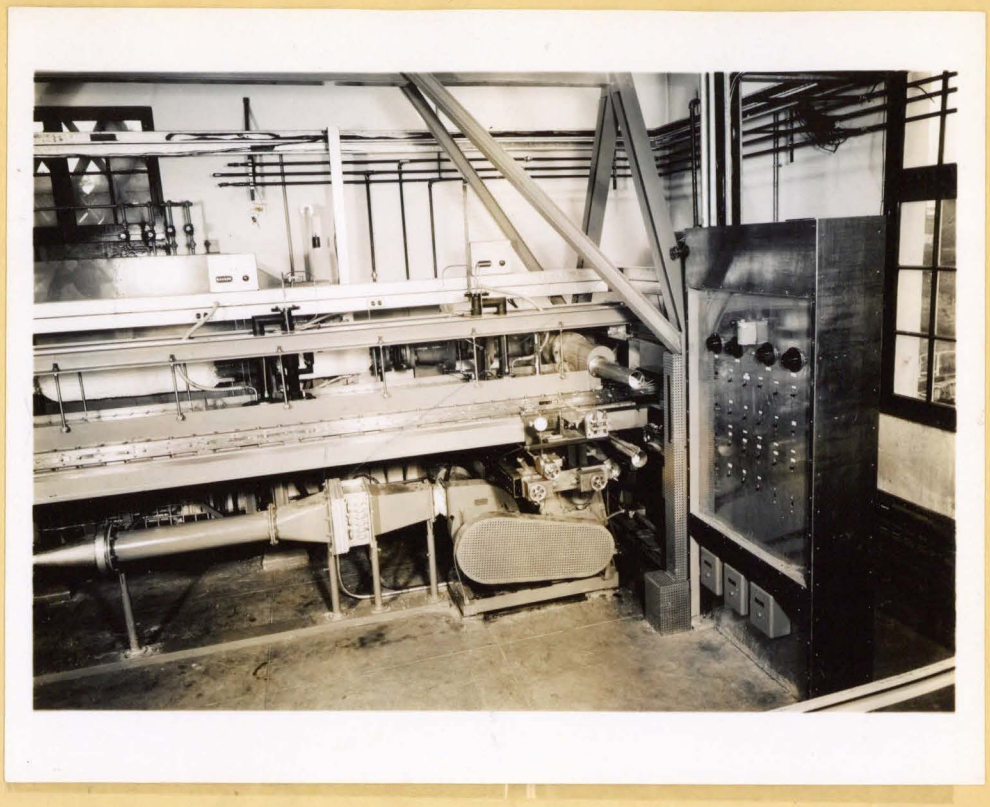

Figure 3

Downstream End of the Apparatus

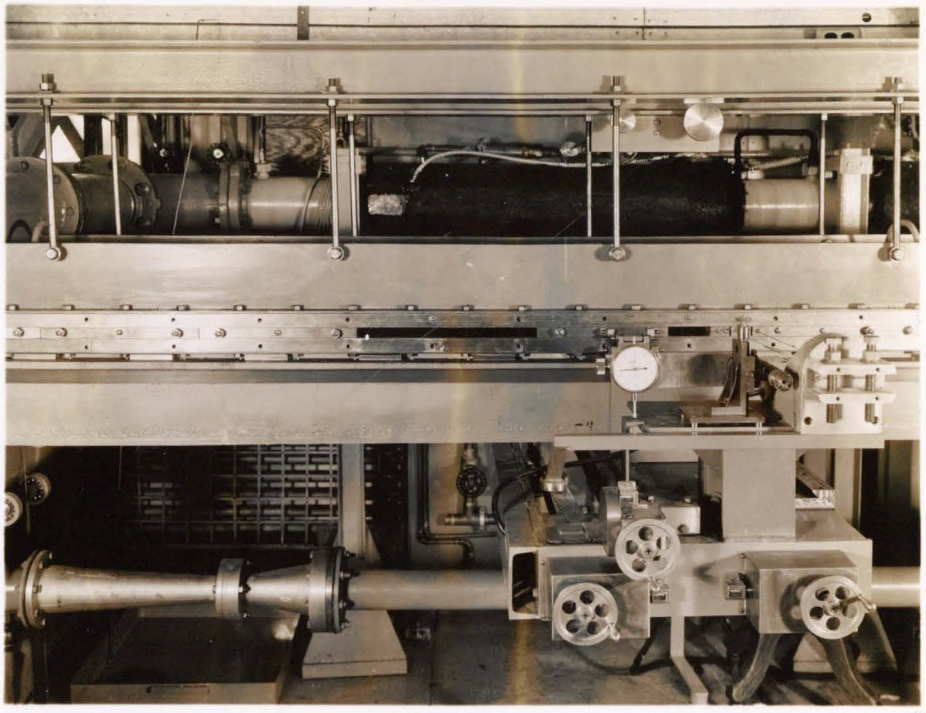

Figure 4

View of the Working Section and The Traversing Gear.

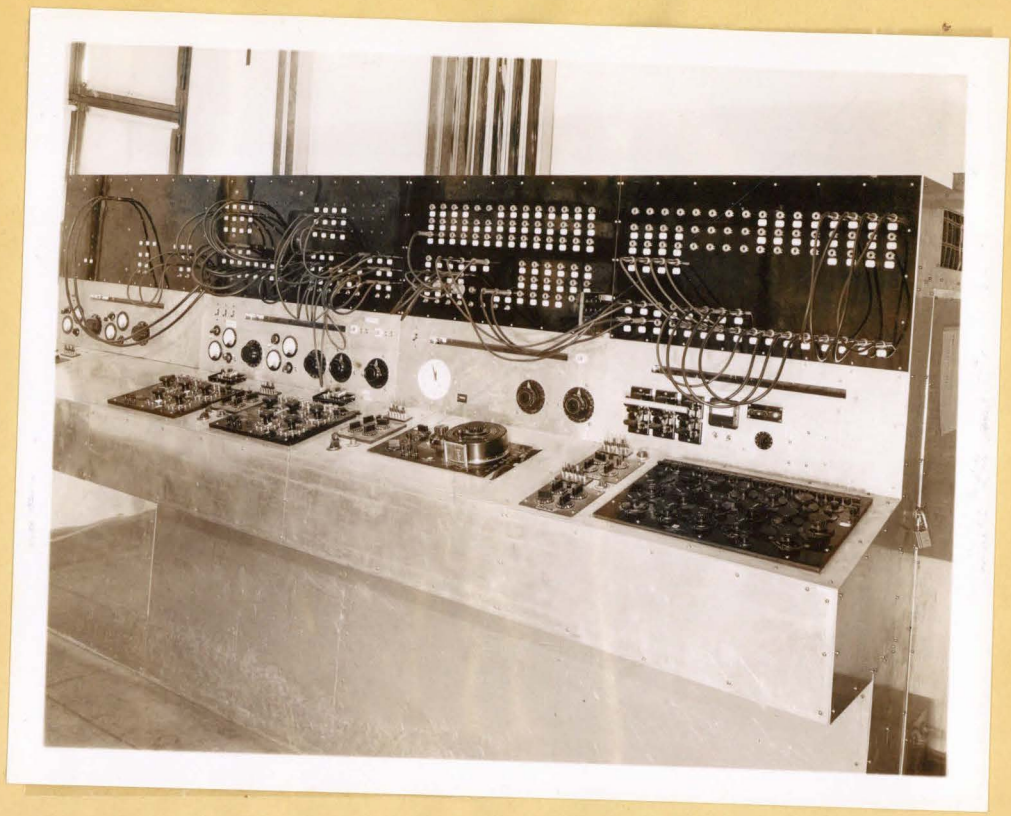

Figure 5

The "Temperature Bench", Centralized Location for all Electrical Measurements.

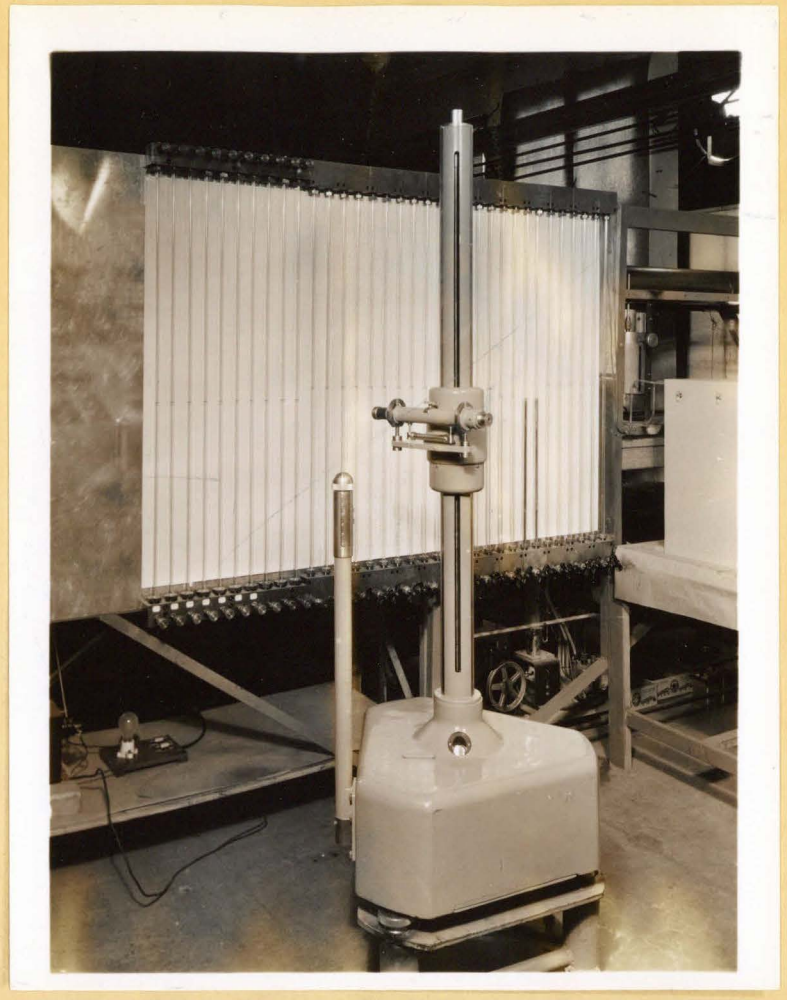

Figure 6

Manometer Bank and Cathetometer

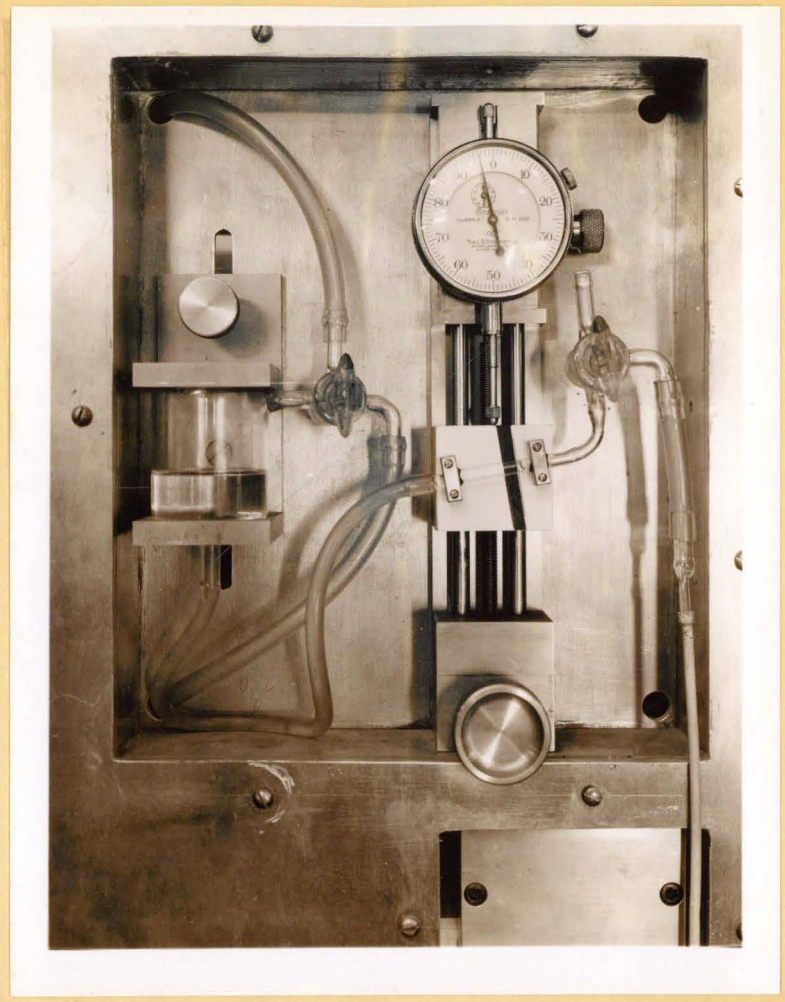

Figure 7

Micromanometer used with pitot tube measurements

Figure 8

Heat Flux Calorimeter

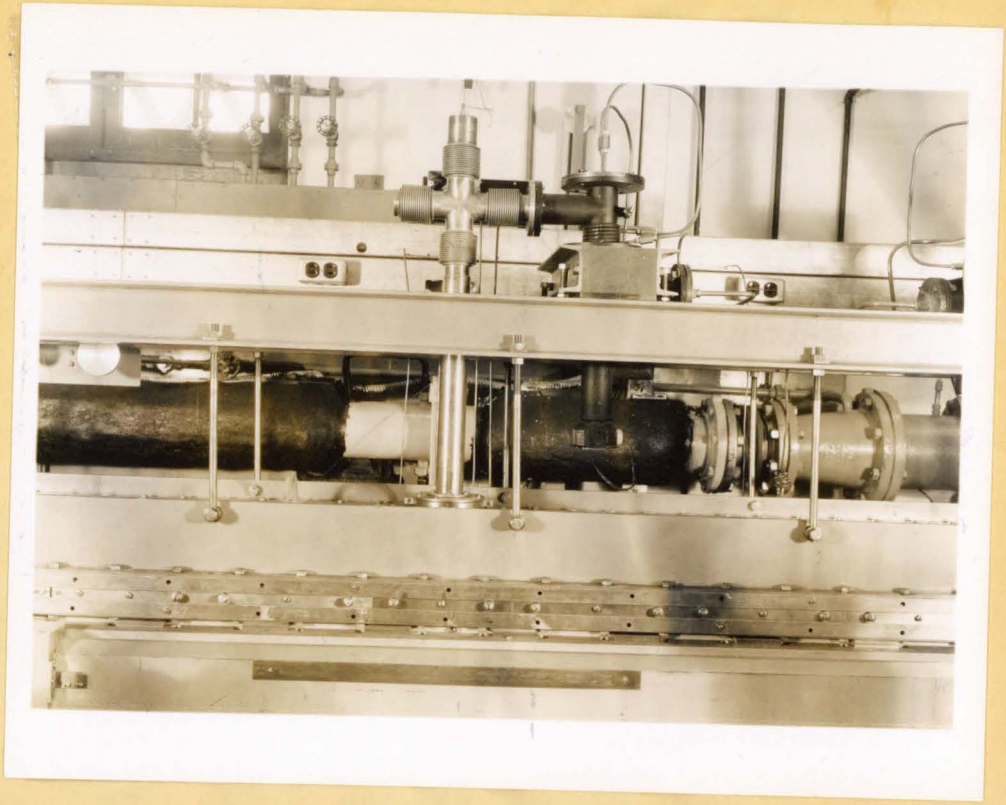

Figure 9

Heat Flux Calorimeter mounted in Apparatus.

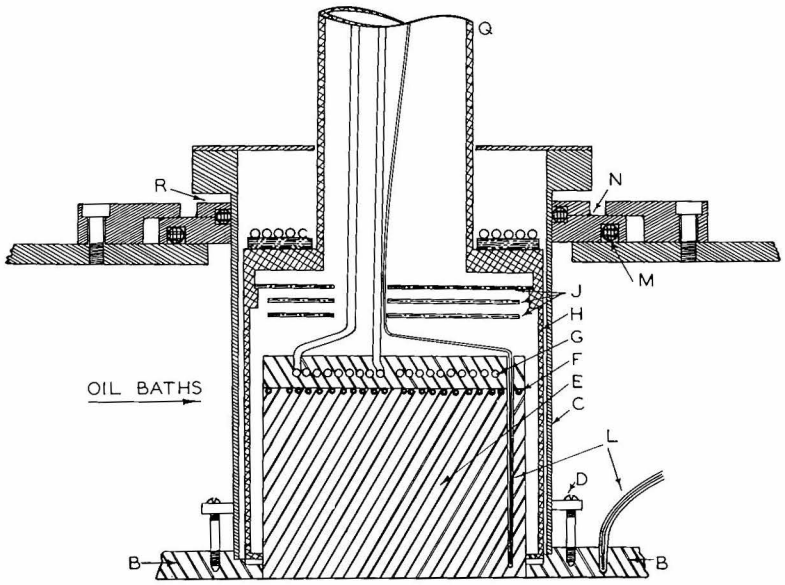

Figure 10

Sectional View of Heat Flux Calorimeters

Legend: B. Upper Copper Plate.

C & D. Oil Bath Dam and mounting.

E. Calorimeter Block.

F. Pancake heater.

G. Cooling Coil, (not used in studies reported in this thesis.)

H.& Q. Vacuum Jacket.

J. Radiation Shields.

L. Differential Thermocouples.

M, N & R. Oil Bath Dam Seals.

Nominal Plate Temperatures °F	Nominal Bulk Velocities ft./sec.					
	90	60	30	15	10	7.5
Upper Plate 130 Lower Plate 70	Test 33	Test 32	Test 31	Test 30		Test 34
Upper Plate 115 Lower Plate 85				Test 46		
Upper Plate 105 Lower Plate 95	Test 44	Test 41	Test 40	Test 45		
Upper Plate 100 Lower Plate 100	Test 43	Test 50	Test 39 Test 37	Test 48	Test 49	

Figure 11

Index to Nominal Experimental Conditions

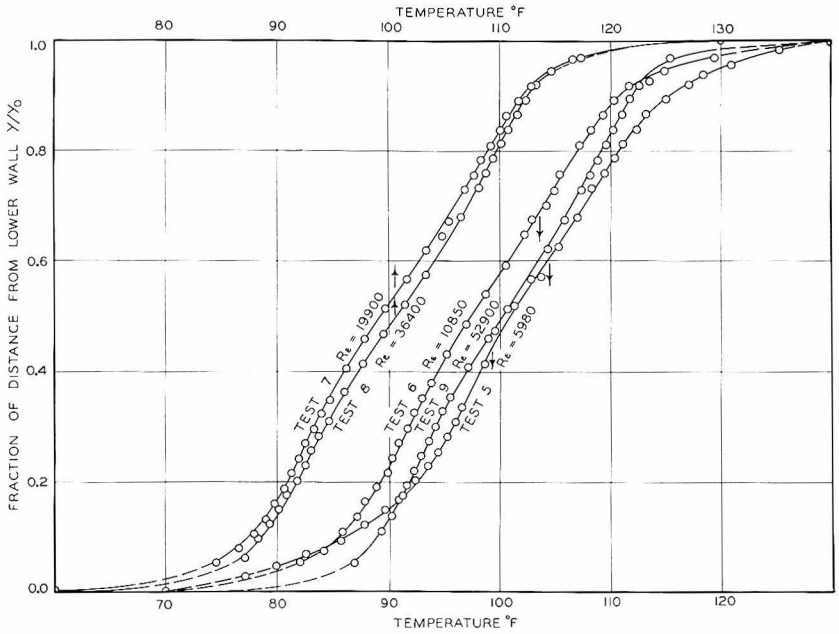

Figure 12

Temperature Distributions,
Tests 30, 31, 32, 33 & 34

Legend:

Test 30 is indicated as test 6 in this figure.

Test 31 is indicated as test 7 in this figure.

Test 32 is indicated as test 8 in this figure.

Test 33 is indicated as test 9 in this figure.

Test 34 is indicated as test 5 in this figure.

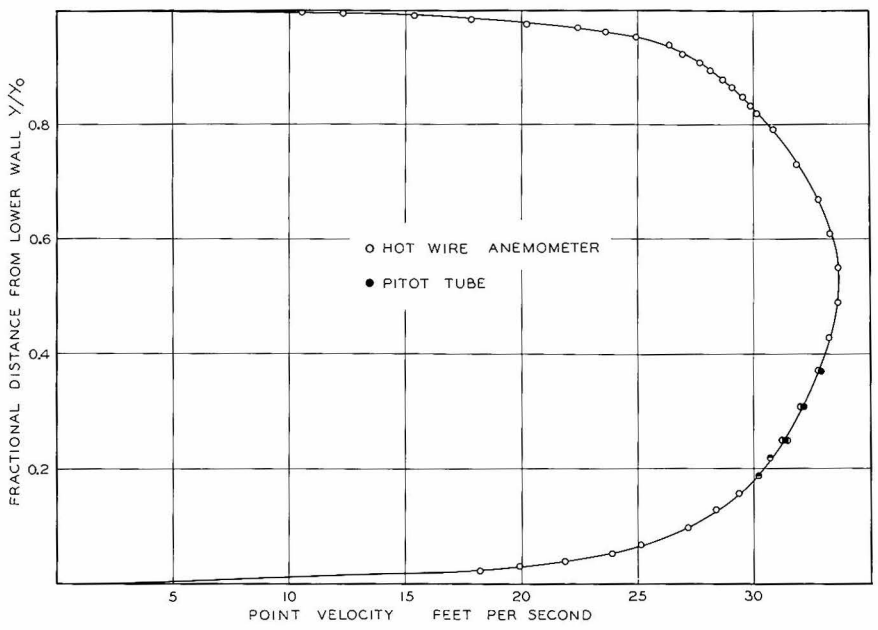

Figure 13

Velocity Distribution, Test 39

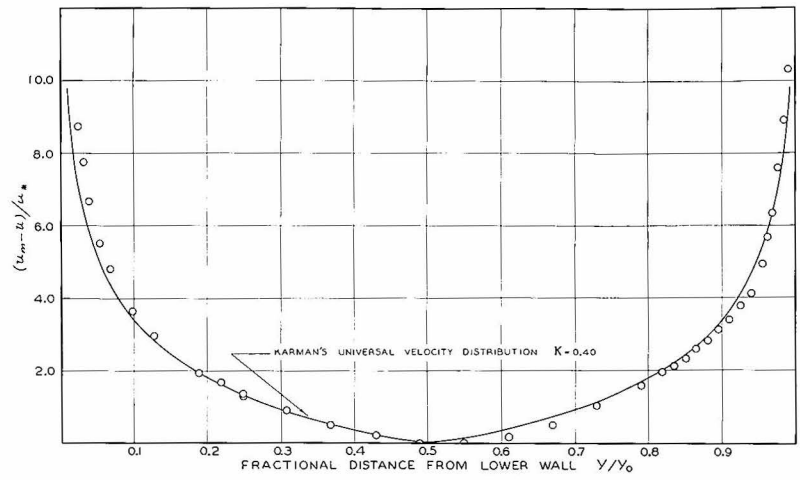

Figure 14

Distribution of the Ratio of the Velocity Deficiency to the Friction Velocity, Test 20.

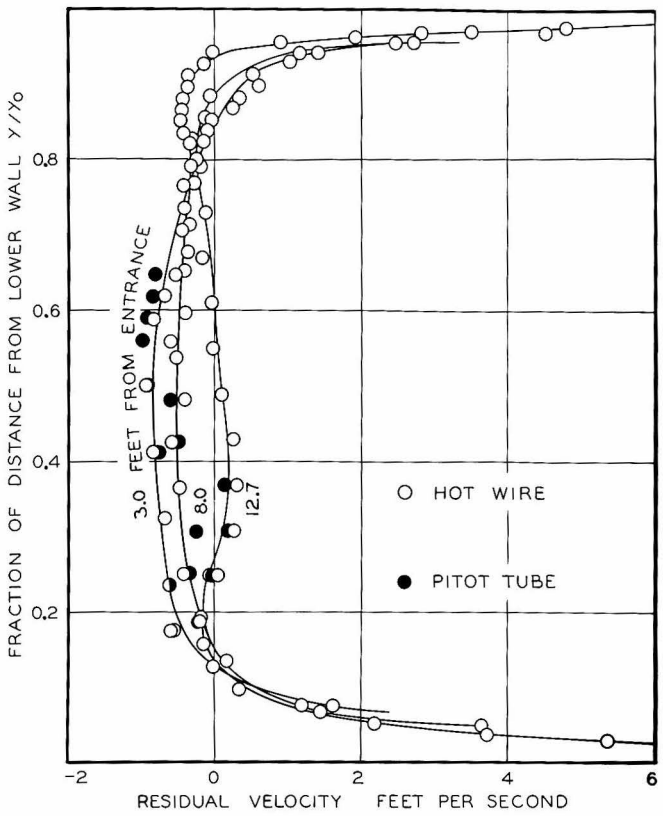

Figure 15

Residual Velocity Profiles,
Tests 37, 37,1 & 39.

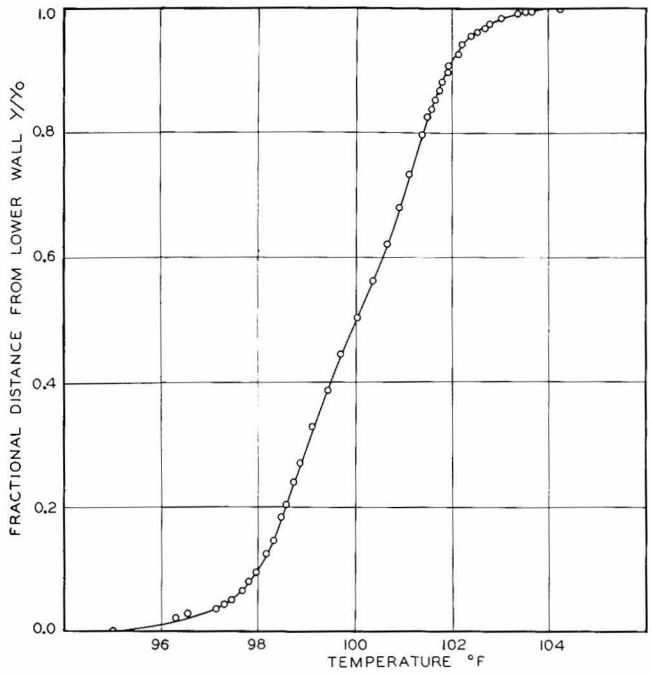

Figure 16

Temperature Distribution,
Test 40

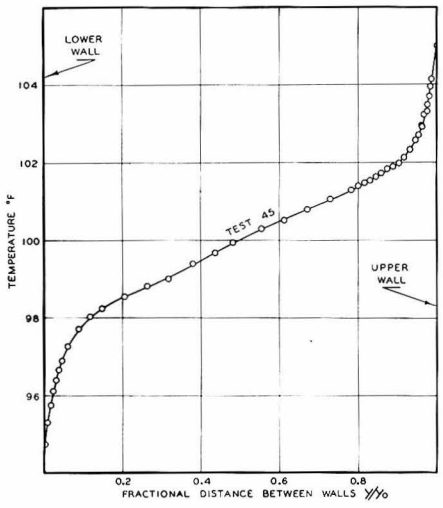

Figure 17

Temperature Distribution,
Test 45

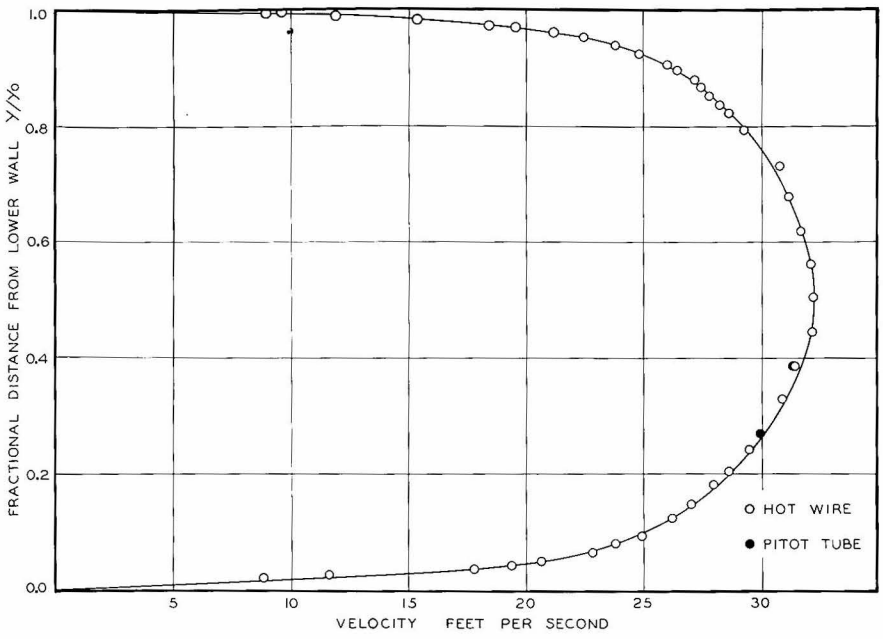

Figure 18

Velocity Distribution, Test 40

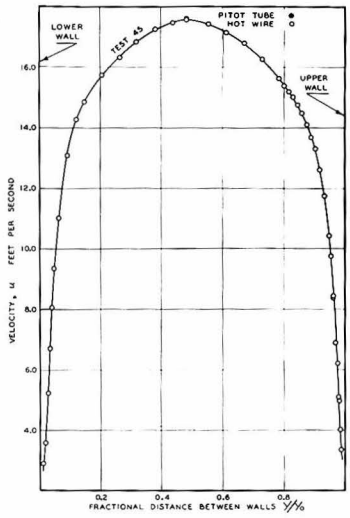

Figure 19

Velocity Distribution, Test 45

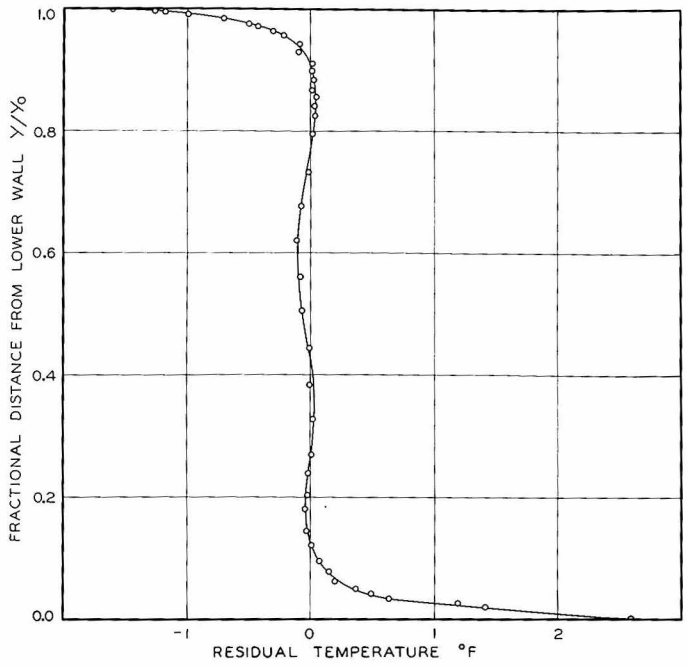

Figure 20

Residual Temperature Distribution, Test 40

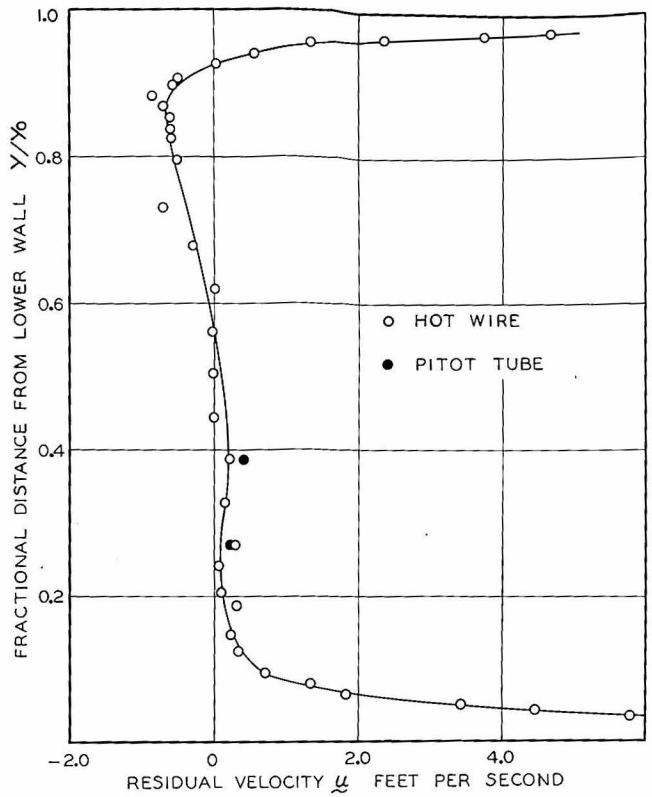

Figure 21

Residual Velocity Distribution,
Test 40

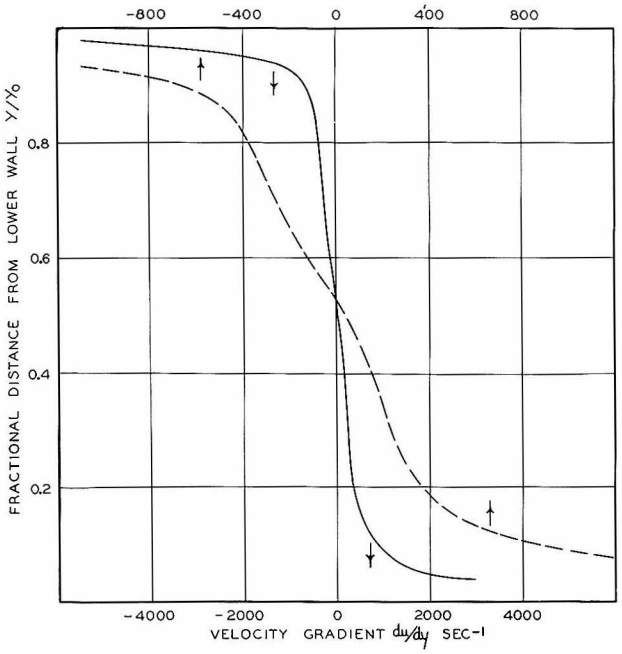

Figure 22

Velocity Gradient Distribution, Test 39

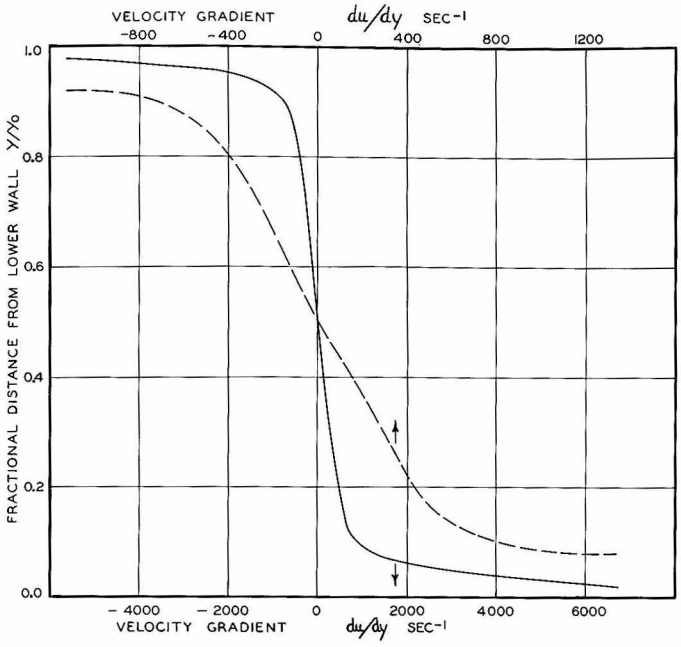

Figure 23

Velocity Gradient Distribution, Test 40

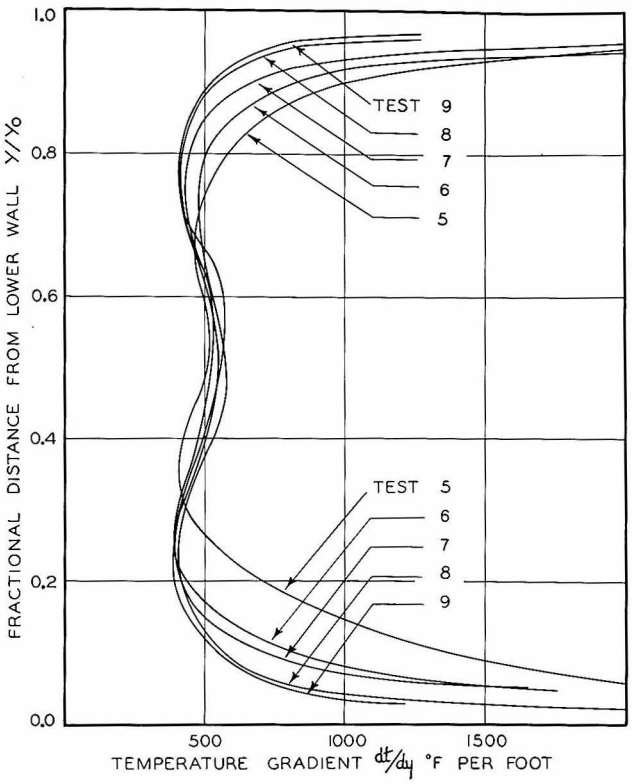

Figure 24

Temperature Gradient Distributions

Tests 30, 31, 32, 33 & 34

Legend:

Test 30 is indicated as test 6 in this figure.

Test 31 is indicated as test 7 in this figure.

Test 32 is indicated as test 8 in this figure.

Test 33 is indicated as test 9 in this figure.

Test 34 is indicated as test 5 in this figure.

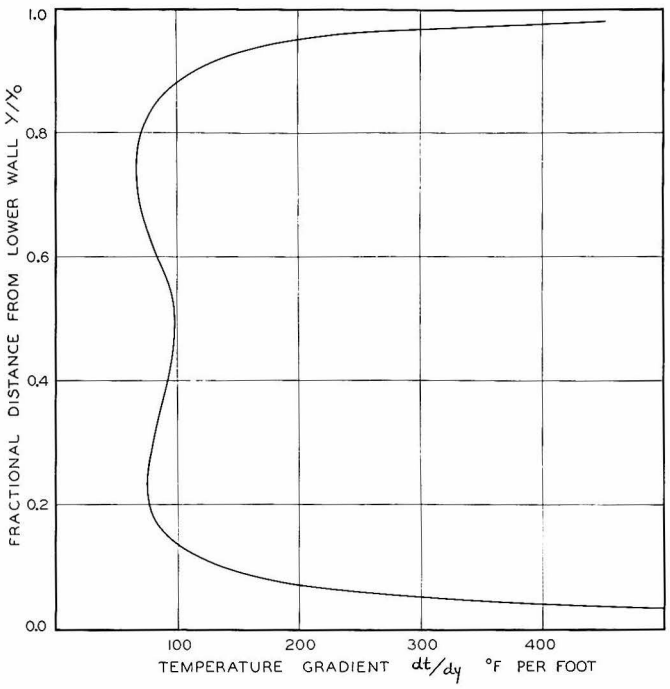

Figure 25

Temperature Gradient Distribution,
Test 40

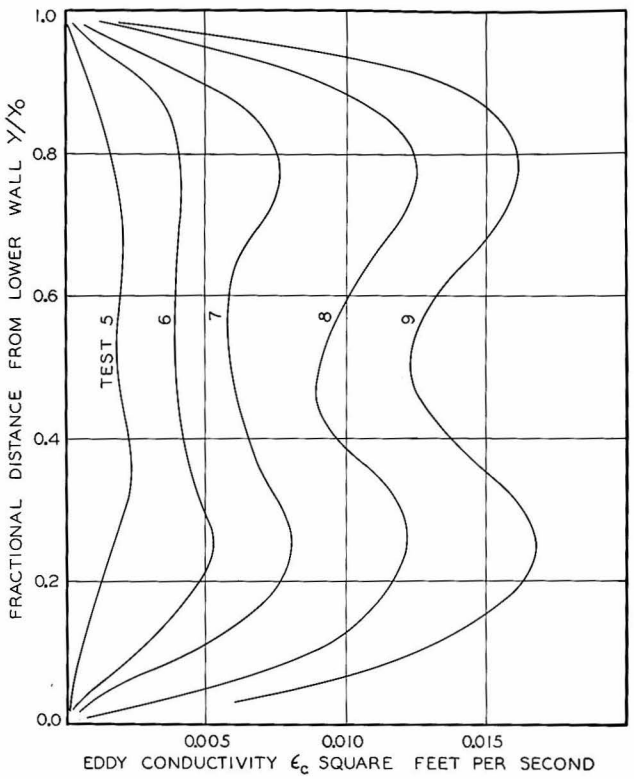

Figure 26

Eddy Conductivity Distributions

Tests 30, 31, 32, 33 & 34

Legend:

Test 30 is indicated as test 6 in this figure.

Test 31 is indicated as test 7 in this figure.

Test 32 is indicated as test 8 in this figure.

Test 33 is indicated as test 9 in this figure.

Test 34 is indicated as test 5 in this figure.

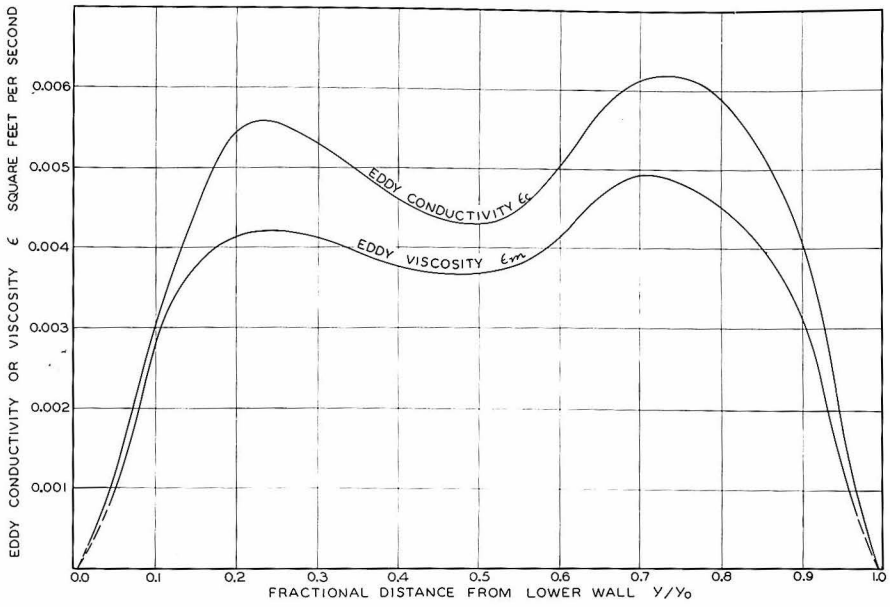

Figure 27

Eddy Property Distributions, Test 40

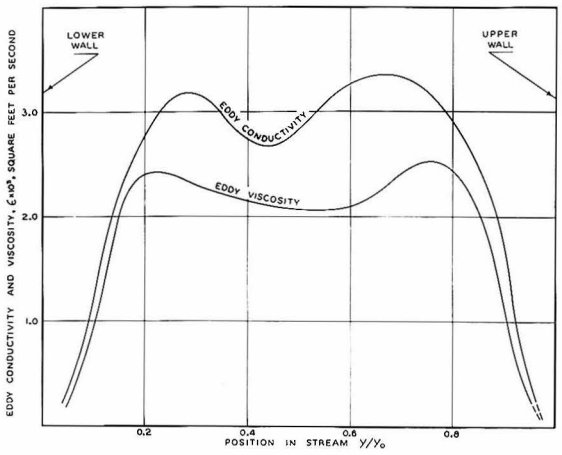

Figure 28

Eddy Property Distributions, Test 45

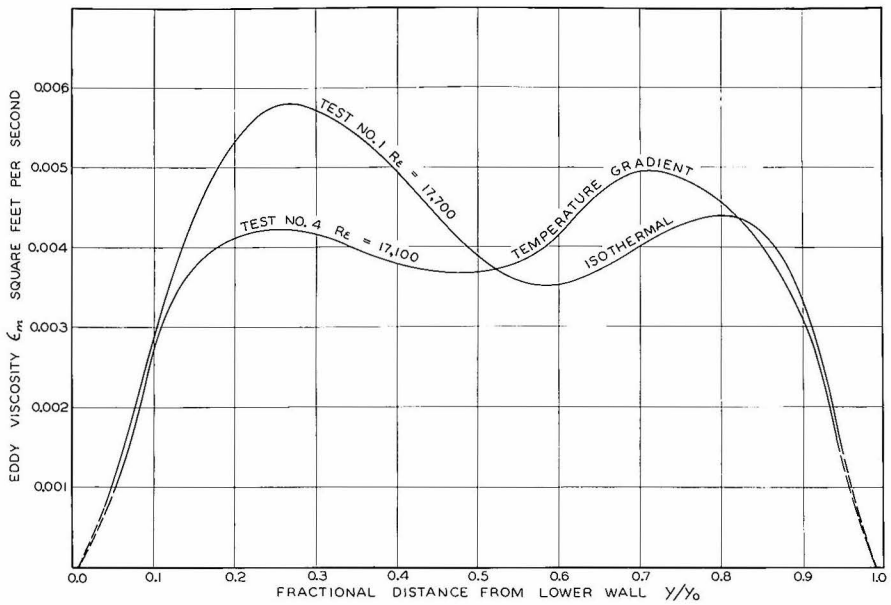

Figure 29

Eddy Viscosity Distributions, Tests 39 and 40

Legend:

Test 39 is indicated as Test 1 in this figure

Test 40 is indicated as Test 4 in this figure

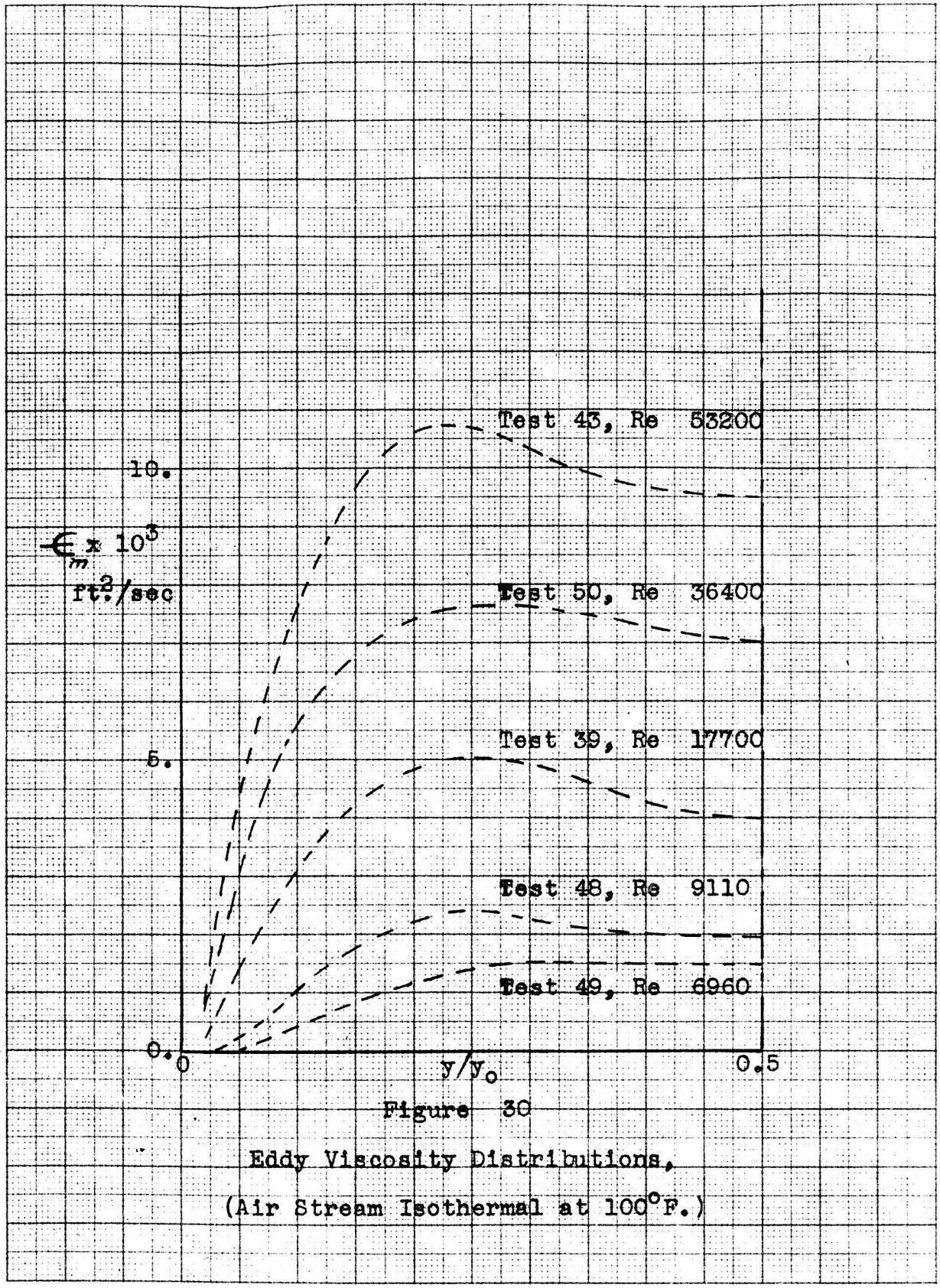

Figure 30

Eddy Viscosity Distributions,

(Air Stream Isothermal at 100°F.)

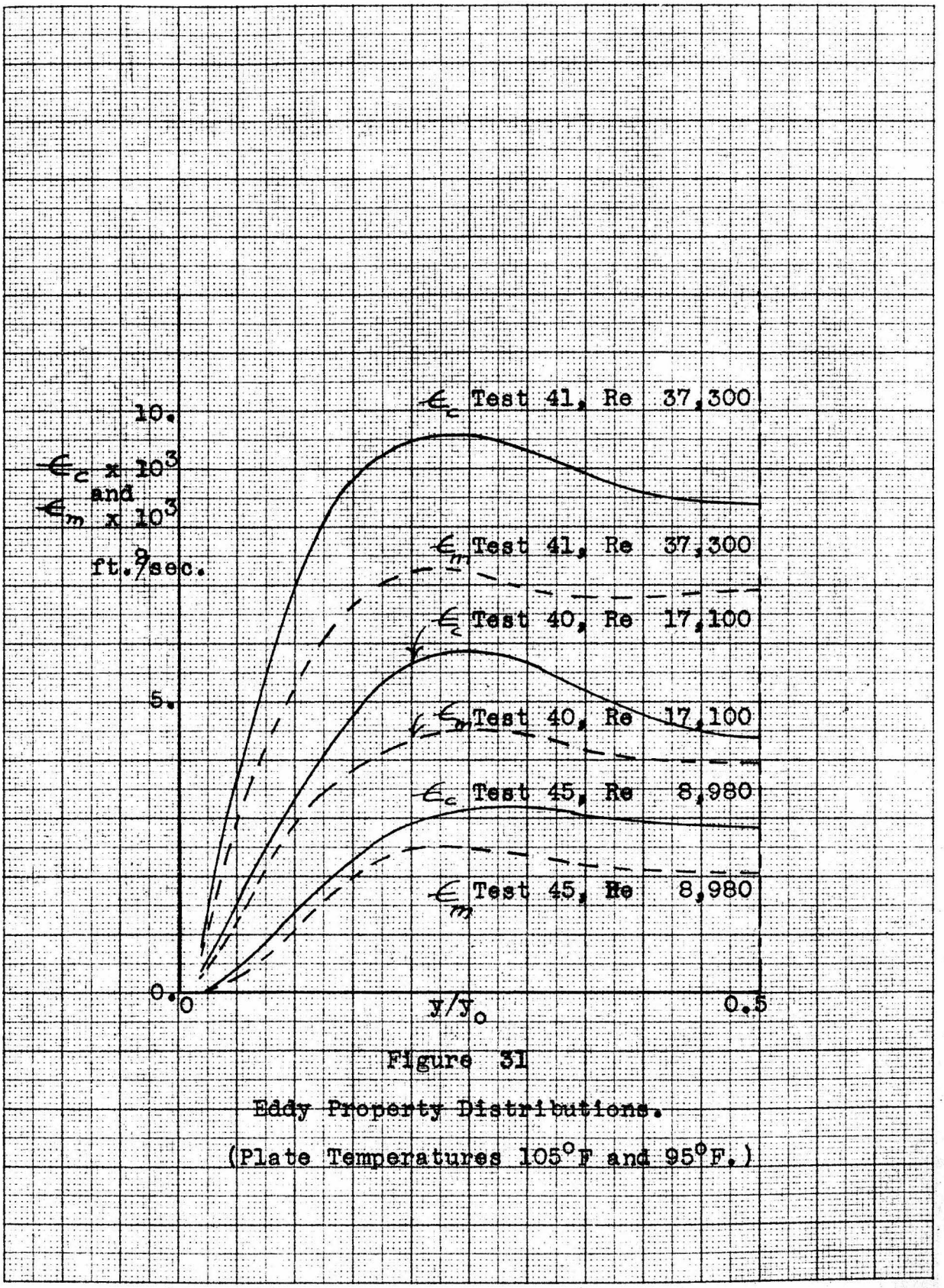

Figure 31

Eddy Property Distributions.

(Plate Temperatures 105°F and 95°F.)

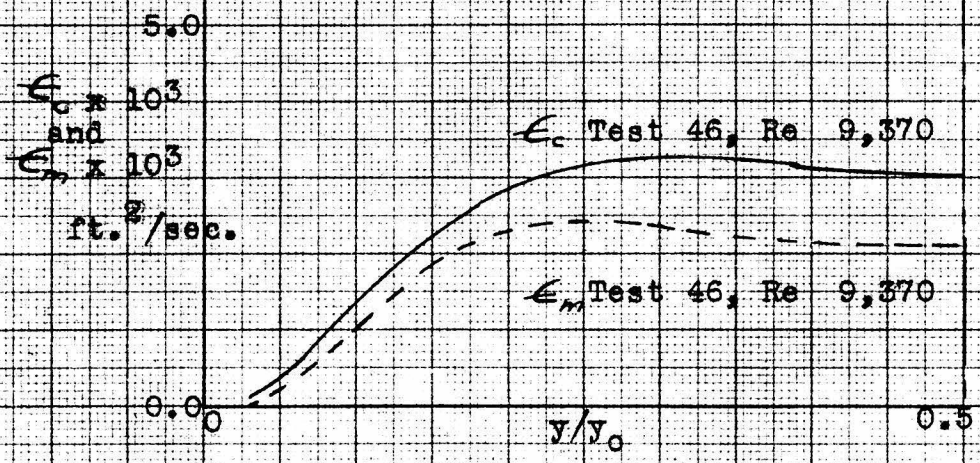

Figure 32

Eddy Property Distributions

(Plate Temperatures 115°F and 85°F.)

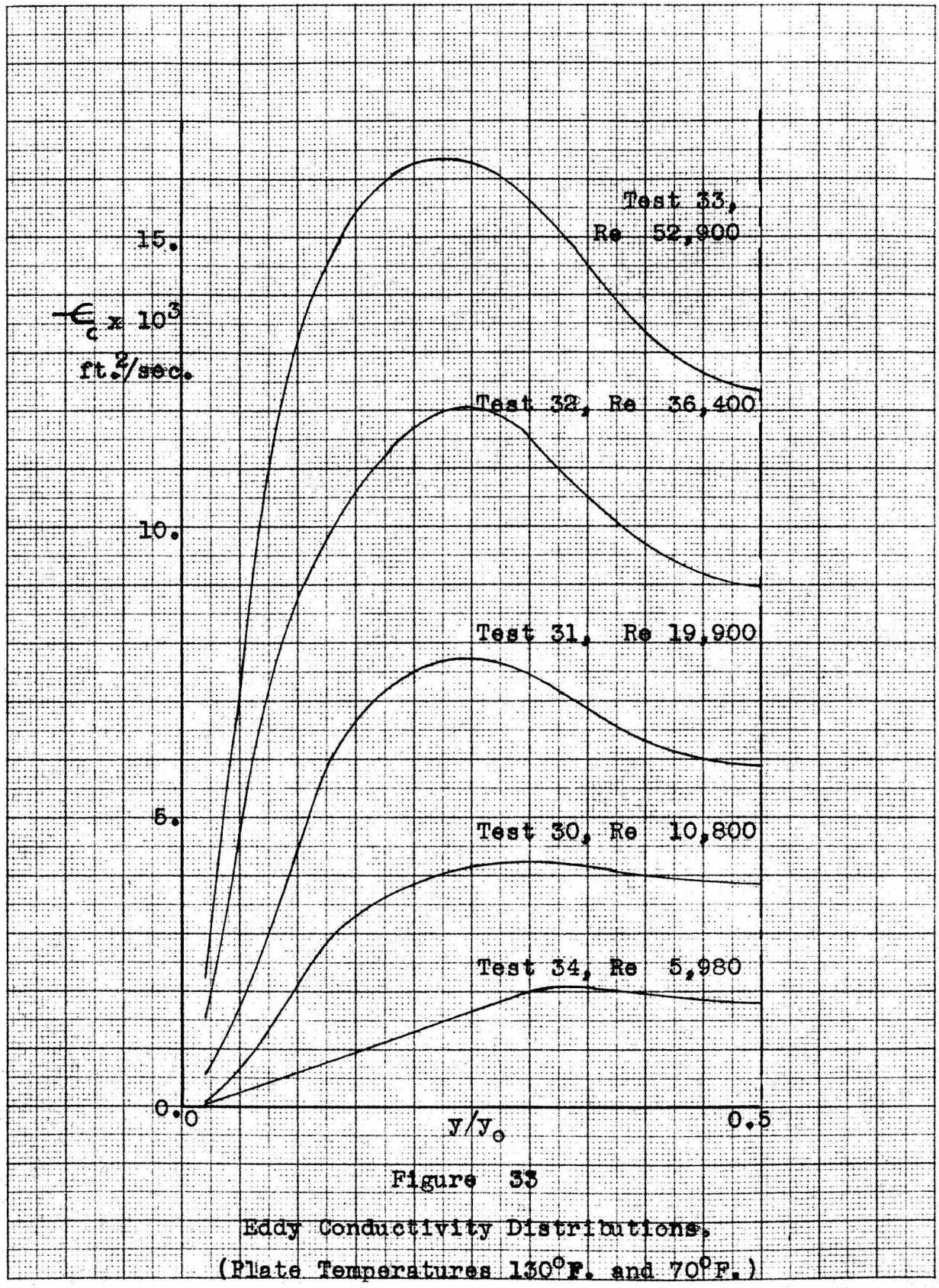

Figure 33

Eddy Conductivity Distributions.
(Plate Temperatures 130°F. and 70°F.)

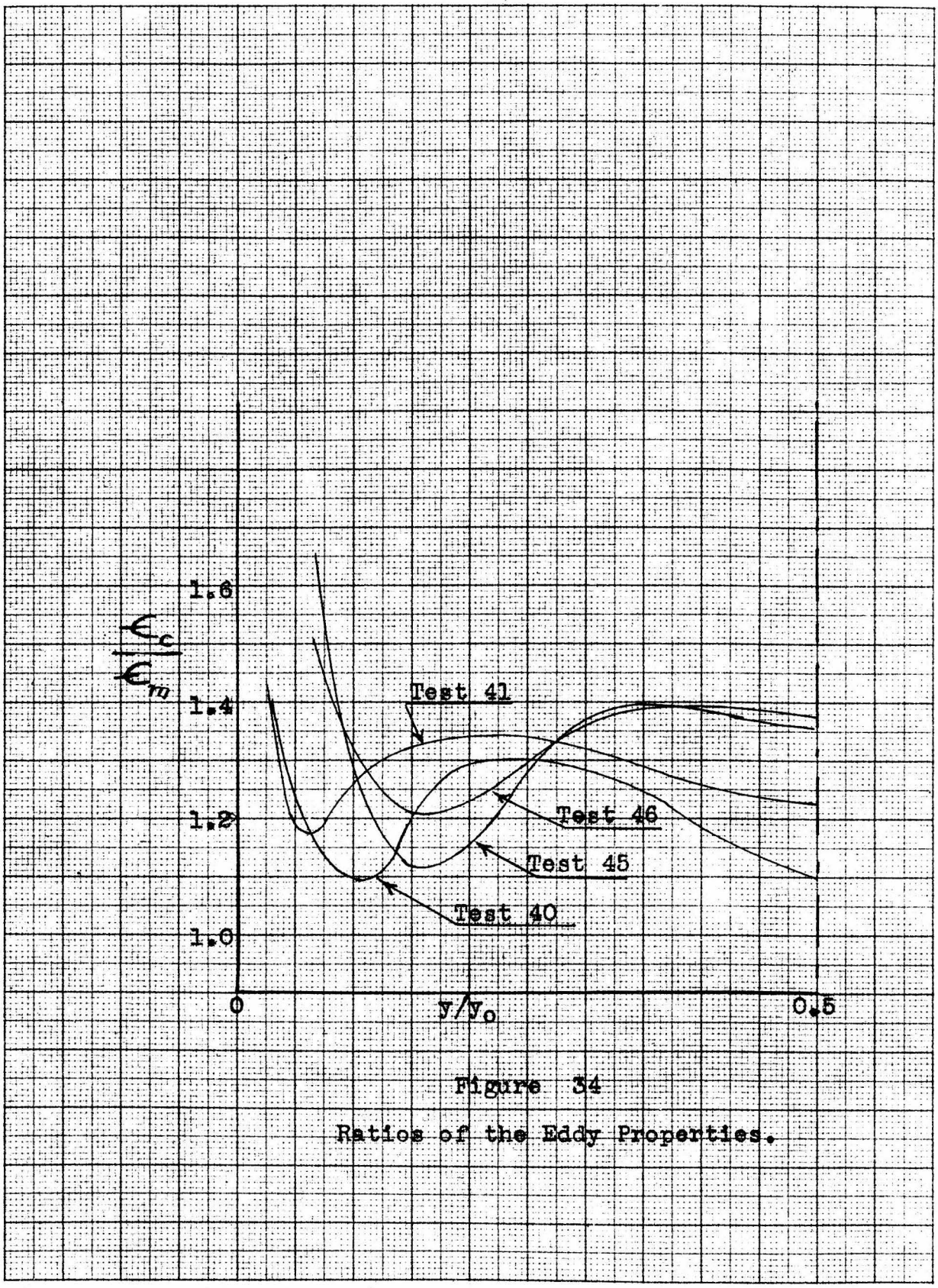

Figure 34

Ratios of the Eddy Properties.

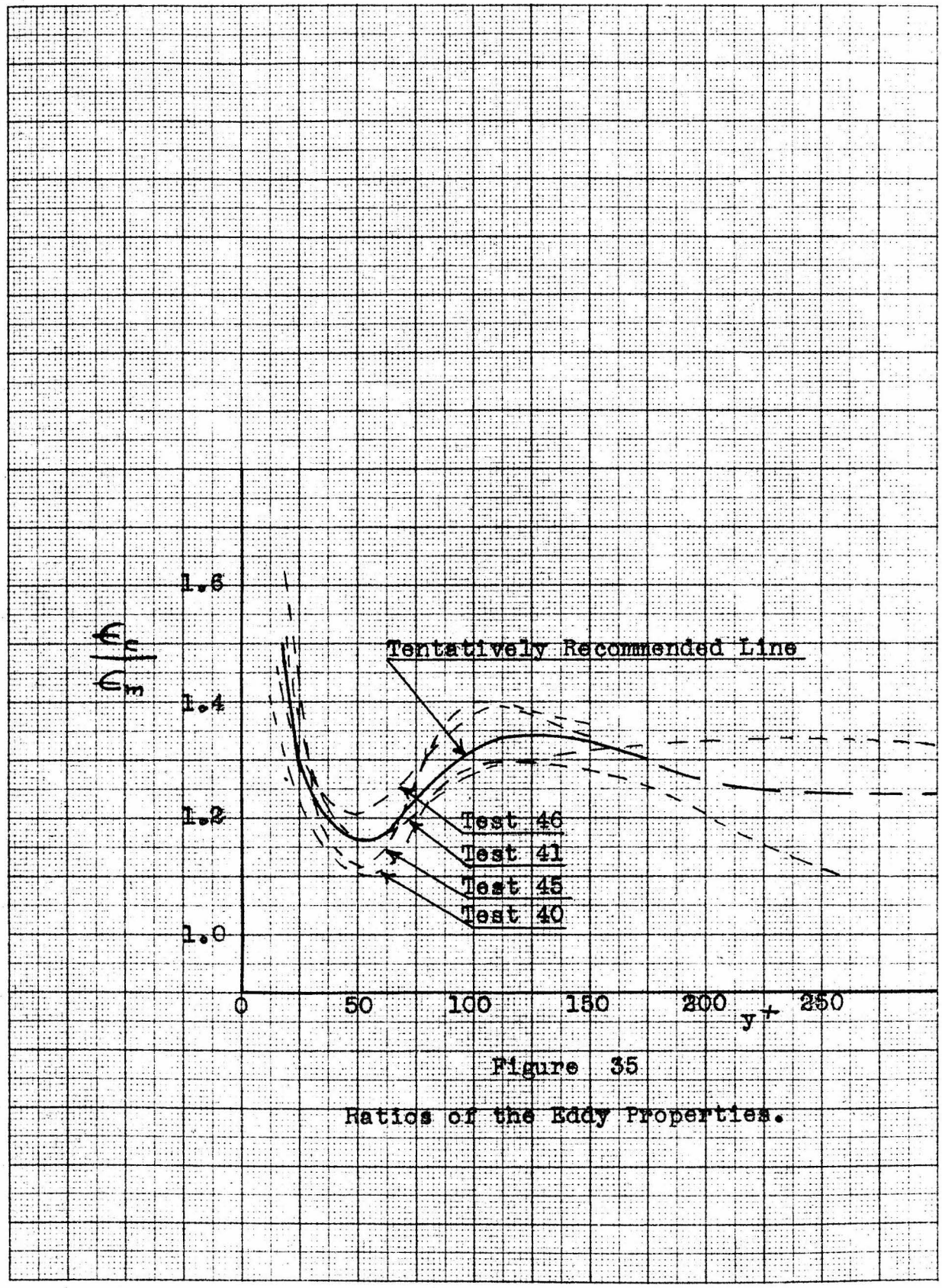

Figure 35

Ratios of the Eddy Properties.

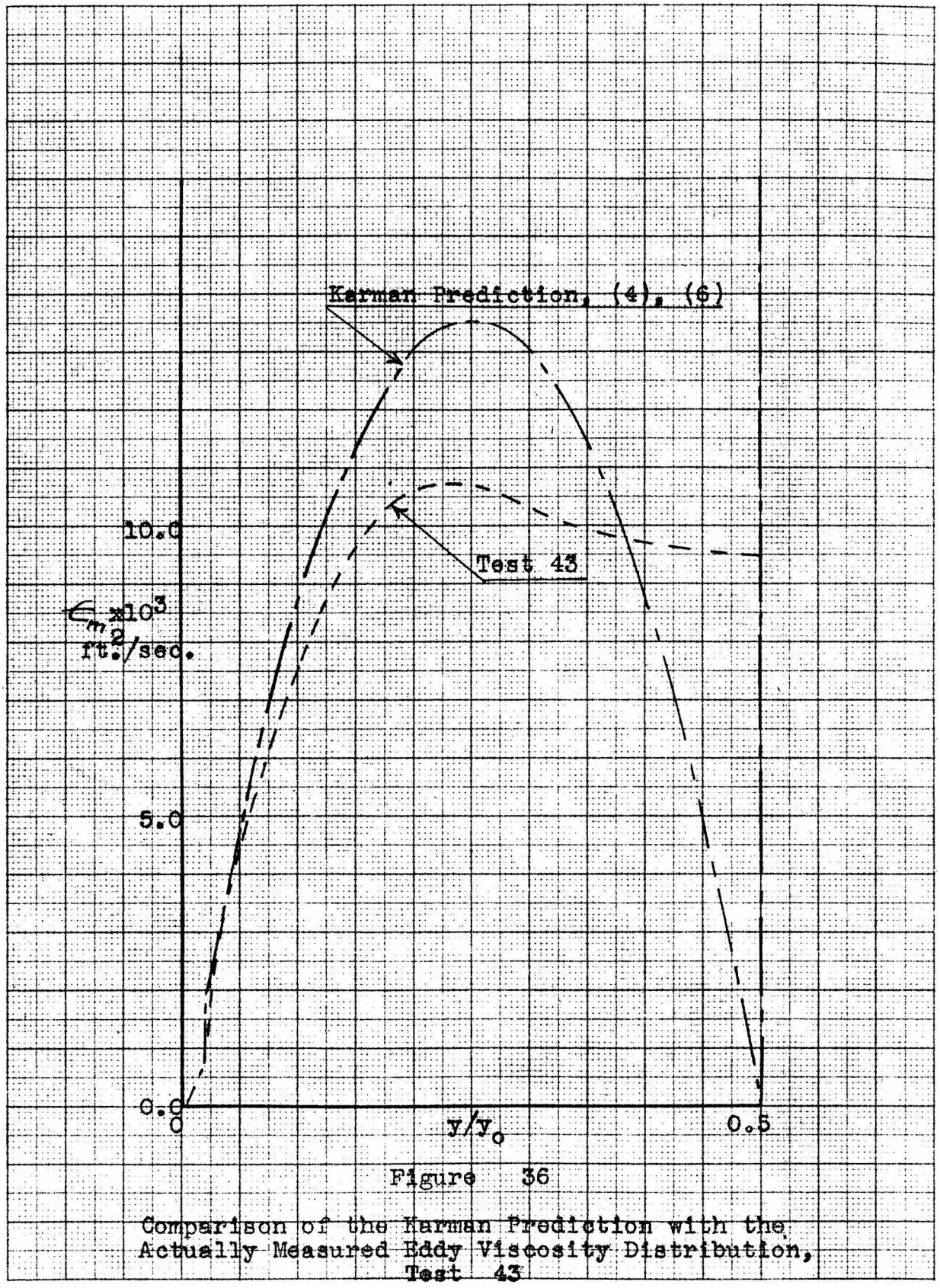

Figure 36

Comparison of the Karman Prediction with the Actually Measured Eddy Viscosity Distribution, Test 43

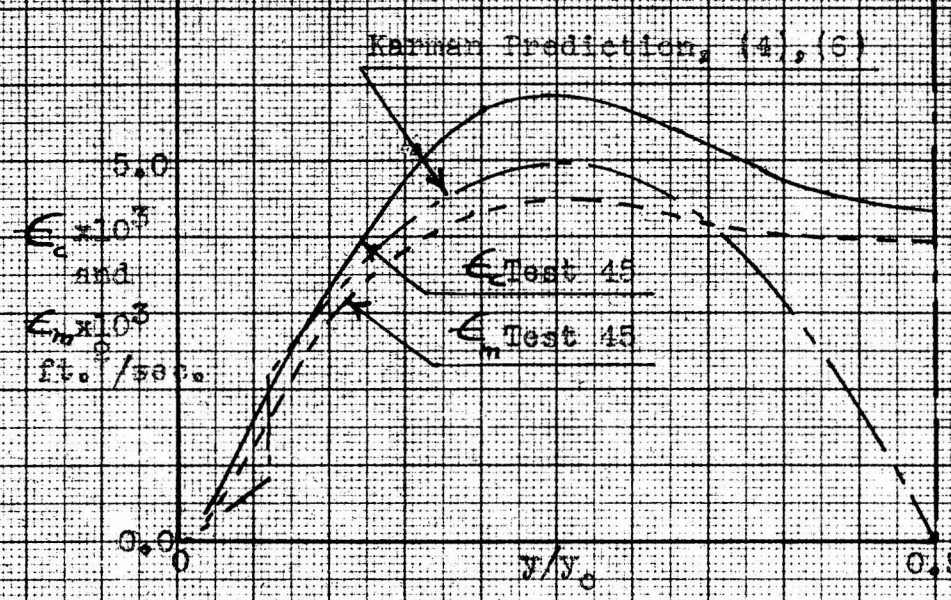

Figure 37

Comparison of the Karman Prediction with the Actually Measured Eddy Property Distributions, Test 45.

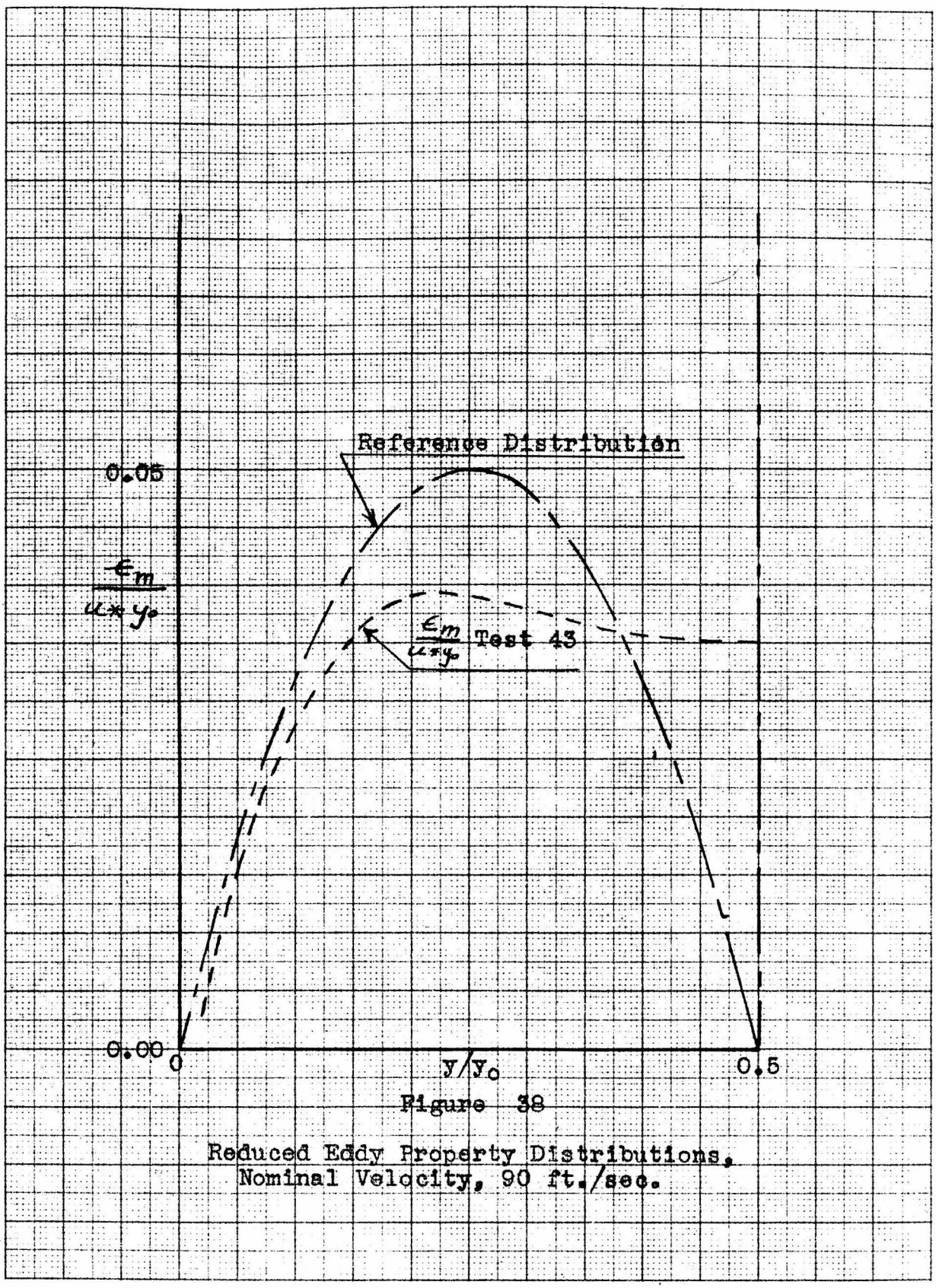

Figure 38

Reduced Eddy Property Distributions,
Nominal Velocity, 90 ft./sec.

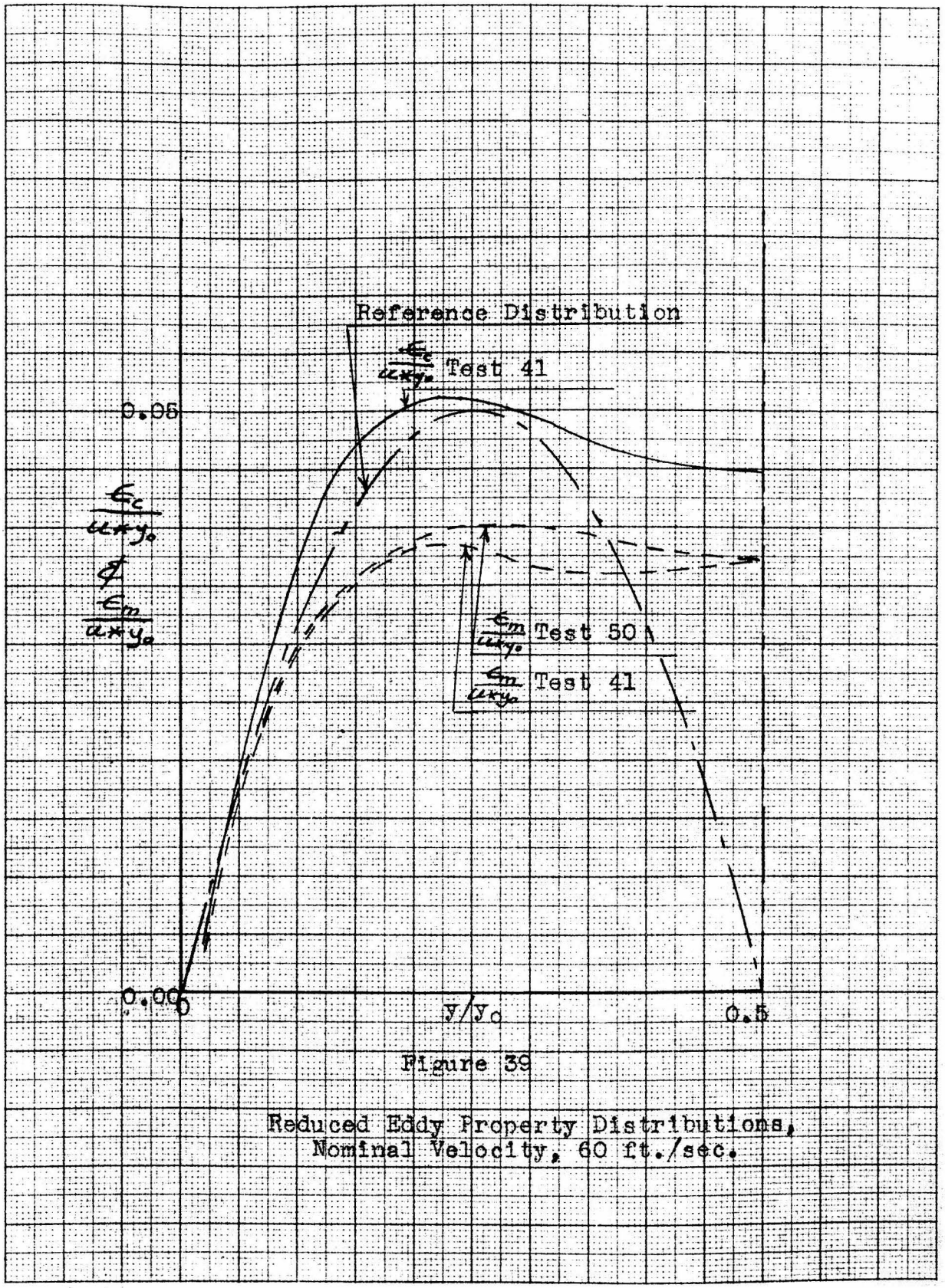

Figure 39

Reduced Eddy Property Distributions,
Nominal Velocity, 60 ft./sec.

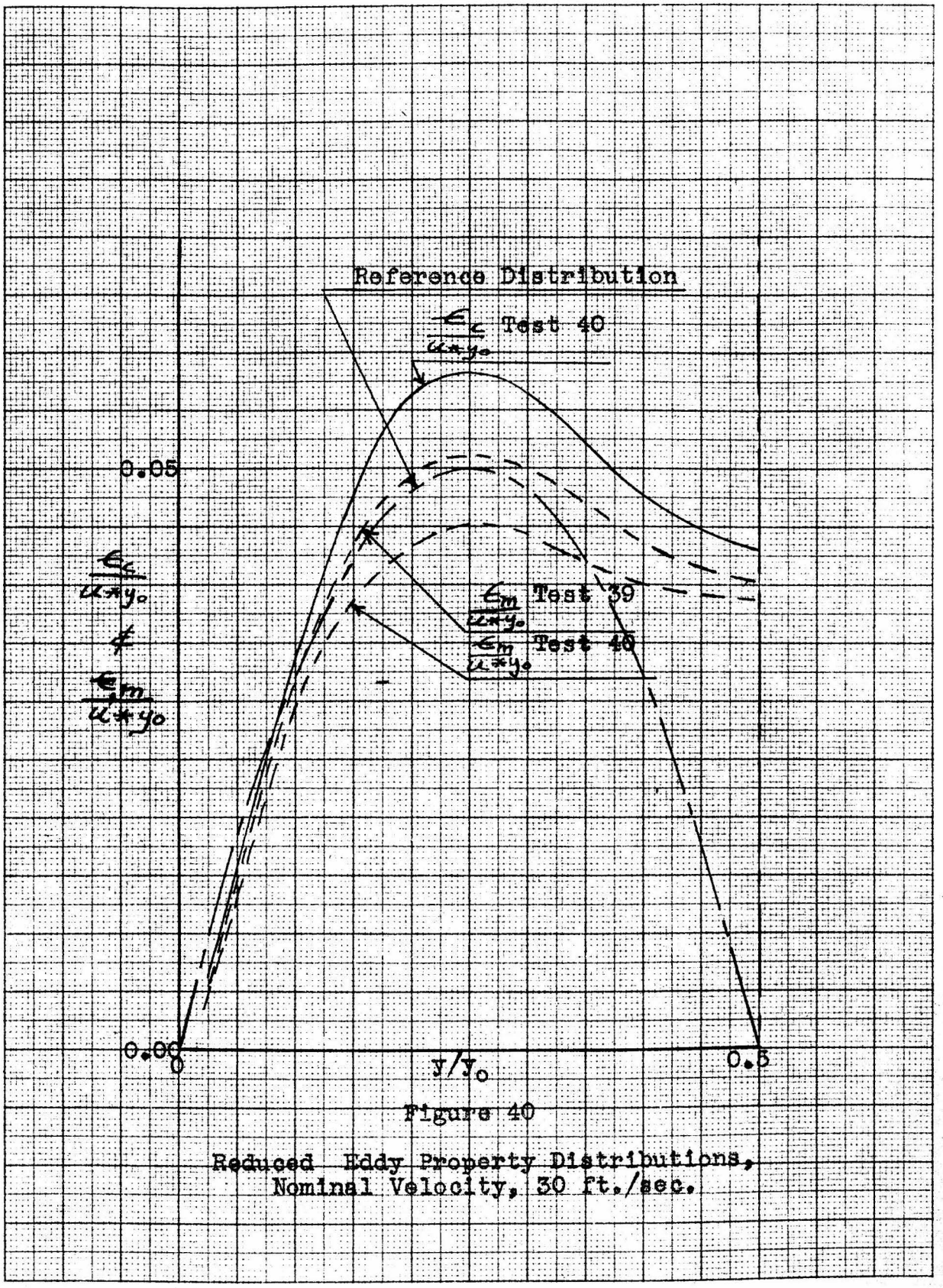

Figure 40

Reduced Eddy Property Distributions,
Nominal Velocity, 30 ft./sec.

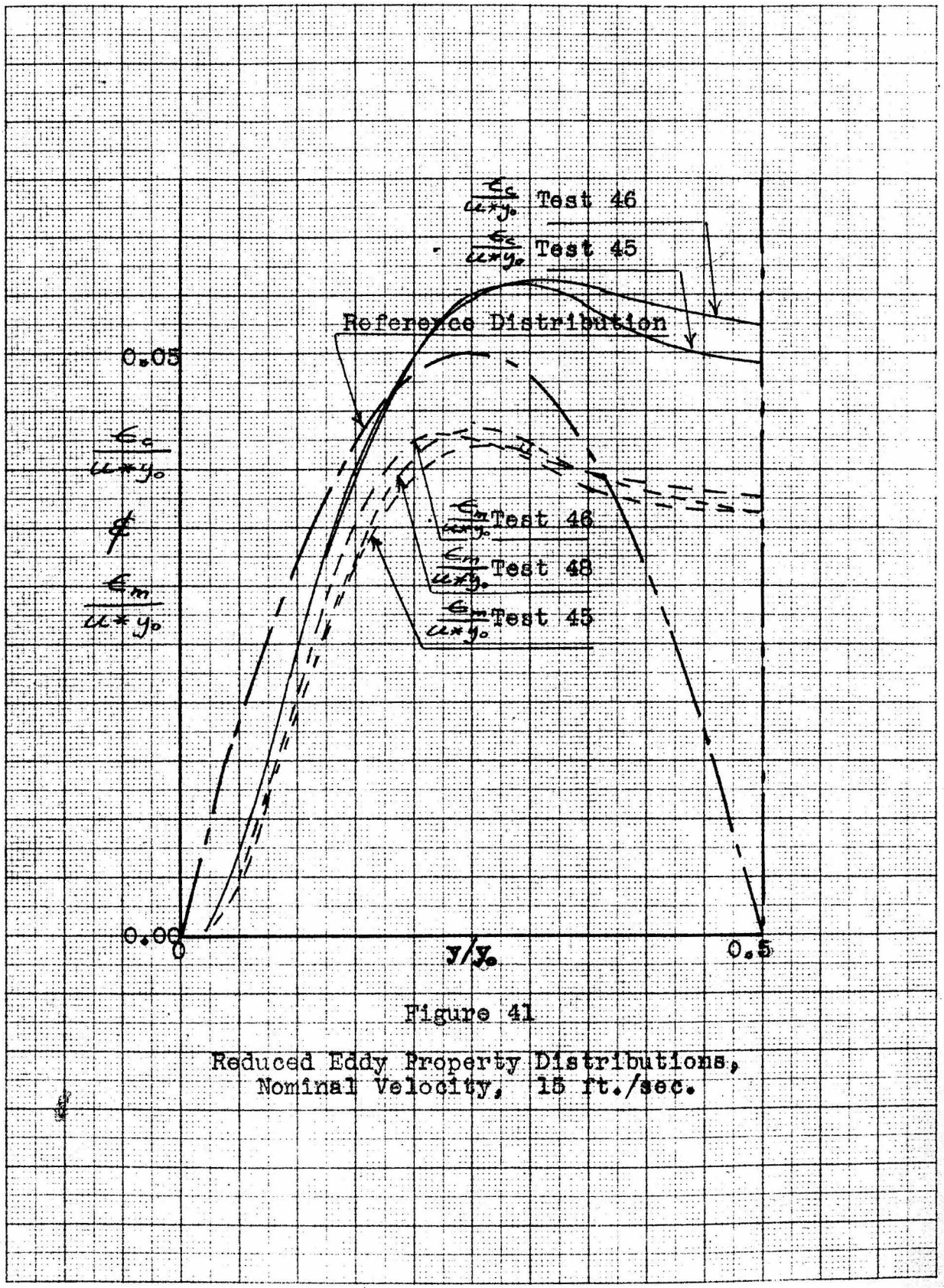

Figure 41

Reduced Eddy Property Distributions,
Nominal Velocity, 15 ft./sec.

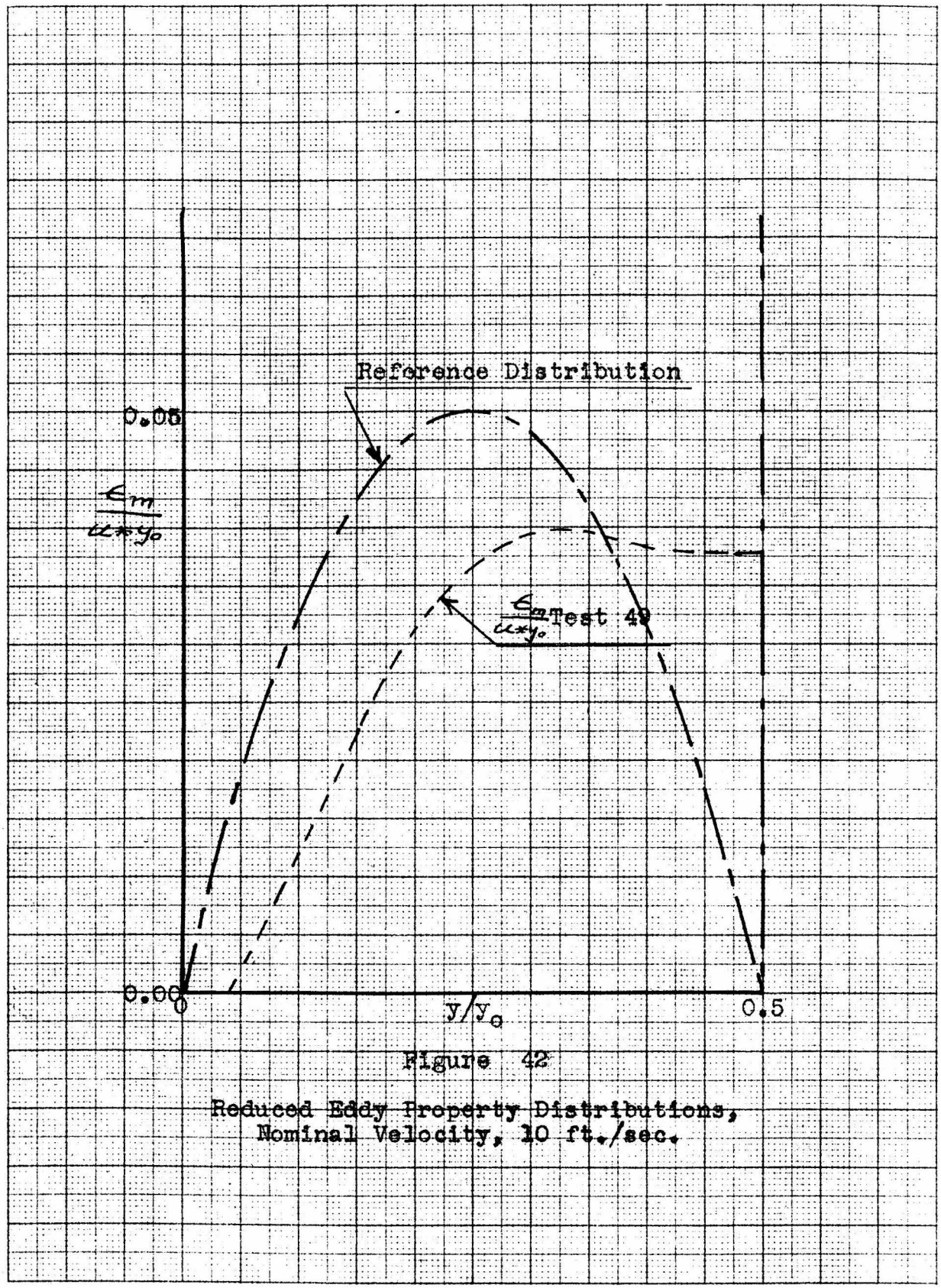

Figure 42

Reduced Eddy Property Distributions,
Nominal Velocity, 10 ft./sec.

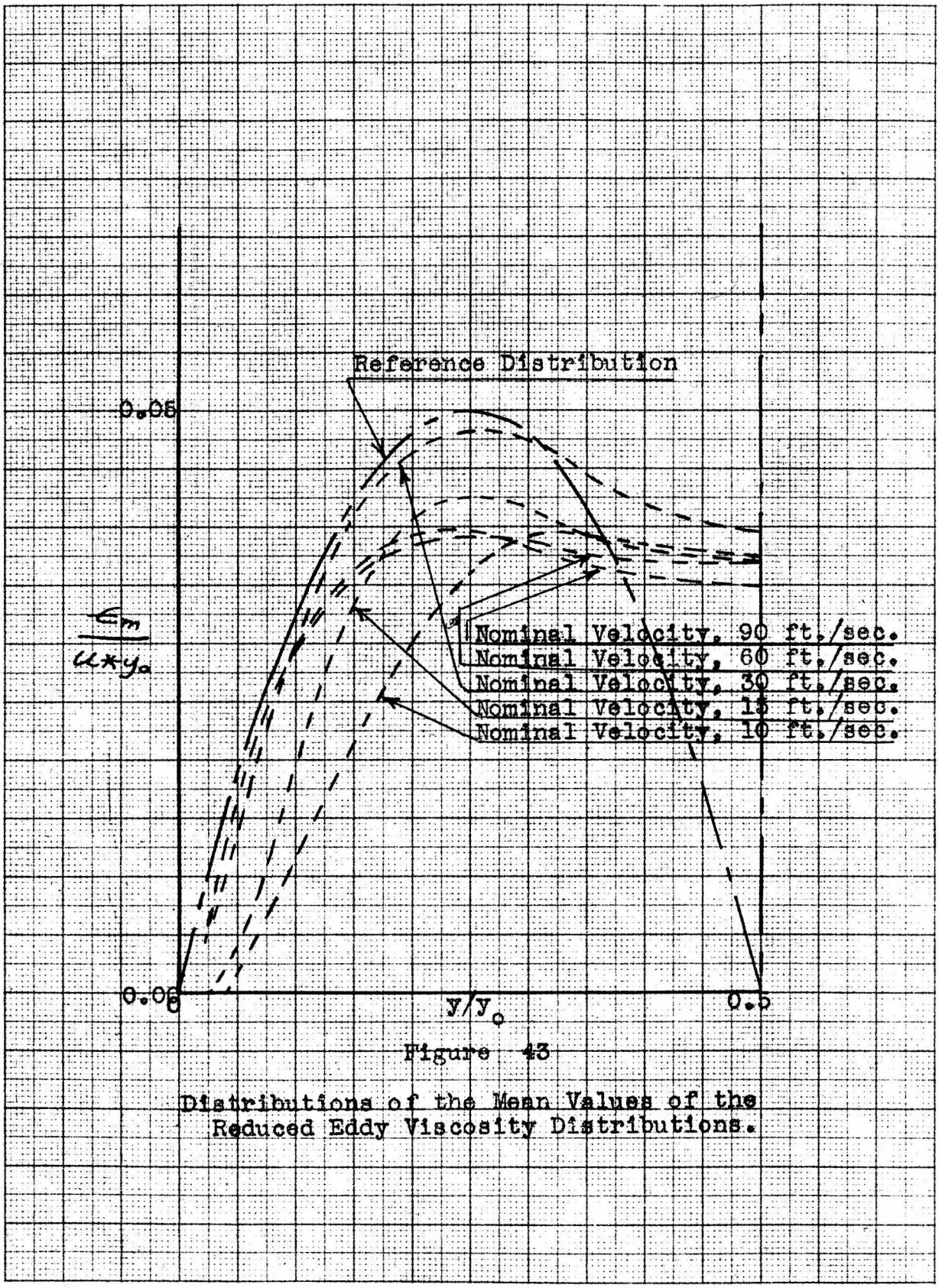

Figure 43

Distributions of the Mean Values of the Reduced Eddy Viscosity Distributions.

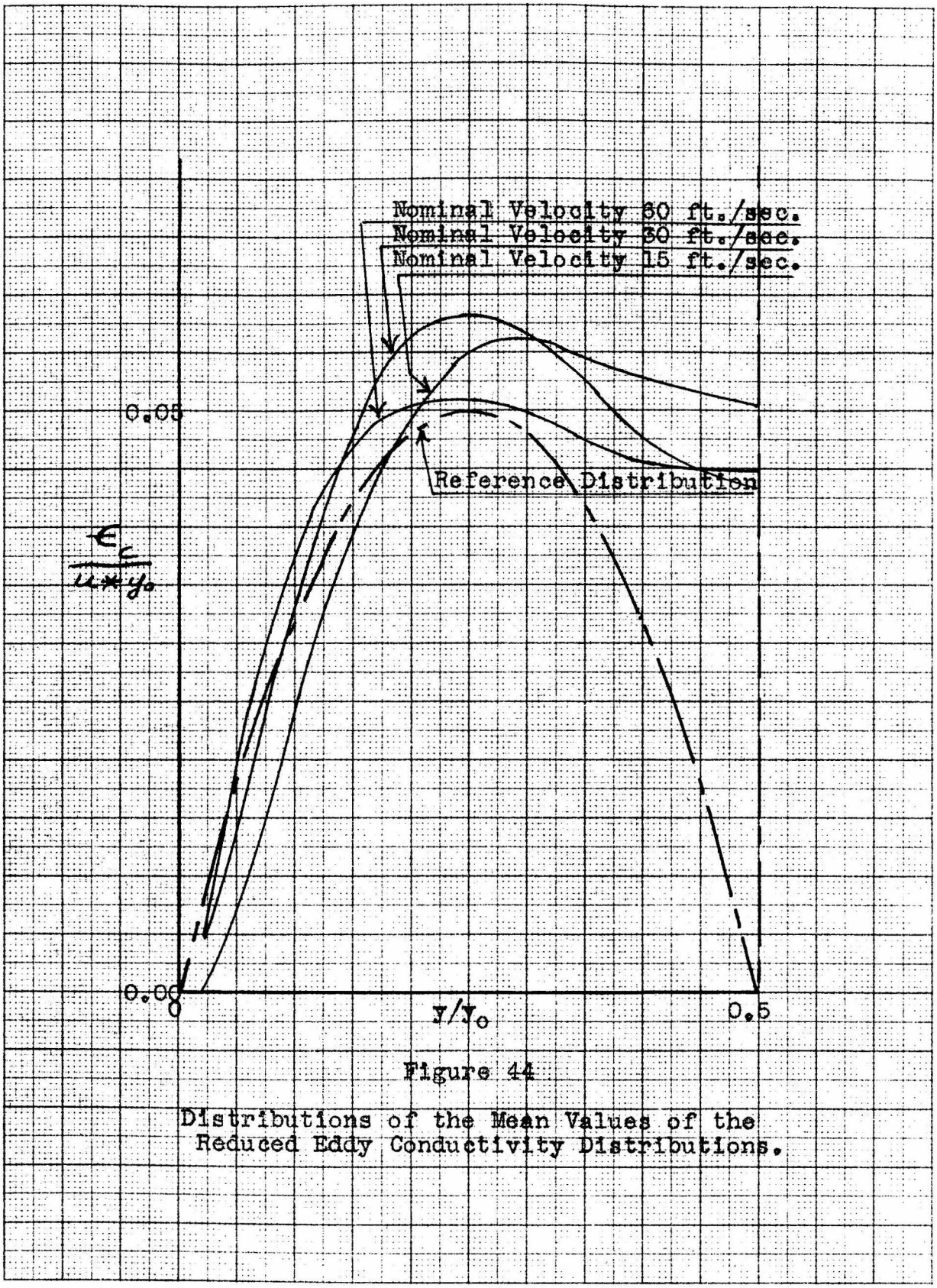

Figure 44

Distributions of the Mean Values of the Reduced Eddy Conductivity Distributions.

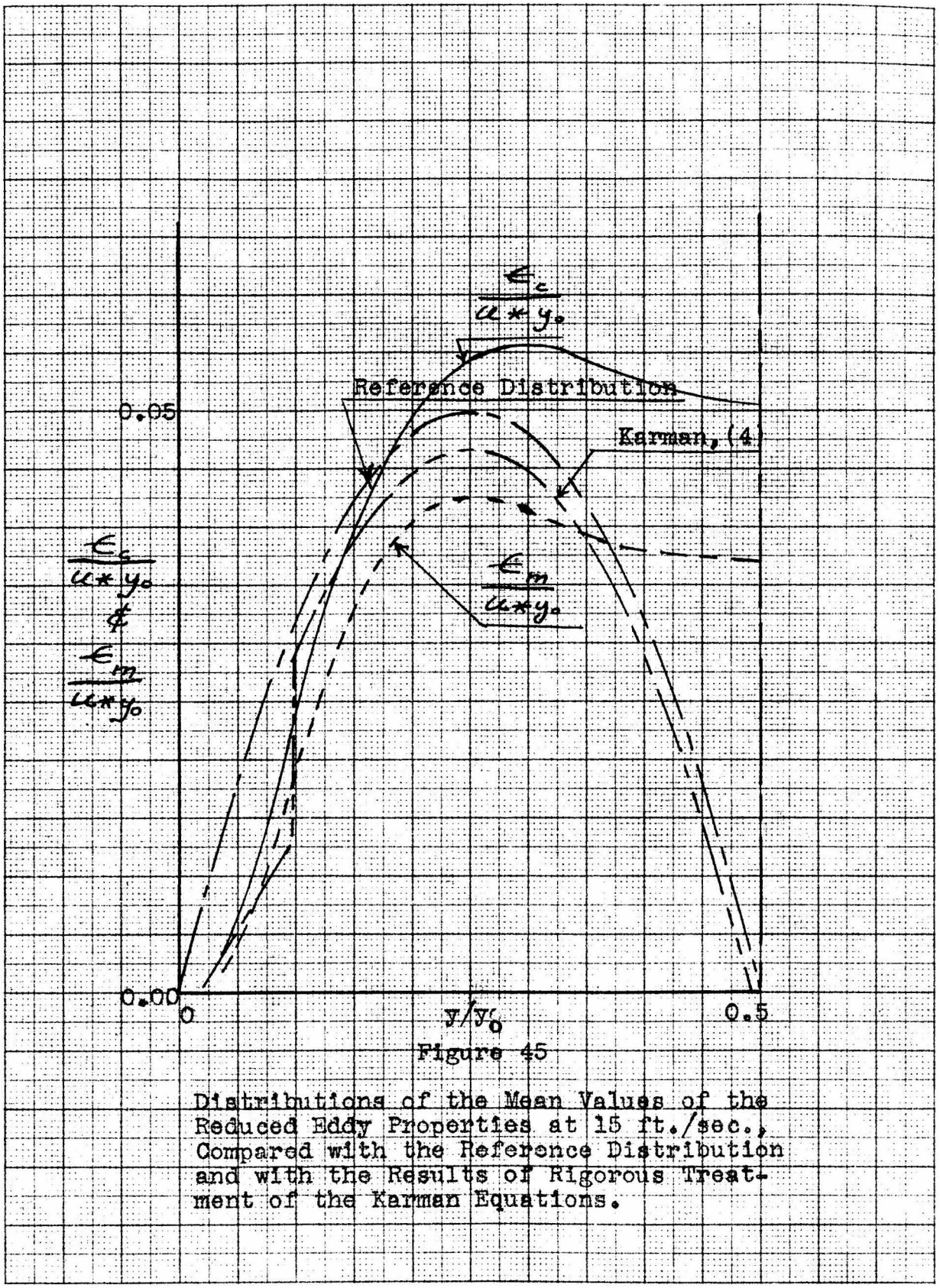

Figure 45

Distributions of the Mean Values of the Reduced Eddy Properties at 15 ft./sec., Compared with the Reference Distribution and with the Results of Rigorous Treatment of the Karman Equations.

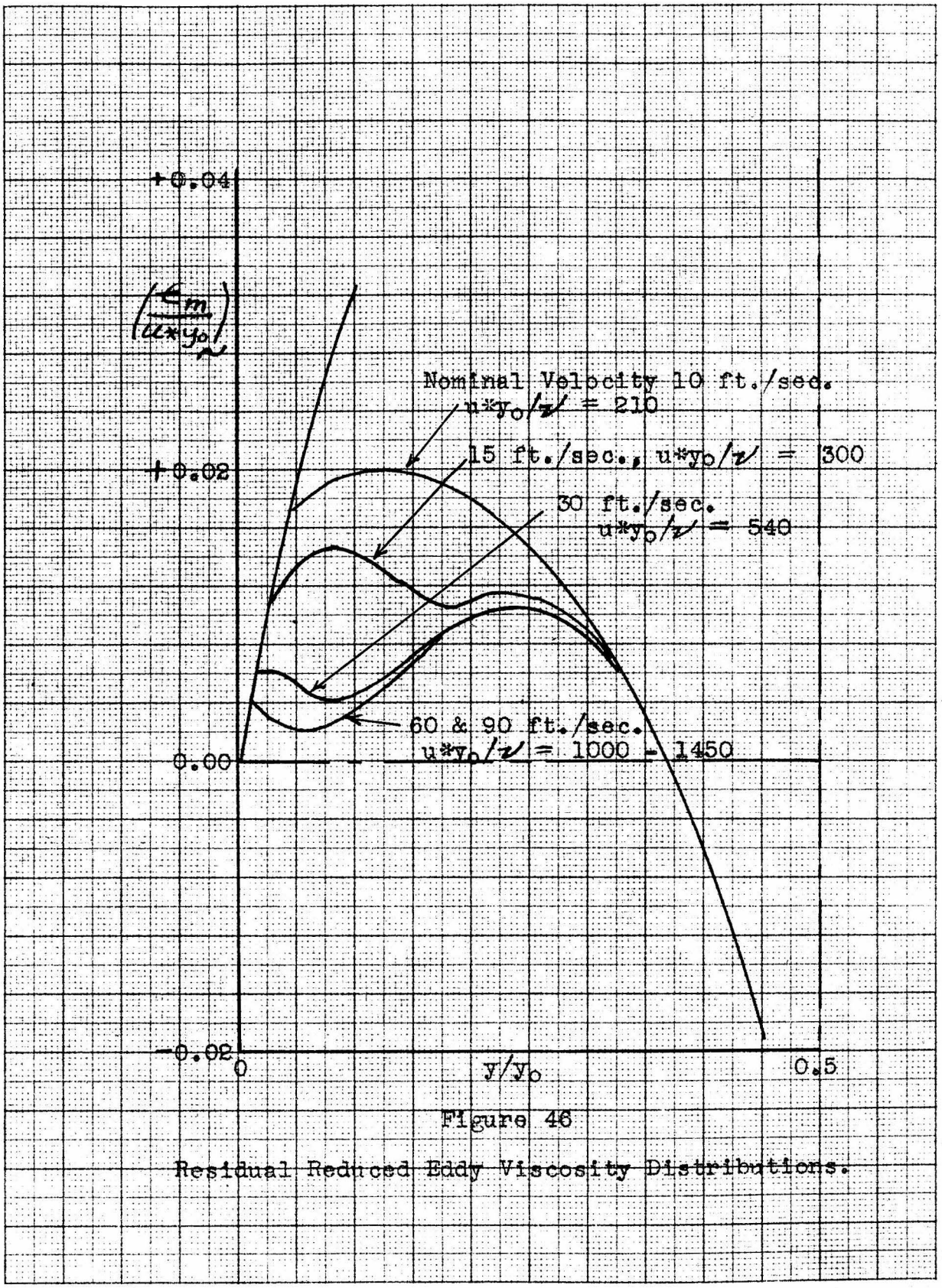

Figure 46

Residual Reduced Eddy Viscosity Distributions.

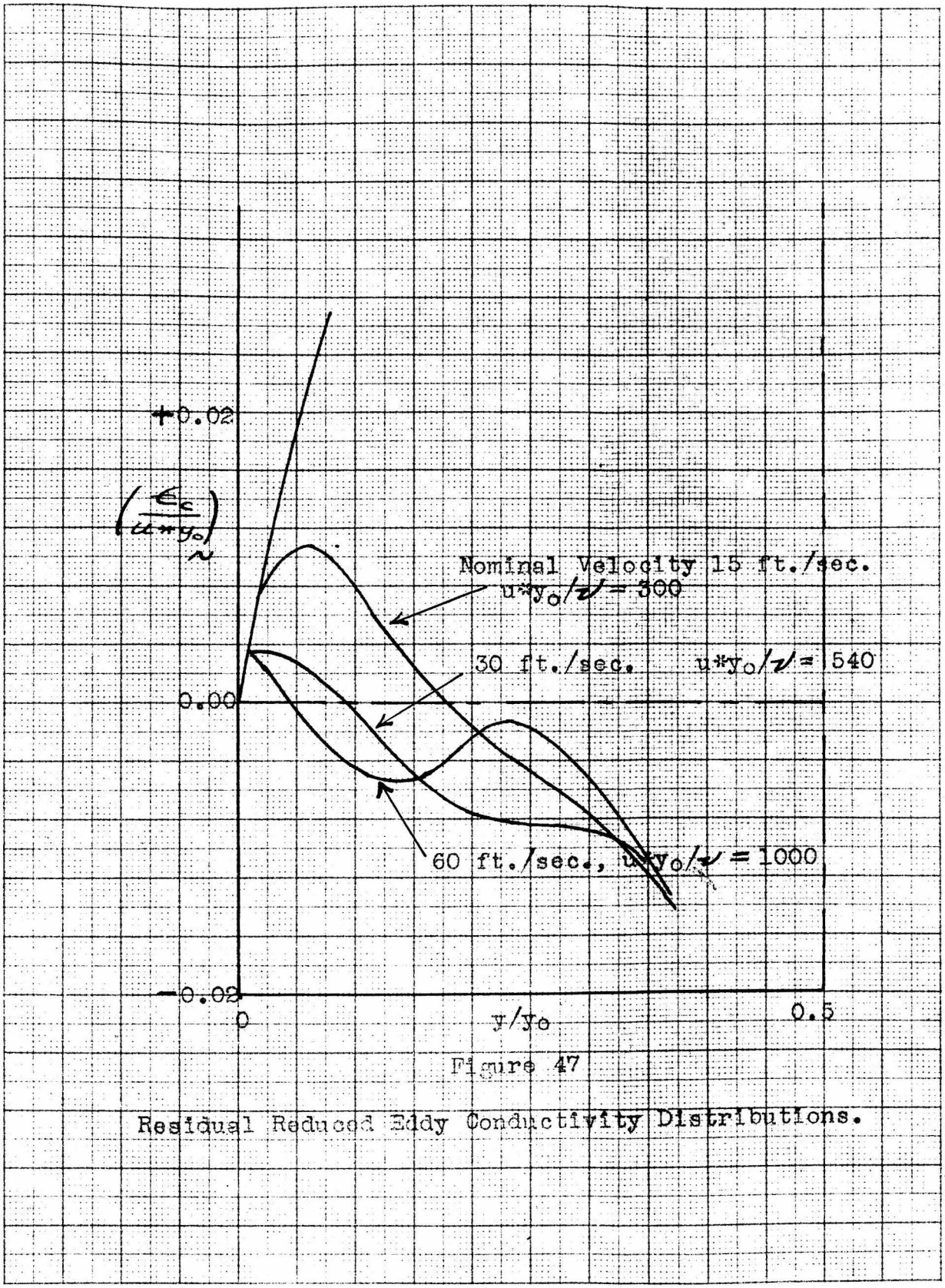

Figure 47

Residual Reduced Eddy Conductivity Distributions.

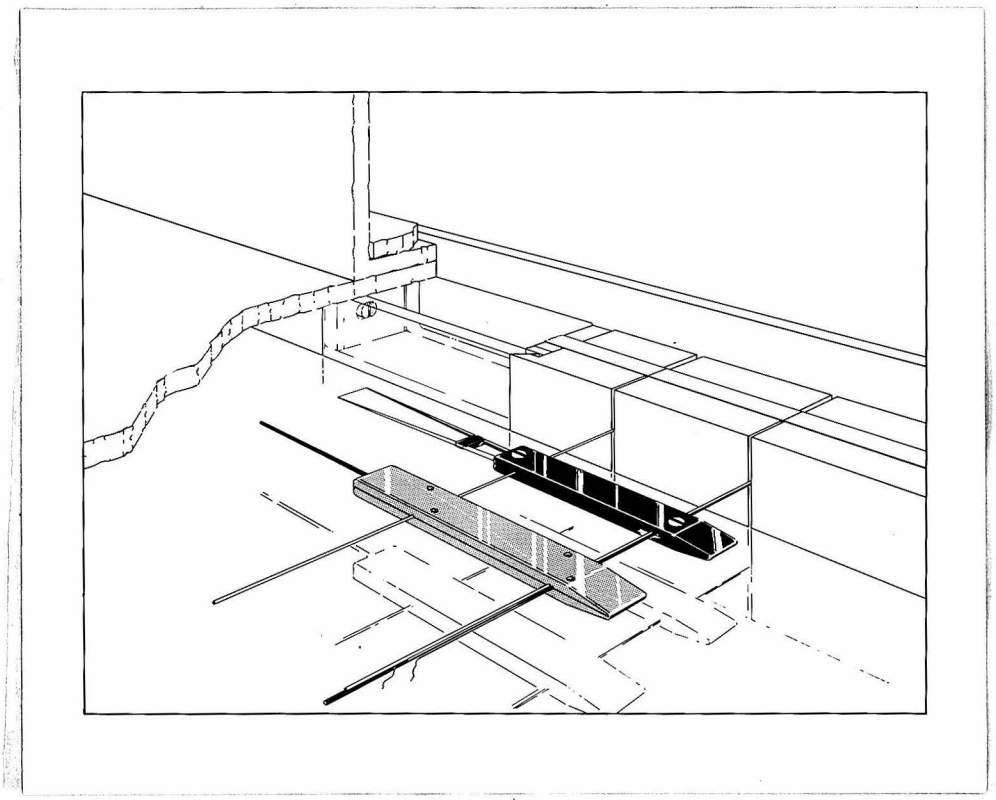

Figure 48

Pitot Tube and Thermanemometer

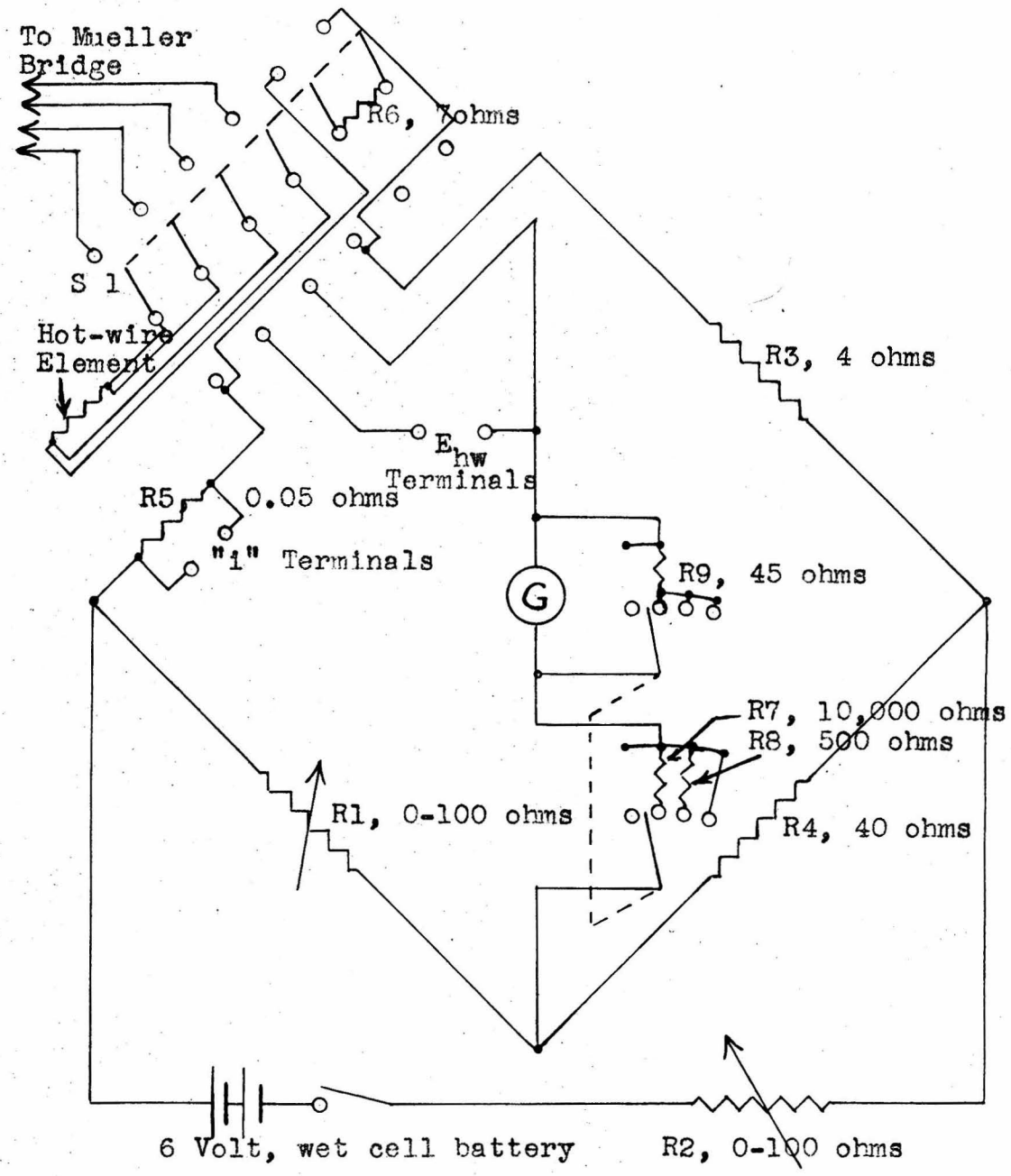

Figure 49

Circuit Diagram, Thermanemometer

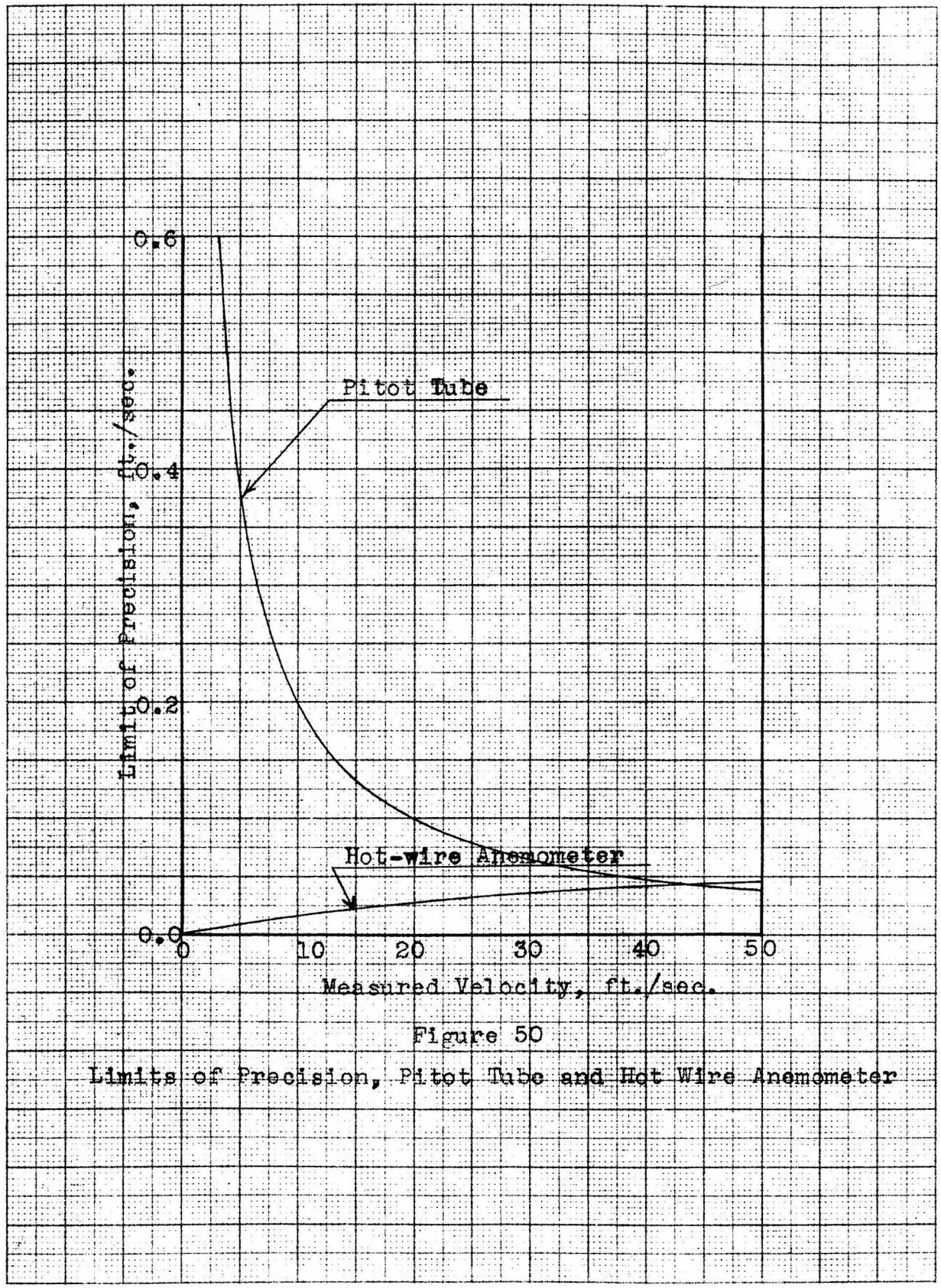

Figure 50

Limits of Precision, Pitot Tube and Hot Wire Anemometer

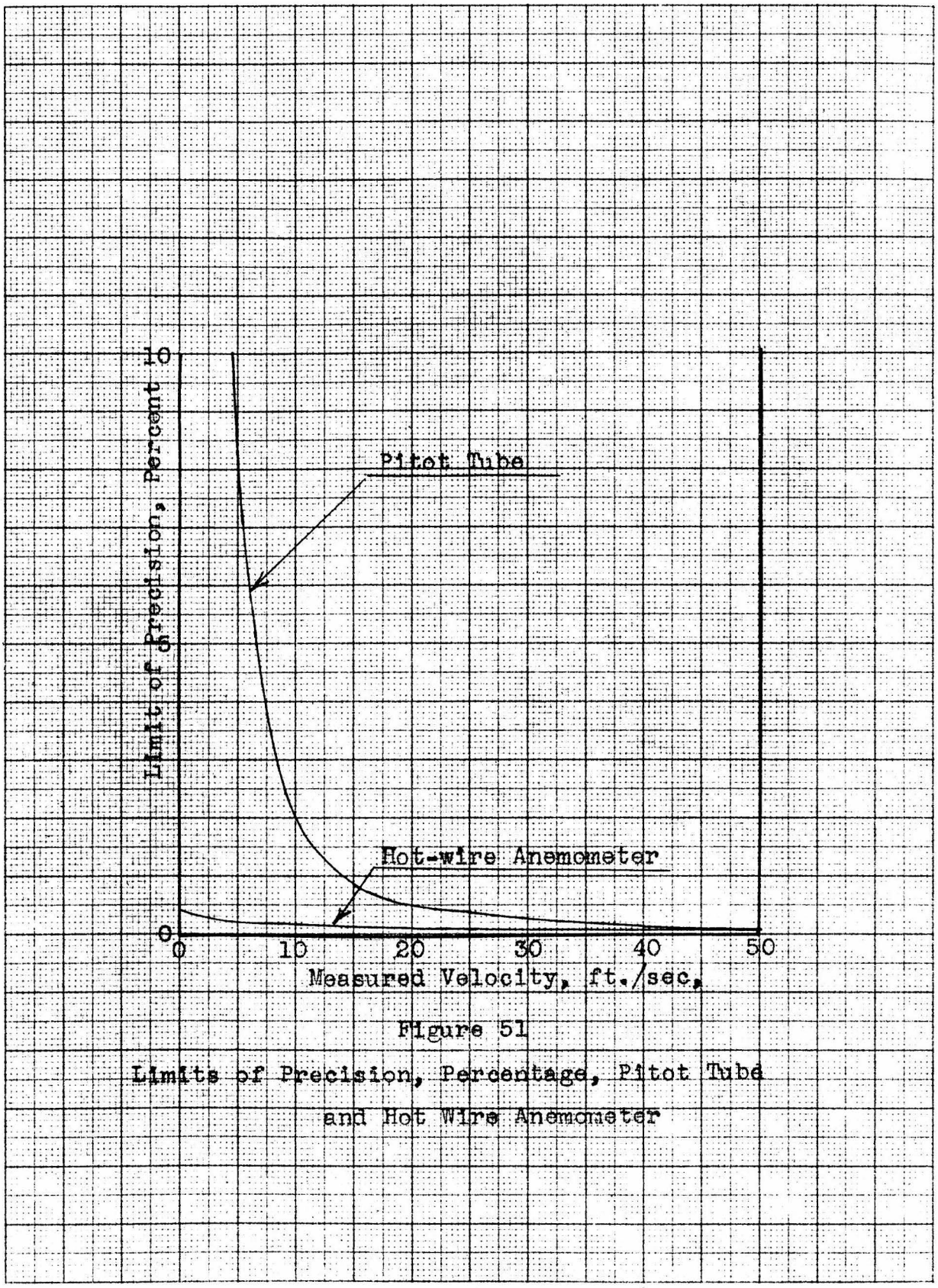

Figure 51

Limits of Precision, Percentage, Pitot Tube and Hot Wire Anemometer

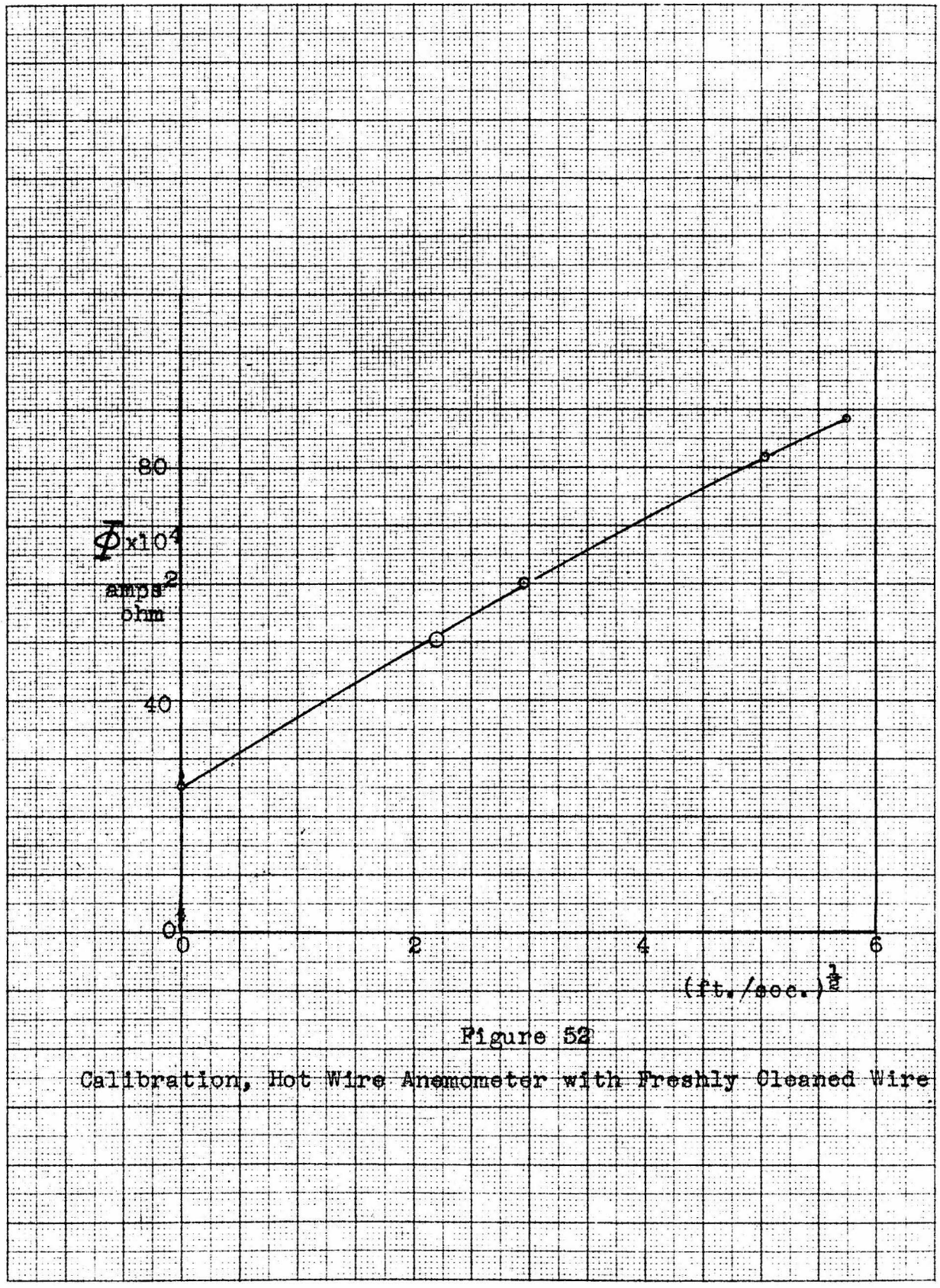

Figure 52

Calibration, Hot Wire Anemometer with Freshly Cleaned Wire

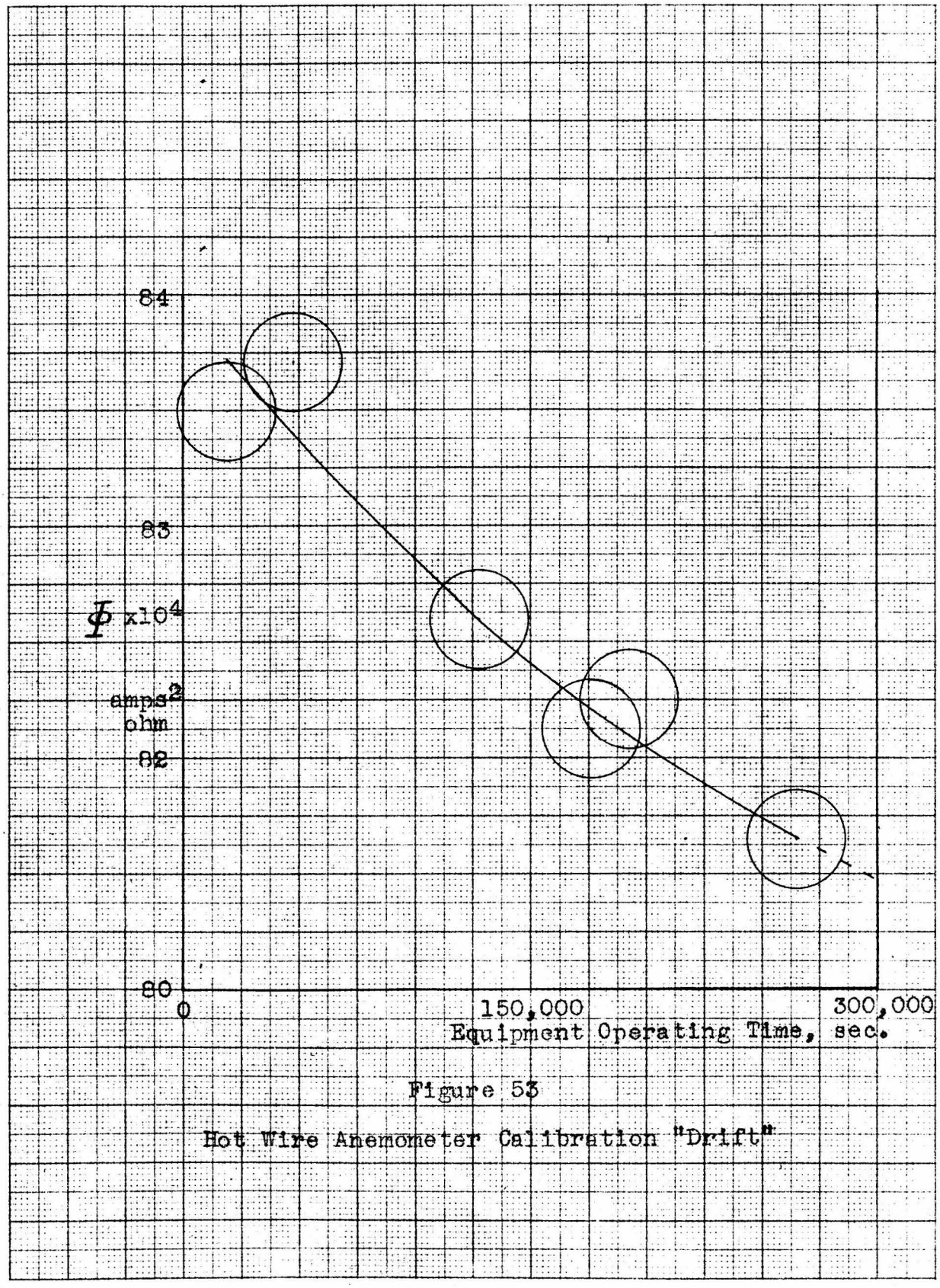

Figure 53

Hot Wire Anemometer Calibration "Drift"

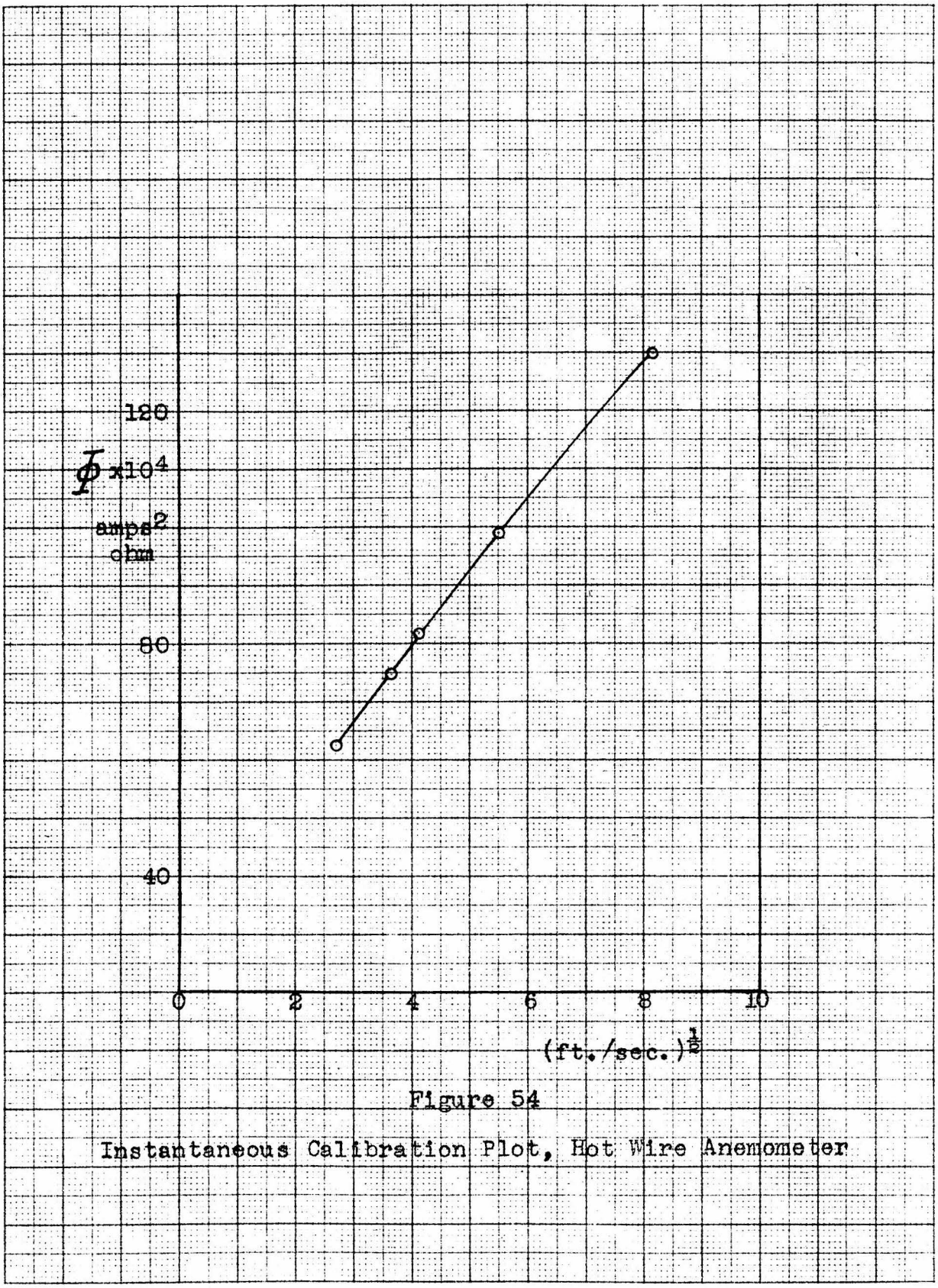

Figure 54

Instantaneous Calibration Plot, Hot Wire Anemometer

List of Tables

Table I

Traverse Conditions

Quantity Reported	Symbol	Units	Test 30	Test 31
Measured Quantities				
Distance Between Copper Plates	y_o	ft.	0.0616	0.0616
Traverse Location(a)		ft.	10.3	10.3
Incoming Air Temperature		°F	100.0	100.0
Upper Plate Temperature		°F	130.0	130.0
Lower Plate Temperature		°F	70.0	70.0
Bulk Velocity (b)	U	ft/sec	16.3	29.3
Pressure (c)	P	lbs/ft^2	14.352	14.368
Pressure Gradient(d)	dP/dx	lbs/ft^3	-0.071 (d)	-0.195(d)
Heat Flux Density	Q^o	$\frac{BTU}{(ft^2)(sec)}$	0.0353	0.0555
Weight Fraction of Water		lb/lb	0.0072	0.0088
Derived Quantities				
Reynolds Number (b)	Re		10850.	19900.
Fanning Factor (b)	f		(d)	(d)
"Friction Velocity"(b)	u^*	ft/sec	(d)	(d)

(a)All traverses reported were conducted on the longitudinal centerline of the apparatus. The distance reported above is downstream of the converging section.

(b)See page 13 for definitions of U, Re, f and u^*.

(c)Piezometric pressure at the traversing point.

(d)The pressure gradient and shear for Tests 30, 31, 32, 33 and 34 were determined from a friction factor plot. The Fanning factor and "friction velocity" were thus not independently available.

Table I, cont'd

Traverse Conditions

Quantity Reported	Test 32	Test 33	Test 34
Measured Quantities			
Distance Between Copper Plates	0.0626	0.0618	0.0625
Traverse Location	110.3	110.3	110.3
Incoming Air Temperature	100.0	100.0	100.0
Upper Plate Temperature	130.0	130.0	130.0
Lower Plate Temperature	70.0	70.0	70.0
Bulk Velocity	54.2	79.2	8.89
Pressure	14.381	14.336	14.446
Pressure Gradient	-0.59 (d)	-1.18 (d)	-0.023 (d)
Heat Flux Density	0.0865	0.116	0.0173
Weight Fraction of Water	0.0088	0.0088	0.0062
Derived Quantities			
Reynolds Number	36400.	52900.	5980.
Fanning Factor	(d)	(d)	(d)
"Friction Velocity"	(d)	(d)	(d)

Table I, cont'd.

Traverse Conditions

Quantity Reported	Test 37	Test 37.1	Test 39
Measured Quantities			
Distance Between Copper Plates	0.0567	0.0578	0.0554
Traverse Location	8.0	3.0	12.7
Incoming Air Temperature	100.0	100.0	100.0
Upper Plate Temperature	100.0	100.0	100.0
Lower Plate Temperature	100.0	100.0	100.0
Bulk Velocity	29.94	29.55	30.02
Pressure	14.335	14.426	14.252
Pressure Gradient	-0.233	-0.220	-0.238
Heat Flux Density	0	0	0
Weight Fraction of Water	0.0058	0.0084	0.014
Derived Quantities			
Reynolds Number	17500.	18400.	17700..
Fanning Factor	0.0069	0.0068	0.0069
"Friction Velocity"	1.76	1.72	1.77

Table I, cont'd.

Traverse Conditions

Quantity Reported	Test 40	Test 41	Test 41.1
Measured Quantities			
Distance Between Copper Plates	0.0571	0.0568	0.0565
Traverse Location	12.7	12.7	8.0
Incoming Air Temperature	100.0	100.0	100.0
Upper Plate Temperature	104.2	105.1	105.1
Lower Plate Temperature	95.0	94.6	94.6
Bulk Velocity	28.13	60.96	
Pressure	14.252	14.297	14.285
Pressure Gradient	-0.227	-0.835	-0.841
Heat Flux Density	0.00732	0.0126	0.0126
Weight Fraction of Water	0.014	0.0081	0.0083
Derived Quantities			
Reynolds Number	17100.	37300.	
Fanning Factor	0.0077	0.0059	
"Friction Velocity"	1.75	3.32	

Table I, cont'd.

Traverse Conditions

Quantity Reported	Test 43	Test 43.1	Test 44
Measured Quantities			
Distance Between Copper Plates	0.0570	0.0561	0.0564
Traverse Location	12.7	8.0	12.7
Incoming Air Temperatures	100.0	100.0	100.0
Upper Plate Temperature	99.9	99.9	105.1
Lower Plate Temperature	100.0	100.0	94.4
Bulk Velocity	88.68	90.21	88.43
Pressure	14.073	14.121	14.108
Pressure Gradient	-1.658	-1.686	-1.629
Heat Flux Density	0	0	0.0156
Weight Fraction of Water	0.0128	0.0104	0.0139
Derived Quantities			
Reynolds Number	53200.		52500.
Fanning Factor	0.0057		0.0056
"Friction Velocity"	4.75		4.68

Table I, cont'd.

Traverse Conditions

Quantity Reported	Test 44.1	Test 45	Test 45.1
Measured Quantities			
Distance Between Copper Plates	0.0566	0.0574	0.0571
Traverse Location	8.0	12.7	8.0
Incoming Air Temperature	100.0	100.0	100.0
Upper Plate Temperature	105.0	105.0	105.0
Lower Plate Temperature	94.5	94.7	94.7
Bulk Velocity	88.35	14.77	15.56
Pressure	14.165	14.156	14.232
Pressure Gradient	-1.670	-0.0742	-0.0768
Heat Flux Density	0.0156	0.0045	0.0045
Weight Fraction of Water	0.0143	0.0154	0.0174
Derived Quantities			
Reynolds Number	52900.	8980.	
Fanning Factor		0.0093	
"Friction Velocity"		1.008	

Table I, cont'd.

Traverse Conditions

Quantity Reported	Test 46	Test 48	Test 48.1
Measured Quantities			
Distance Between Copper Plates	0.0576	0.0574	0.0574
Traverse Location	12.7	12.7	8.0
Incoming Air Temperature	100.0	100.0	100.0
Upper Plate Temperature	115.3	100.0	100.0
Lower Plate Temperature	84.6	100.0	100.0
Bulk Velocity	15.29	14.84	15.30
Pressure	14.199	14.282	14.292
Pressure Gradient	-0.0755	-0.0670	-0.0709
Heat Flux Density	0.0139	0	0
Weight Fraction of Water	0.0114	0.0118	0.0124
Derived Quantities			
Reynolds Number	9370.	9110.	
Fanning Factor	0.0088	0.0082	
"Friction Velocity"	1.013	0.950	

Table I, cont'd.

Traverse Conditions

Quantity Reported	Test 49	Test 49.1	Test 50
Measured Quantities			
Distance Between Copper Plates	0.0575	0.0575	0.0580
Traverse Location	12.7	8.0	12.7
Incoming Air Temperature	100.0	100.0	100.0
Upper Plate Temperature	100.0	100.0	100.0
Lower Plate Temperature	100.0	100.0	100.0
Bulk Velocity	11.32	12.29	58.72
Pressure	14.277	14.303	14.265
Pressure Gradient	-0.0343	-0.0371	-0.785
Heat Flux Density	0	0	0
Weight Fraction of Water	0.0149	0.0112	0.0156
Derived Quantities			
Reynolds Number	6960.		36400.
Fanning Factor	0.0072		0.0062
"Friction Velocity"	0.681		3.28

Table I, cont'd.

Traverse Conditions

Quantity Reported	Test 50.1
Measured Quantities	
Distance Between Copper Plates	0.0575
Traverse Location	8.0
Incoming Air Temperature	100.0
Upper Plate Temperature	100.0
Lower Plate Temperature	100.0
Bulk Velocity	61.96
Pressure	14.300
Pressure Gradient	-0.783
Heat Flux Density	0
Weight Fraction of Water	0.0122
Derived Quantities	
Reynolds Number	
Fanning Factor	
"Friction Velocity	

Table II

Temperature and Velocity Data

y/y_o [a]	t °F	u ft./sec.	y/y_o	t °F	u ft./sec.
	Test 30			Test 30, cont'd.	
1.000	130.0	0	0.785		17.67
0.969	119.36		0.704		18.53
0.946	114.92		0.622		18.98
0.919	111.61		0.543		19.10
0.892	110.22		0.462		19.06
0.865	109.25		0.382		18.73
0.838	108.09		0.301		18.21
0.811	107.08		0.220		17.41
0.783	106.25		0.140		15.99
0.756	105.36		0.086		14.06
0.729	104.82		0.052		13.37
0.702	104.16		0.000	70.0	0
0.675	102.87				
0.648	102.16				
0.594	100.51				
0.540	98.76			Test 31	
0.486	96.99				
0.432	95.29		1.000	130.0	0
0.378	93.84		0.969	117.26	
0.350	93.07		0.946	114.59	
			0.919	112.77	
0.323	92.33		0.891	111.61	
0.296	91.73				
0.269	90.91		0.864	110.57	
0.241	90.34		0.837	109.83	
0.215	89.98		0.810	109.07	
			0.783	108.33	
0.188	88.98		0.756	107.61	
0.161	87.90				
0.134	87.17		0.729	106.91	
0.107	85.92		0.674	105.41	
0.073	84.19		0.620	103.39	
			0.566	101.62	
0.054	82.04		0.512	99.78	
- - - - - - -					
0.964		6.18			
0.919		14.49			
0.866		16.30			

(a); y/y_o is the fractional distance from the lower plate.

Table II, cont'd.

Temperature and Velocity Data

y/y_o	t, °F	u, ft./sec.
Test 31, cont'd.		
0.457	97.87	
0.403	96.24	
0.347	94.64	
0.321	93.91	
0.294	93.22	
0.267	92.56	
0.240	91.89	
0.213	91.21	
0.186	90.58	
0.159	89.68	
0.130	88.88	
0.104	87.94	
0.077	86.49	
0.052	84.52	
- - - - - - -		
0.983		6.60
0.966		16.67
0.947		22.81
0.920		26.15
0.894		27.89
0.867		28.99
0.841		29.33
0.814		30.36
0.788		31.29
0.761		31.78
0.735		32.16
0.682		32.50
0.629		33.47
0.576		34.02
0.523		34.09
0.469		34.06
0.416		33.21
0.363		33.93
0.310		32.99
0.257		31.76
0.231		31.59
0.204		30.56
0.178		29.84
0.151		28.44
0.125		27.64
0.098		26.94
0.072		24.94
0.045		19.82
0.028		12.69
0.000	70.0	0
Test 32		
1.000	130.0	0
0.968	116.43	
0.947	114.58	
0.920	113.25	
0.893	112.24	
0.867	111.50	
0.840	110.73	
0.814	110.01	
0.787	109.40	
0.760	108.62	
0.734	108.06	
0.680	106.48	
0.627	104.85	
0.574	103.42	
0.512	101.46	
0.467	99.57	
0.414	97.67	
0.361	96.01	
0.308	94.61	
0.281	93.78	

Table II, cont'd.

Temperature and Velocity Data

y/y_o	t, °F	u, ft./sec.	y/y_o	t, °F	u, ft./sec.
	Test 32, cont'd.			Test 33	
0.254	93.05		1.000	130.0	0
0.288	92.42		0.969	115.35	
0.201	91.82		0.946	113.49	
0.174	90.75		0.919	112.50	
0.148	90.10		0.892	111.62	
0.121	89.28		0.865	110.90	
0.095	88.26		0.838	110.11	
0.062	87.15		0.818	109.43	
- - - - - - -			0.784	108.71	
0.985		22.59	0.757	108.05	
0.969		39.33	0.730	107.30	
0.947		45.56	0.676	105.83	
0.920		48.30	0.622	104.25	
0.893		49.48	0.568	102.74	
0.867		50.54	0.514	100.73	
0.840		51.49	0.460	98.95	
0.813		52.69	0.406	97.22	
0.787		52.74	0.352	95.62	
0.760		52.75	0.326	94.98	
0.733		53.57	0.298	94.31	
0.680		54.72	0.271	93.66	
0.627		54.73	0.244	92.93	
0.573		54.79	0.217	92.24	
0.520		53.85	0.190	91.66	
0.467		54.17	0.163	90.99	
0.413		54.41	0.136	90.34	
0.000	70.0	0	0.109	89.37	
			0.049	86.81	
			- - - - - - -		
			0.984		26.3
			0.966		41.6
			0.946		50.3
			0.920		60.0
			0.893		63.3
			0.866		71.2

Table II, cont'd.

Temperature and Velocity Data

y/y$_o$	t °F	u ft./sec.	y/y$_o$	t °F	u ft./sec.
Test 33, cont'd			**Test 34, cont'd**		
0.839		72.0	0.920	117.13	
0.812		76.3	0.893	115.02	
0.786		78.9	0.867	113.14	
0.759		83.3	0.840	112.30	
0.732		84.6	0.813	111.03	
0.678		88.9	0.787	110.31	
0.625		92.3	0.759	109.34	
0.571		97.0	0.734	108.20	
0.517		98.0	0.680	106.90	
0.464		95.7	0.627	105.18	
0.410		97.4	0.573	103.64	
0.357		93.8	0.520	101.32	
0.303		91.3	0.467	99.57	
0.249		86.8	0.413	98.70	
0.223		84.3	0.333	96.67	
0.196		81.5	0.307	96.07	
0.169		79.2	0.280	95.36	
0.142		75.9	0.253	94.47	
0.115		70.8	0.227	93.52	
0.088		65.6	0.200	92.47	
0.062		56.8	0.173	91.26	
0.035		45.6	0.147	89.66	
0.000	70.0	0	0.120	87.84	
			0.093	85.66	
			0.067	82.60	
			0.045	79.98	
			0.027	77.13	
	Test 34		- - - - - - - -		
1.000	130.0	0	0.984		0.54
0.983	125.15		0.966		2.13
0.969	122.80				
0.956	120.87		0.947		4.14
0.939	118.33		0.919		6.73
			0.894		7.55
			0.868		8.45
			0.841		8.89

Table II, cont'd.

Temperature and Velocity Data

y/y$_o$	t °F	u ft./sec.
Test 34, cont'd.		
0.815		9.47
0.788		9.94
0.762		10.22
0.735		10.41
0.682		10.57
0.641		10.46
0.571		11.24
0.536		11.11
0.470		11.08
0.417		10.98
0.364		11.17
0.338		10.91
0.311		10.06
0.285		9.66
0.258		9.54
0.232		9.60
0.205		9.51
0.179		9.29
0.152		8.86
0.126		8.57
0.098		7.58
0.073		6.36
0.046		5.23
0.020		0.88
0.000	70.0	0
Test 37		
1.000	100.0	0
0.998	99.75	8.58
0.987	99.70	11.02
0.979	99.63	17.88
0.971	99.63	20.96
Test 37, cont'd.		
0.956	99.65	22.23
0.941	99.65	24.23
0.926	99.61	24.82
0.912	99.61	25.74
0.897	99.57	26.11
0.882	99.59	26.81
0.868	99.57	27.28
0.853	99.59	27.97
0.838	99.59	28.39
0.824	99.60	28.80
0.794	99.60	29.51
0.765	99.60	30.32
0.735	99.60	30.86
0.706	99.60	30.36
0.676	99.56	31.72
0.647	99.56	32.23
0.647		32.48*
0.618	99.54	32.63
0.618		32.78*
0.588	99.60	33.01
0.588		33.08*
0.559	99.56	32.95
0.559		33.31*
0.500	99.54	33.39
0.500		33.36*
0.412	99.49	33.01
0.412		32.94*
0.324	99.53	32.00
0.324		32.53*
0.235	99.42	30.49
0.235		30.49*
0.176	99.44	29.21
0.176		29.19*
0.076	99.43	24.13
0.022	99.57	11.90

*: Throughout this table, an asterisk indicates pitot tube data; all other data determined with the thermanemometer.

Table II, cont'd.

Temperature and Velocity Data

y/yo	t °F	u ft./sec.
Test 37, cont'd.		
0.000	100.0	0
Test 37.1		
1.000	100.0	0
0.996	99.51	9.43
0.991	99.51	9.73
0.986	99.49	16.08
0.978	99.45	17.91
0.971	99.46	20.40
0.957	99.49	22.92
0.942	99.43	24.45
0.913	99.41	26.32
0.885	99.38	27.70
0.856	99.37	28.56
0.827	99.38	29.46
0.798	99.37	30.09
0.769	99.40	30.74
0.711	99.41	31.85
0.653	99.43	32.71
0.596	99.45	33.22
0.538	99.47	33.63
0.481	99.47	33.57
0.481		33.73*
0.423	99.46	33.52
0.423		33.44*
0.365	99.47	32.96
0.307	99.51	32.02*
0.250	99.59	31.23
0.250		31.15*
0.192	99.68	29.77
0.134	99.64	27.98
0.076	99.[illegible]	[illegible]
0.048	99.66	21.93

y/yo	t °F	u ft./sec.
Test 37.1, cont'd.		
0.025	99.69	15.09
0.000	100.0	0
Test 39		
1.000	100.0	0
0.997	100.1	10.52
0.994	99.93	12.31
0.991	99.99	15.40
0.985	100.01	17.88
0.977	100.05	20.21
0.970	100.10	22.41
0.962	100.09	23.63
0.955	100.13	24.90
0.940	100.17	26.36
0.925	100.12	26.97
0.910	100.11	27.67
0.895	100.04	28.14
0.880	100.00	28.64
0.865	100.14	29.09
0.850	100.12	29.52
0.835	100.11	29.86
0.820	100.11	30.15
0.790	100.10	30.84
0.729	100.07	31.83
0.669	100.11	32.79
0.609	100.02	33.30
0.549	100.07	33.63
0.489	100.14	33.62
0.429	100.13	33.24
0.368	100.13	32.74
0.368		32.87*
0.308	100.13	32.04
0.308		32.15*
0.248	100.12	31.23

Table II, cont'd.

Temperature and Velocity Data

y/y_o	t °F	u ft./sec.
Test 39, cont'd.		
0.248		31.34*
0.248	100.13	31.37
0.218	100.11	30.67
0.218		30.67*
0.188	100.10	30.20
0.188		30.22*
0.158	100.11	29.39
0.128	100.13	28.39
0.098	100.08	27.20
0.068	100.08	25.12
0.053	100.07	23.88
0.038	100.06	21.84
0.030	100.07	19.92
0.023	100.06	18.20
0.000	100.0	0
Test 40		
1.000	104.2	0
0.997	103.65	8.96
0.994	103.54	9.60
0.991	103.35	11.96
0.985	103.03	15.43
0.975	102.78	18.47
0.971	102.69	19.55
0.964	102.52	21.21
0.956	102.41	22.50
0.942	102.20	23.82
0.927	102.14	24.85
0.908	101.94	26.05
0.898	101.90	26.45
0.883	101.81	27.20
0.869	101.75	27.48
Test 40, cont'd		
0.854	101.65	27.83
0.839	101.60	28.24
0.825	101.52	28.61
0.796	101.41	29.26
0.731	101.14	30.81
0.679	100.94	31.21
0.620	100.68	31.70
0.562	100.39	32.17
0.503	100.08	32.30
0.445	99.74	32.18
0.387	99.46	31.56
0.387		31.36*
0.329	99.15	30.97
0.270	98.88	29.86
0.270		29.94*
0.241	98.77	29.51
0.205	98.60	28.65
0.183	98.51	27.99
0.147	98.33	27.02
0.124	98.19	26.21
0.095	97.98	24.93
0.080	97.82	23.81
0.066	97.71	22.81
0.051	97.46	20.68
0.044	97.30	19.41
0.037	97.13	17.80
0.029	96.55	11.65
0.022	96.29	8.87
0.000	95.0	0

Table II, cont'd.

Temperature and Velocity Data

y/y_o	t, °F	u, ft./sec.
Test 41		
1.000	105.1	0
0.988	102.89	30.71
0.985	102.89	31.92
0.981	102.56	37.87
0.976	102.43	40.64
0.968	102.26	44.13
0.962	102.17	45.63
0.954	102.09	47.53
0.947	102.02	48.62
0.932	101.86	50.91
0.918	101.75	52.69
0.903	101.67	54.15
0.888	101.57	55.59
0.874	101.50	56.61
0.859	101.39	57.79
0.845	101.33	58.84
0.830	101.29	59.81
0.815	101.21	60.82
0.799	101.16	61.53
0.786	101.09	62.39
0.724	100.83	64.93
0.669	100.58	66.93
0.610	100.34	68.39
0.551	100.02	69.67
0.493	99.72	69.39
0.434	99.42	69.06
0.375	99.18	67.91
0.375		67.80*
0.317	99.86	66.18
0.258	98.58	63.87
0.199	98.32	61.23
0.136	98.02	57.37
0.111	97.89	55.64
0.081	97.69	52.33
0.050	97.40	48.30
0.038	97.23	45.44
0.031	97.13	43.73
0.023	96.89	38.99
0.016	96.53	31.19
0.000	94.6	0
Test 41.1		
1.000	105.1	0
0.982	102.84	34.25
0.975	102.60	40.41
0.969	102.54	43.89
0.960	102.44	47.24
0.954	102.36	48.80
0.939	101.98	51.54
0.925	101.89	53.51
0.903	101.74	55.80
0.873	101.64	58.35
0.844	101.49	60.31
0.814	101.38	61.70
0.755	101.15	64.38
0.696	100.91	66.34
0.637	100.66	67.95
0.578	100.39	68.72
0.519	100.10	69.24
0.519		69.16*
0.460	99.79	68.92
0.401	99.47	67.98
0.401		68.07*
0.342	99.16	66.34
0.283	98.89	64.42
0.224	98.60	61.81
0.165	98.34	58.58

Table II, cont'd.

Temperature and Velocity Data

y/y_o	t °F	u ft./sec.
Test 41.1, cont'd.		
0.106	98.04	54.32
0.077	97.82	51.12
0.040	97.45	45.16
0.015	96.60	28.83
0.000	94.6	0
Test 43		
1.000	99.9	0
0.985	99.80	50.10
0.984	99.80	51.38
0.979	99.76	58.05
0.976	99.76	60.30
0.973	99.76	62.51
0.966	99.77	66.34
0.959	99.77	69.12
0.951	99.77	71.67
0.943	99.75	73.26
0.928	99.73	75.97
0.913	99.73	78.59
0.900	99.75	80.17
0.886	99.81	82.14
0.867	99.82	84.40
0.856	99.85	85.51
0.842	99.74	86.86
0.827	99.73	88.02
0.813	99.80	89.42
0.796	99.76	90.31
0.782	99.77	91.24
0.725	99.77	94.73
0.666	99.97	97.63
0.608	99.78	99.86
0.541	99.80	101.12
Test 43, cont'd.		
0.491	99.80	101.16
0.432	99.75	100.56
0.374	99.80	98.92
0.374		99.18*
0.315	99.78	96.65
0.257	99.76	93.68
0.197	99.75	89.87
0.136	99.76	84.94
0.103	99.76	80.91
0.082	99.77	77.67
0.064	99.78	74.58
0.052	99.78	72.40
0.045	99.80	69.97
0.035	99.80	66.80
0.030	99.79	64.67
0.022	99.80	58.20
0.016	99.67	48.76
0.000	100.0	0
Test 43.1		
1.000	99.9	0
0.981	99.89	58.02
0.973	99.89	64.84
0.966	99.88	67.39
0.957	99.89	70.36
0.939	99.88	74.80
0.929	99.90	76.67
0.914	99.90	79.48
0.899	99.91	81.58
0.884	99.92	83.50

Table II, cont'd.

Temperature and Velocity Data

y/y_o	t, °F	u, ft./sec.
Test 43.1, cont'd.		
0.868	99.91	85.15
0.854	99.91	86.47
0.833	99.94	88.38
0.810	99.94	90.46
0.780	99.95	92.54
0.721	99.95	96.02
0.661	99.98	99.02
0.602	99.98	100.90
0.542	100.00	102.13
0.483	99.99	102.54
0.483		102.48*
0.423	99.99	101.95
0.362	99.98	99.84
0.304	99.94	97.28
0.245	99.93	93.95
0.181	99.94	89.26
0.128	99.92	84.27
0.059	99.91	74.87
0.037	99.89	69.52
0.022	99.88	61.20
0.007	99.85	43.10
0.000	100.0	0
Test 44		
1.000	105.1	0
0.989	103.37	49.22
0.988	103.03	51.11
0.984	103.43	55.41
0.979	103.28	60.13
0.976	103.18	62.73
0.967	103.04	67.54
0.964	103.00	67.95
0.954	102.88	70.80
0.947	102.82	72.59
0.932	102.73	75.26
0.917	102.64	77.37
0.902	102.57	79.10
0.886	102.49	81.11
0.870	102.44	82.54
0.860	102.37	83.28
0.843	102.33	84.77
0.829	102.24	86.17
0.808	102.18	87.82
0.795	102.13	88.59
0.777	102.05	89.93
0.724	101.87	92.76
0.666	101.61	95.65
0.607	101.31	97.30
0.548	101.11	98.88
0.489	100.78	99.18
0.421	100.37	99.68
0.421		99.73*
0.371	100.11	98.37
0.312	99.82	96.36
0.252	99.54	93.39
0.193	99.26	89.10
0.134	98.95	83.39
0.075	98.59	77.16
0.060	98.49	74.65
0.046	98.31	70.59
0.028	98.05	64.56
0.021	97.85	59.78
0.012	97.42	47.62
0.000	94.4	0

Table II, cont'd.

Temperature and Velocity Data

y/y$_o$	t °F	u ft./sec.	y/y$_o$	t °F	u ft/sec.
	Test 44.1			**Test 44.1, cont'd.**	
1.000	105.0	0	0.020	97.41	52.34
0.985	103.14	52.29	0.013	96.82	35.69
0.976	102.85	62.27	0.000	94.5	0
0.970	102.75	65.90			
0.961	102.63	68.44			
0.955	102.57	70.21			
0.948	102.51	71.98		**Test 45**	
0.933	102.42	73.98			
0.920	102.37	76.34	1.000	105.0	0
0.904	102.25	78.73	0.986	104.15	3.37
			0.983	103.95	4.04
0.889	102.18	81.05	0.980	103.71	4.98
0.874	102.18	82.26	0.977	103.50	5.11
0.845	102.09	85.08			
0.815	101.96	87.44	0.974	103.32	6.22
0.756	101.79	91.60	0.967	103.24	6.91
			0.960	102.92	8.44
0.727	101.72	94.09	0.960	102.87	8.48
0.668	101.50	97.36	0.953	102.72	9.76
0.609	101.21	99.10			
0.609	101.23	98.96	0.945	102.59	10.45
0.550	100.97	100.56	0.931	102.32	11.76
			0.916	102.12	12.62
0.491	100.68	101.02	0.902	102.97	13.32
0.432	100.34	100.20	0.887	101.88	13.68
0.373	100.06	98.82			
0.373		98.92*	0.873	101.83	14.11
0.315	99.76	97.02	0.858	101.72	14.49
			0.844	101.62	14.72
0.256	99.49	93.94	0.829	101.53	15.02
0.197	99.29	88.96	0.815	101.47	15.19
0.138	98.97	84.05			
0.108	98.73	80.82	0.800	101.39	15.39
0.094	98.60	79.17	0.783	101.28	15.63
			0.728	101.05	16.27
0.079	98.43	77.26	0.670	101.79	16.80
0.064	98.36	74.91	0.612	101.52	17.15
0.049	98.13	70.98			
0.035	97.94	65.82			
0.027	97.79	62.19			

Table II, cont'd.

Temperature and Velocity Data

y/y$_o$	t °F	u ft./sec.
Test 45, cont'd.		
0.554	100.29	17.44
0.481	99.93	17.56
0.481		17.61*
0.437	99.67	17.46
0.379	99.38	17.26
0.317	99.01	16.84
0.263	98.82	16.33
0.205	98.55	15.73
0.147	98.23	14.85
0.118	98.03	14.27
0.089	97.71	13.09
0.060	97.26	11.22
0.046	96.88	9.36
0.038	96.66	8.06
0.031	96.40	6.70
0.024	96.11	5.22
0.017	95.75	3.58
0.009	95.31	2.90
0.000	94.7	0
Test 45.1		
1.000	105.0	0
0.981	103.89	4.72
0.973	103.66	6.46
0.966	103.40	8.04
0.959	103.21	9.29
0.952	102.99	10.41
0.944	102.85	11.25
0.930	102.58	12.52
0.915	102.45	13.40
0.900	102.34	14.08
Test 45.1, cont'd.		
0.871	102.00	15.02
0.842	101.94	15.66
0.784	101.65	16.56
0.725	101.46	17.40
0.667	101.06	17.72
0.608	100.80	18.23
0.550	100.68	18.56
0.492	100.26	18.46
0.492		18.52*
0.433	100.01	18.40
0.375	99.72	18.05
0.316	99.42	17.62
0.258	99.16	17.17
0.200	98.86	16.34
0.141	98.49	15.18
0.112	98.18	14.30
0.083	97.78	12.93
0.054	97.31	10.63
0.039	96.76	8.09
0.032	96.47	6.74
0.024	96.25	5.32
0.017	95.78	3.46
0.000	94.7	0
Test 46		
1.000	115.3	0
0.990	112.92	2.89
0.986	112.66	3.34
0.977	111.36	4.97
0.971	110.60	6.43

Table II, cont'd.

Temperature and Velocity Data

y/y_o	t °F	u ft./sec.	y/y_o	t °F	u ft./sec.
Test 46, cont'd.			Test 48		
0.961	109.56	8.20	1.000	100.0	0
0.954	109.02	9.30	0.993	99.71	3.62
0.949	108.51	10.48	0.991	99.73	3.73
0.935	107.59	11.75	0.988	99.78	3.78
0.906	106.39	13.62	0.984	99.78	5.03
0.877	105.71	14.54	0.982	99.78	5.51
0.848	105.13	15.28	0.975	99.79	6.74
0.789	104.13	16.22	0.968	99.76	8.04
0.733	103.39	16.83	0.961	99.68	9.25
0.675	102.62	17.46	0.958	99.71	9.45
0.614	101.76	17.83	0.953	99.68	9.92
0.559	101.05	18.00	0.939	99.67	11.37
0.501	100.18	18.20	0.910	99.68	12.96
0.443	99.30	18.01	0.881	99.68	13.91
0.443		17.88*	0.852	99.70	14.62
0.385	98.41	17.80	0.823	99.68	15.04
0.327	97.62	17.44	0.765	99.70	15.82
0.267	96.80	16.92	0.707	99.65	16.31
0.212	96.06	16.32	0.649	99.65	16.80
0.154	95.12	15.37	0.591	99.62	17.16
0.123	94.42	14.61	0.533	99.62	17.37
0.096	93.63	13.60	0.533		17.80*
0.081	93.12	12.94	0.475	99.71	17.31
0.058	92.07	11.34	0.416	99.70	17.27
0.048	91.48	10.17	0.358	99.71	16.97
0.035	90.27	8.34	0.293	99.74	16.45
0.029	89.56	6.80	0.242	99.74	16.01
0.022	88.48	4.93	0.184	99.72	15.34
0.015	87.14	2.97	0.126	99.71	14.28
0.000	84.6	0	0.097	99.72	13.38
			0.083	99.71	12.64
			0.068	99.71	11.75
			0.051	99.72	10.38
			0.029	99.73	7.52
			0.000	100.0	0

Table II, cont'd.

Temperature and Velocity Data

y/y_o	t °F	u ft./sec.	y/y_o	t °F	u ft./sec.
	Test 48.1			Test 49	
1.000	100.0	0	1.000	100.0	0
0.994	99.81	3.61	0.990	99.69	2.21
0.990	99.85	3.54	0.990	99.69	2.25
0.983	99.90	5.38	0.987	99.71	1.87
0.976	99.90	6.99	0.987	99.75	1.87
0.968	99.91	7.71	0.984	99.75	2.04
0.954	99.84	10.13	0.979	99.72	2.75
0.939	99.82	11.73	0.970	99.81	4.03
0.910	99.79	13.84	0.963	99.82	4.85
0.881	99.80	14.28	0.954	99.87	6.10
0.823	99.80	15.52	0.949	99.73	6.77
0.765	99.76	16.22	0.935	99.70	8.33
0.716	99.74	16.79	0.921	99.70	8.99
0.649	99.77	17.41	0.906	99.70	9.95
0.620	99.78	17.59	0.874	99.75	10.89
0.562	99.76	17.80	0.847	99.78	11.38
0.563	99.66	17.82	0.819	99.82	12.01
0.563		18.80*	0.787	99.78	12.20
0.507	99.77	17.93	0.737	99.76	12.62
0.494	99.73	17.77	0.674	99.81	13.04
0.446	99.76	17.88	0.616	99.77	13.26
0.388	99.74	17.58	0.561	99.76	13.48
0.330	99.67	17.25	0.561		13.55*
0.272	99.65	16.70	0.492	99.81	13.46
0.214	99.64	16.10	0.432	99.81	13.40
0.156	99.72	15.25	0.381	99.81	13.24
0.098	99.72	13.92	0.326	99.76	12.91
0.084	99.72	13.40	0.276	99.78	12.65
0.069	99.70	12.28	0.210	99.74	12.11
0.055	99.69	11.21	0.152	99.74	11.30
0.040	99.72	9.21	0.090	99.72	9.63
0.026	99.73	7.04	0.065	99.78	8.41
0.000	100.0	0	0.050	99.78	7.05
			0.036	99.82	5.44
			0.018	99.78	3.14
			0.000	100.0	0

Table II, cont'd.

Temperature and Velocity Data

y/y_o	t °F	u ft./sec.	y/y_o	t °F	u ft./sec.
	Test 49.1			Test 50	
1.000	100.0	0	1.000	100.0	0
0.994	99.72	2.59	0.989	99.84	19.14
0.990	99.72	2.41	0.986	99.88	22.75
0.983	99.66	3.61	0.983	99.83	29.27
0.968	99.71	5.53	0.978	99.79	37.04
0.954	99.73	7.84	0.966	99.76	42.94
0.939	99.68	8.89	0.963	99.78	43.78
0.906	99.70	10.91	0.959	99.80	45.54
0.881	99.68	11.74	0.948	99.81	47.32
0.856	99.64	12.22	0.933	99.87	49.48
0.798	99.56	12.89	0.920	99.90	51.28
0.736	99.52	13.56	0.906	99.67	52.52
0.678	99.30	13.91	0.877	99.63	54.92
0.620	99.38	14.12	0.848	99.63	57.79
0.555	99.12	14.35	0.820	99.61	58.20
0.555		14.65*	0.791	99.64	60.28
0.500	99.30	14.43	0.733	99.70	62.20
0.439	99.40	14.33	0.676	99.72	63.74
0.384	99.40	14.20	0.618	99.72	65.38
0.330	99.57	13.91	0.561	99.70	66.21
0.272	99.69	13.62	0.561		66.15*
0.214	99.84	13.24	0.499	99.72	66.83
0.156	99.91	12.45	0.446	99.74	66.52
0.098	99.54	11.30	0.389	99.74	65.69
0.069	99.51	9.47	0.331	99.73	63.84
0.040	99.60	6.92	0.274	99.68	61.78
0.026	99.63	4.40	0.216	99.66	59.48
0.000	100.0	0	0.159	99.67	56.44
			0.101	99.68	52.52
			0.072	99.68	50.00
			0.058	99.68	47.87
			0.044	99.70	45.23
			0.029	99.65	42.60
			0.022	99.61	40.03
			0.016	99.54	38.42

Table II, cont'd.

Temperature and Velocity Data

y/y$_o$	t °F	u ft./sec.
Test 50, cont'd.		
0.000	100.0	0
Test 50.1		
1.000	100.0	0
0.988	99.64	16.32
0.985	99.59	25.39
0.978	99.51	35.50
0.978	99.50	35.50
0.963	99.43	44.74
0.948	99.34	49.04
0.934	99.27	51.77
0.901	99.54	56.01
0.876	99.55	58.97
0.876	99.56	58.32
0.847	99.52	60.00
0.789	99.49	63.73
0.789	99.47	63.73
0.731	99.47	66.99
0.672	99.39	69.52
0.612	99.28	71.32
0.563	99.17	72.05
0.563		66.50*
0.557	99.27	70.46
0.557	99.22	70.14
0.557	99.36	69.46
0.499	99.40	70.09
0.441	99.41	69.64
0.383	99.46	68.52
0.325	99.59	67.04
0.267	99.65	64.85
0.209	99.76	61.90
0.151	99.72	58.52
0.093	99.72	54.14
0.064	99.76	50.98
0.035	99.75	45.79
0.021	99.75	40.79
0.000	100.0	0

Table III

Eddy Property Distributions in a Two-Dimensional, Turbulent Air Stream.

y/y_o	Test 30 $\epsilon_c \times 10^3$ ft.²/sec.	Test 31 $\epsilon_x \times 10^3$ ft.²/sec.	Test 32 $\epsilon_x \times 10^3$ ft.²/sec.	Test 33 $\epsilon_x \times 10^3$ ft.²/sec.	Test 34 $\epsilon_x \times 10^3$ ft.²/sec.
0.02	---	0.47	1.87	---	0.07
0.04	---	1.18	4.05	---	0.17
0.06	0.84	2.13	5.07	7.31	0.25
0.08	1.08	3.06	7.89	10.5	0.37
0.10	2.50	4.30	8.99	12.5	0.48
0.15	3.31	6.45	10.1	14.8	0.73
0.20	3.87	7.69	11.2	17.2	1.19
0.25	4.50	8.08	12.6	16.7	1.67
0.30	4.85	7.61	11.5	16.2	2.10
0.35	4.49	7.06	11.0	15.1	2.31
0.40	4.33	6.69	9.63	13.6	2.24
0.45	3.94	6.06	8.54	12.8	1.96
0.50	3.84	5.77	9.23	12.3	1.76
0.55	3.75	5.78	9.60	12.5	1.75
0.60	3.76	5.72	10.1	13.2	1.86
0.65	3.96	6.64	10.4	14.4	2.02
0.70	4.02	7.50	10.9	15.4	1.91
0.75	4.17	7.64	14.4	15.9	1.75
0.80	3.86	7.40	12.1	16.2	1.51
0.85	3.41	6.84	11.5	15.2	1.21
0.90	3.24	4.87	9.02	13.6	0.78
0.92	1.49	3.64	7.53	12.5	0.57
0.94	0.82	2.73	5.53	9.63	0.34
0.96	0.46	1.47	3.89	5.47	0.20
0.98	---	0.71	1.56	1.91	0.08

Table III, cont'd.

Eddy Property Distributions in a Two-Dimensional, Turbulent Air Stream.

	Test 39	Test 40	Test 40	Test 41	Test 41
	$\epsilon_m \times 10^3$	$\epsilon_c \times 10^3$	$\epsilon_m \times 10^3$	$\epsilon_c \times 10^3$	$\epsilon_m \times 10^3$
y/y_c	$ft^2/sec.$	$ft^2/sec.$	$ft^2/sec.$	$ft^2/sec.$	$ft^2/sec.$
0.02	---	0.31	0.25	0.68	0.38
0.04	0.84	0.83	0.56	2.41	2.10
0.06	1.60	1.48	1.00	3.98	3.52
0.08	2.22	2.31	1.94	5.50	4.40
0.10	2.88	2.99	2.75	6.78	5.14
0.15	4.38	4.45	3.74	8.38	6.64
0.20	5.32	5.50	4.12	9.05	7.32
0.25	5.79	5.56	4.22	9.20	7.18
0.30	5.71	5.30	4.14	8.94	6.65
0.35	5.37	4.96	3.97	8.55	6.30
0.40	4.97	4.62	3.77	8.36	6.25
0.45	4.40	4.37	3.71	8.32	6.46
0.50	3.82	4.29	4.	8.36	6.84
0.55	3.60	4.49	4.2	8.51	7.08
0.60	3.52	5.04	3.94	8.78	7.12
0.65	3.71	5.72	4.75	9.20	7.04
0.70	3.99	6.15	4.68	9.61	7.92
0.75	4.26	6.15	4.80	9.80	6.88
0.80	4.39	5.90	4.57	9.64	6.82
0.85	4.20	5.06	4.00	9.05	6.47
0.90	3.39	3.56	3.19	7.32	5.36
0.92	2.70	2.92	2.49	5.92	4.60
0.94	1.91	2.34	1.74	4.48	3.60
0.96	0.79	1.55	0.84	3.06	2.26
0.98	0.33	0.64	0.48	1.12	0.80

Table III, cont'd.

Eddy Property Distributions in a Two-Dimensional, Turbulent Air Stream.

	Test 43	Test 44*	Test 44*	Test 45	Test 45
y/y_o	$\epsilon_m \times 10^3$ ft.²/sec.	$\epsilon_c \times 10^3$ ft.²/sec.	$\epsilon_m \times 10^3$ ft.²/sec.	$\epsilon_c \times 10^3$ ft.²/sec.	$\epsilon_m \times 10^3$ ft.²/sec.
0.02	1.08	1.18	0.92	0.04	0.03
0.04	3.10	3.48	3.16	0.23	0.14
0.06	5.00	6.14	4.94	0.49	0.31
0.08	6.42	7.90	6.30	0.83	0.56
0.10	7.61	8.74	7.17	1.22	0.96
0.15	9.67	9.98	8.23	2.24	2.04
0.20	10.62	10.84	8.79	2.83	2.41
0.25	10.77	11.25	9.15	3.11	2.40
0.30	10.50	11.24	9.42	3.18	2.30
0.35	10.11	10.87	9.64	2.98	2.22
0.40	9.77	10.48	9.83	2.75	2.16
0.45	9.55	10.18	10.05	2.67	2.11
0.50	9.44	10.07	10.32	2.82	2.08
0.55	9.48	10.18	10.77	3.18	2.07
0.60	9,63	10.50	11.40	3.27	2.09
0.65	9.86	11.24	11.92	3.35	2.21
0.70	10.15	13.29	12.02	3.33	2.41
0.75	10.48	14.09	11.75	3.20	2.52
0.80	10.52	14.00	11.15	2.92	2.43
0.85	9.66	13.11	10.45	2.46	2.06
0.90	7.60	10.82	9.96	1.65	1.15
0.92	6.38	9.57	7.84	1.10	0.73
0.94	4.86	7.88	6.02	0.64	0.40
0.96	3.12	5.24	3.72	0.39	0.17
0.98	1.20	1.88	1.32	0.02	0.01

* Eddy Properties for Test 44 are of doubtful validity because of unsmoothness of original data.

Table III, cont'd.

Eddy Property Distributions in a Two-Dimensional, Turbulent Air Stream.

y/y_o	Test 46 $\epsilon_c \times 10^3$ ft.^{2}/sec.	Test 46 $\epsilon_m \times 10^3$ ft.^{2}/sec.	Test 48 $\epsilon_m \times 10^3$ ft.^{2}/sec.	Test 49 $\epsilon_m \times 10^3$ ft.^{2}/sec.	Test 50 $\epsilon_m \times 10^3$ ft.^{2}/sec.
0.02	0.02	0.03	0.02	0.00	0.86
0.04	0.25	0.12	0.17	0.05	2.00
0.06	0.55	0.31	0.37	0.17	3.40
0.08	0.92	0.63	0.59	0.31	4.87
0.10	1.34	0.92	0.86	0.47	5.81
0.15	2.37	1.82	1.70	0.87	6.97
0.20	3.05	2.36	2.23	1.22	7.15
0.25	3.28	2.54	2.30	1.44	6.91
0.30	3.34	2.50	2.16	1.49	6.63
0.35	3.26	2.23	2.00	1.43	6.49
0.40	3.00	2.12	1.94	1.42	6.54
0.45	2.90	2.15	1.94	1.45	6.74
0.50	2.98	2.25	1.97	1.50	7.06
0.55	3.16	2.35	2.03	1.57	7.48
0.60	3.29	2.39	2.13	1.62	7.98
0.65	3.32	2.40	2.26	1.63	8.44
0.70	3.27	2.49	2.40	1.58	8.66
0.75	3.10	2.40	2.45	1.45	8.36
0.80	2.76	2.24	2.30	1.18	7.65
0.85	2.25	1.86	1.85	0.83	6.61
0.90	1.42	1.09	1.10	0.43	5.24
0.92	0.97	0.67	0.73	0.24	4.52
0.94	0.57	0.33	0.44	0.08	3.62
0.96	0.29	0.14	0.21	0.00	2.38
0.98	0.10	0.04	0.04	0.00	0.80

Table IV

Smoothed and Symmetrical Distributions of the Eddy Properties and of their Ratio.

	Test 30	Test 31	Test 32	Test 33	Test 34
	$\epsilon_c \times 10^3$	$\epsilon_c \times 10^3$	$\epsilon_c \times 10^3$	$\epsilon_c \times 10^3$	$\epsilon_c \times 10^3$
y/y_o	$ft.^2/sec.$	$ft.^2/sec.$	$ft.^2/sec.$	$ft.^2/sec.$	$ft.^2/sec.$
0.02	0.00	0.55	1.60	2.22	0.08
0.04	0.38	1.36	3.70	5.46	0.18
0.06	0.82	2.26	5.84	9.04	0.33
0.08	1.52	3.28	7.72	11.40	0.46
0.10	2.26	4.47	8.93	13.00	0.60
0.15	3.35	6.66	10.50	15.27	0.95
0.20	3.89	7.55	11.67	16.60	1.34
0.25	4.23	7.78	12.65	16.28	1.69
0.30	4.32	7.50	11.53	15.66	2.00
0.35	4.23	6.90	10.58	14.60	2.11
0.40	4.06	6.33	9.76	13.35	2.01
0.45	3.90	5.94	9.22	12.63	1.86
0.50	3.84	5.78	8.98	12.33	1.80

Table IV, cont'd.

Smoothed and Symmetrical Distributions of the Eddy Properties and of their Ratio.

	Test 39	Test 40	Test 40	Test 40	Test 41
	$\epsilon_m \times 10^3$	$\epsilon \times 10^3$	$\epsilon_m \times 10^3$	ϵ/ϵ_m	$\epsilon \times 10^3$
y/y_o	$ft.^2/sec.$	$ft.^2/sec.$	$ft.^2/sec.$		$ft.^2/sec.$
0.02	0.16	0.42	0.30	1.40	0.88
0.04	0.89	1.13	0.87	1.30	2.72
0.06	1.70	1.87	1.58	1.18	4.30
0.08	2.47	2.59	2.35	1.10	5.66
0.10	3.10	3.25	2.98	1.09	6.87
0.15	4.23	4.73	3.87	1.22	8.79
0.20	4.82	5.61	4.32	1.30	9.42
0.25	5.00	5.81	4.50	1.29	9.53
0.30	4.89	5.64	4.42	1.28	9.28
0.35	4.59	5.23	4.18	1.25	8.90
0.40	4.27	4.76	4.00	1.19	8.57
0.45	4.06	4.44	3.94	1.13	8.41
0.50	3.95	4.32	3.92	1.10	8.37

Table IV, cont'd.

Smoothed and Symmetrical Distributions of the Eddy Properties and of their Ratio.

	Test 41	Test 41	Test 43	Test 44*	Test 44*
	$\epsilon_m \times 10^3$	ϵ_c/ϵ_m	$\epsilon_m \times 10^3$	$\epsilon_c \times 10^3$	$\epsilon_m \times 10^3$
y/y_c	$ft^2/sec.$		$ft^2/sec.$	$ft^2/sec.$	$ft^2/sec.$
0.02	0.60	1.47	0.78	1.56	1.52
0.04	2.28	1.19	3.40	3.88	3.94
0.06	3.68	1.17	5.00	6.90	6.84
0.08	4.60	1.28	6.40	8.68	8.82
0.10	5.32	1.29	7.40	9.83	10.20
0.15	6.62	1.33	9.66	11.54	11.78
0.20	7.16	1.32	10.60	12.46	12.48
0.25	7.14	1.34	10.58	12.68	12.60
0.30	6.90	1.35	10.28	13.38	12.13
0.35	6.76	1.32	9.92	11.66	11.21
0.40	6.77	1.27	9.68	10.86	10.34
0.45	6.84	1.23	9.52	10.40	10.26
0.50	6.88	1.22	9.46	10.20	10.16

* Eddy Property Data for Test 44 are of doubtful validity because of unsmoothness of original data.

Table IV, cont'd.

Smoothed and Symmetrical Distributions of the Eddy Properties and of their Ratio.

y/yo	Test 44* ϵ_c/ϵ_m	Test 45 $\epsilon_c \times 10^3$ ft²/sec.	Test 45 $\epsilon_m \times 10^3$ ft²/sec.	Test 45 ϵ_c/ϵ_m	Test 46 $\epsilon_c \times 10^3$ ft²/sec.
0.02	1.03	0.00	0.06	---	0.02
0.04	0.99	0.27	0.13	---	0.25
0.06	1.01	0.58	0.35	1.66	0.57
0.08	0.98	0.96	0.68	1.41	0.97
0.10	0.96	1.36	1.06	1.28	1.38
0.15	0.98	2.27	2.03	1.12	2.24
0.20	1.00	2.87	2.46	1.17	2.84
0.25	1.01	3.17	2.46	1.29	3.16
0.30	1.02	3.23	2.34	1.38	3.27
0.35	1.04	3.10	2.20	1.41	3.23
0.40	1.05	2.96	2.14	1.38	3.16
0.45	1.01	2.87	2.11	1.36	3.10
0.50	1.00	2.84	2.09	1.36	3.05

* Eddy property data fpr Test 44 are of doubtful validity because of unsmoothness of original data.

Table IV, cont'd.

Smoothed and Symmetrical Distributions of the Eddy Properties and of their Ratio.

	Test 46	Test 46	Test 48	Test 49	Test 50
	$\epsilon_m \times 10^3$	ϵ_c/ϵ_m	$\epsilon_m \times 10^3$	$\epsilon_m \times 10^3$	$\epsilon_m \times 10^3$
y/y_o	$ft.^2/sec.$		$ft.^2/sec.$	$ft.^2/sec.$	$ft.^2/sec.$
0.02	0.06	---	0.00	0.00	0.81
0.04	0.14	---	0.17	0.00	2.30
0.06	0.37	1.54	0.42	0.13	3.60
0.08	0.72	1.35	0.71	0.30	4.84
0.10	1.07	1.29	1.03	0.46	5.68
0.15	1.87	1.20	1.75	0.85	6.81
0.20	2.30	1.24	2.23	1.20	7.37
0.25	2.43	1.30	2.38	1.43	7.62
0.30	2.39	1.37	2.30	1.54	7.60
0.35	2.30	1.40	2.14	1.54	7.46
0.40	2.25	1.40	2.04	1.50	7.27
0.45	2.22	1.40	1.99	1.48	7.12
0.50	2.20	1.39	1.97	1.48	7.04

Propositions

Chemical Engineering:

1. The thermal resistance of a metal-to-metal joint, when "controlled" by roughness and not by waviness, may be approximated by the following formula:

$$h = \frac{\sqrt{2}}{4r}\left[k_m\left(\frac{P}{\sigma}\right) + 2k_a\right]$$

Nomenclature; (see also p.58):

h = $Q^\circ/\Delta t$, the reciprocal of the thermal resistance, BTU/(ft.^{2})(sec.)($^\circ$F).

k_a = the thermal conductivity of the ambient fluid, BTU/(ft.)(sec.)($^\circ$F).

k_m = the thermal conductivity of the metal, BTU/(ft.)(sec.)($^\circ$F).

P = the load per unit area perpendicular to the plane of the joint, lbs./ft.^{2}.

σ = a constant, a property of the metal, of approximately the same magnitude as the yield strength, lbs./ft.^{2}.

r = the r.m.s. roughness of the metal surfaces, ft.

2. Butane, propane, and other light hydrocarbons are suitable "foaming" agents for vinyl plastisols.

3. The wall-to-fluid heat transfer coefficient for any situation not involving appreciable fluid acceleration is given by the generalized expression:

$$h = \tau_0\left(\frac{g\,C_p}{U}\right)(P_r)^{-0.6}$$

4. In the analysis of gas mixtures by the thermal conductivity method, it is suggested that the reference gas consist of the sample gas from which the compound of interest has been removed by a specific absorbent. For example,

Propositions, cont'd.

combustion exhaust gases may be "preoxidized" with CuO and dried and admitted to legs 1 and 3 of the analyzer; "preoxidized" gas is further treated with soda-lime and dried and admitted to legs 2 and 4. The galvanometer reading is expected to be a single valued function of the combustion mixture.

5. Stainless steel shim stock is suggested for use as an electrical analogy in the study of potential field problems such as the flow of fluids through porous media.

6. The eddy viscosity is finite and has a real meaning at the center of a fluid stream.

Mechanical Engineering:

1. The requirements of a given maximum working deflection and the mechanical properties of available materials approximately fix the resonant frequency of a helical spring. This limits the performance of many high speed devices which cannot be allowed to operate at speeds which may cause their springs to surge. This limiting resonant frequency may be increased by approximately the factor $\sqrt{2}$ by the use of hollow wire for the spring.

2. It is suggested that simulated climate and altitude chambers be insulated by making their walls in the form of a stainless steel Dewar flask and that air-cycle refrigeration be used in such chambers.

3. Cobalt is suggested as a possible alloying element for high-strength weldable steels.

4. The differences in corrosion behavior between weldements of titanium stabilized and columbium stabilized austenitic steels are readily explained by considering the differences in the temperatures at which the corresponding carbides became soluble in the austenite.

Propositions, cont'd.

5. Titanium is an effective addition for decreasing the nitrogen content of a steel melt.

Chemistry

1. Long-chain polyester resins with a minimum amount of unsaturation and of styrene cross-linking have optimum properties for the "potting" of miniaturized electronic components, except possibly for use in the microwave ranges.

2. The removal of scale from stainless steel by pickling acids is an electrolytic process, the basis metal going into solution at the anode. Apparently the scale serves as the cathode.

3. In the analysis for nitrogen of titanium-containing metals and alloys, correct results may be obtained if the alloy is dissolved in HCL containing a little HF and if the residue is digested with a H_2SO_4-$NaHSO_4$ mixture containing a little copper sulphate or selenium. The solutions are combined and made alkaline and the nitrogen is "distilled over" and determined in the usual manner.